



Letter

Observation of double parton scattering in same-sign W boson pair production in pp collisions at $\sqrt{s} = 13$ TeV with the ATLAS detector

The ATLAS Collaboration¹

ARTICLE INFO

Editor: M. Doser

Keywords:

DPS

Same-sign WW

ABSTRACT

This letter reports the measurement of double parton scattering in same-sign W boson pair production with the ATLAS detector. The data set used corresponds to an integrated luminosity of 140 fb^{-1} of proton–proton collisions at a center-of-mass energy of 13 TeV, collected during Run 2 of the Large Hadron Collider. The study is performed in final states including two same-charge leptons, electron or muon, missing transverse momentum, and up to one jet. An excess of events is observed over the expected background contributions with a significance of 8.8 standard deviations. The measured fiducial cross section times leptonic branching fraction is $4.59 \pm 0.64 \text{ fb}$. The measurement corresponds to a double parton scattering effective cross section of $10.6 \pm 1.8 \text{ mb}$.

1. Introduction

Multi-parton interactions (MPI) involving hard interactions of more than one pair of incident partons in the same proton–proton (pp) collision have been discussed in theoretical studies since the first days of the parton model [1–3]. This was followed by the generalization of the Altarelli-Parisi evolution equations to the case of multi-parton states [4,5] and theoretical studies of potential correlations in color and spin space [6]. Phenomenological studies of MPI in the framework of perturbative quantum chromodynamics (QCD) for a variety of processes leading to final states such as four leptons, four jets, three jets plus a photon, or a leptonically decaying gauge boson accompanied by two jets are discussed in Refs. [7–15].

The cross sections of the double-parton scattering (DPS) processes, where two partons in each proton initiate two separate hard-scattering processes, can be estimated by using a factorized ansatz that neglects potential complex correlation effects [12,13]. For a DPS process in which a final state $A + B$ is produced at a hadronic center-of-mass energy \sqrt{s} , this simplified formalism yields

$$\sigma_{AB}^{\text{DPS}} = \frac{1}{1 + \delta_{AB}} \frac{\sigma_A \sigma_B}{\sigma_{\text{eff}}}, \quad (1)$$

where σ_{AB}^{DPS} denotes the DPS cross section and σ_A and σ_B denote the production cross sections of final states A and B in a single parton scattering (SPS), respectively. The quantity δ_{AB} is the Kronecker delta used to construct a symmetry factor such that for identical final states with identical phase space, the DPS cross section is divided by two. The parameter σ_{eff} , known as the effective cross section, describes the effective overlap of the spatial distribution of partons in the plane perpendicular to the direction of motion. Experimental measurements of DPS effects

in hadron collisions at different center-of-mass energies from 63 GeV to 8 TeV yield typical values of σ_{eff} ranging from about 10 mb at the lowest energy to 25 mb [16–40].

The study of DPS events is crucial for fully understanding the internal structure of the colliding hadrons, including the correlation effects among the partons that are neglected in the simplified approach of Eq. (1). Recent theoretical developments [41–45] have introduced non-factorized double parton distribution functions including perturbative splittings with impact parameter dependence. The high energy and high integrated luminosity available at the Large Hadron Collider [46] (LHC) offers the possibility to further study these interactions in a variety of processes.

This letter presents the measurement of DPS production of same-sign W boson pairs ($W^\pm W^\pm$) with the ATLAS detector. Observation of the DPS $W^\pm W^\pm$ production at 13 TeV with a significance greater than 5 standard deviations was reported by the CMS Collaboration [47]. The $W^\pm W^\pm$ process is a promising channel to study DPS [48,49] compared to opposite-sign $W^\pm W^\mp$ because of the smaller background contribution from the production of SPS $W^\pm W^\pm$. The SPS $W^\pm W^\pm$ process can indeed be suppressed by selections as two additional partons are needed in the final state at the leading-order (LO) accuracy to produce same-sign W bosons, as seen in Fig. 1.

The measurement is performed in the leptonic decay modes $W^\pm W^\pm \rightarrow \ell^\pm \nu \ell'^\pm \nu$, where both W bosons decay into electrons or muons, $\ell, \ell' = e, \mu$. A set of pp collision data events collected by the ATLAS detector between 2015 and 2018 at $\sqrt{s} = 13$ TeV is used. The dataset corresponds to an integrated luminosity of 140 fb^{-1} [50,51] with a relative uncertainty of 0.83%. Candidate events contain two same charge leptons, moderate missing transverse momentum, and at most one jet. As discussed above, the contribution of the SPS $W^\pm W^\pm$

¹ Authors are listed at the end of this paper.

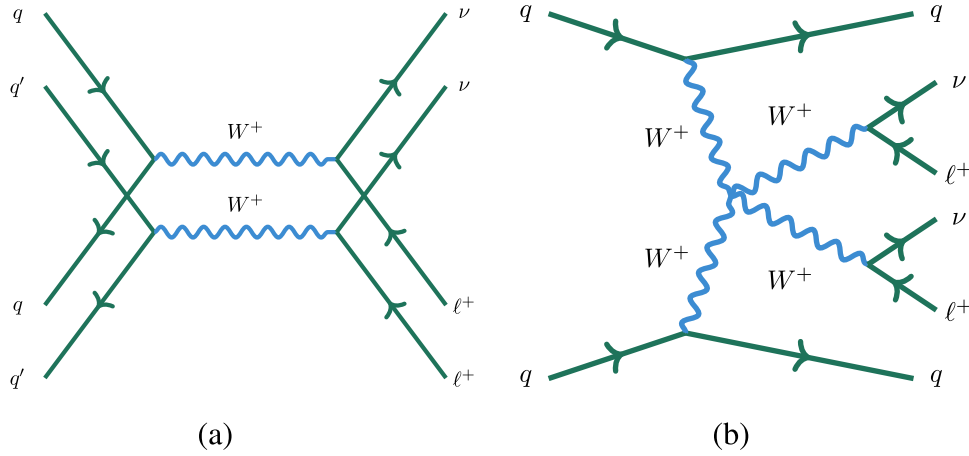


Fig. 1. Representative Feynman diagrams of W^+W^+ process produced via (a) DPS and (b) SPS.

background process is not significant after the requirement on the number of jets. The leading Standard Model (SM) background process is the production of WZ/γ^* boson pairs (referred to as WZ). It contributes when the lepton from the Z boson decay, having an opposite sign to that of the W boson, is not detected, typically because it is outside of the geometrical and kinematical acceptances of the detector. Its contribution is estimated using Monte Carlo (MC) simulated events, with the normalization constrained in a dedicated signal-depleted control region (CR). Data-driven techniques, assisted by MC simulation, are used to estimate backgrounds including electrons or muons not originating from the prompt decay of particles such as W or Z bosons (referred to as non-prompt leptons) and backgrounds including electron charge misidentification. Background events from the production of two overlapping same-sign W bosons originating from separate pp interactions within the same bunch crossing are also considered. Other smaller backgrounds, including contributions mainly from the $V\gamma$ ($V = W, Z/\gamma^*$), SPS $W^\pm W^\pm$, ZZ , and top quark processes, are estimated using MC simulation.

2. ATLAS detector

The ATLAS experiment [52] at the LHC is a multipurpose particle detector with a forward-backward symmetric cylindrical geometry and a near 4π coverage in solid angle.² It consists of an inner tracking detector (ID) surrounded by a thin superconducting solenoid providing a 2 T axial magnetic field, electromagnetic and hadronic calorimeters, and a muon spectrometer. The ID covers the pseudorapidity range $|\eta| < 2.5$. It consists of silicon pixel, silicon microstrip, and transition radiation tracking detectors. Lead/liquid-argon (LAr) sampling calorimeters provide electromagnetic (EM) energy measurements with high granularity within the region $|\eta| < 3.2$. A steel/scintillator-tile hadronic calorimeter covers the central pseudorapidity range ($|\eta| < 1.7$). The endcap and forward regions are instrumented with LAr calorimeters for EM and hadronic energy measurements up to $|\eta| = 4.9$. The muon spectrometer (MS) surrounds the calorimeters and is based on three large superconducting air-core toroidal magnets with eight coils each. The MS includes a sys-

tem of precision tracking chambers up to $|\eta| = 2.7$ and fast detectors for triggering up to $|\eta| = 2.4$. The luminosity is measured mainly by the LUCID-2 [51] detector, which is located close to the beam pipe. A two-level trigger system is used to select events [53]. The first-level trigger is implemented in hardware and uses a subset of the detector information to accept events at a rate close to 100 kHz. This is followed by a software-based trigger that reduces the accepted rate of complete events to 1.25 kHz on average depending on the data-taking conditions. A software suite [54] is used in data simulation, in the reconstruction and analysis of real and simulated data, in detector operations, and in the trigger and data acquisition systems of the experiment.

3. Event simulation

MC simulated event samples are used to model the signal DPS $W^\pm W^\pm$ process as well as other background processes. Simulated events are processed through the ATLAS simulation infrastructure [55] using GEANT4 [56]. The effect of additional pp interactions per bunch crossing (pileup) is accounted for by overlaying the hard-scattering process with Poisson-distributed minimum-bias events generated with PYTHIA [8.186] [57] using the NNPDF2.3LO set of parton distribution functions (PDF) [58] and the A3 set of tuned parameters [59]. Different pileup conditions between data and simulation are taken into account by reweighting the mean number of interactions per bunch crossing in simulation to the number observed in data. The EVTGEN 1.7.0 program [60] was used to model the decays of bottom and charm hadrons. All simulated samples are processed through the same reconstruction algorithms and analysis chain as the data.

The DPS $W^\pm W^\pm$ production is simulated at LO using the PYTHIA [8.307] [61] generator with the A14 [62] set of tuned parameters used for the parton shower. The NNPDF2.3LO PDF set is used. An alternative signal sample is simulated at LO with the Herwig [7.2.13] [63,64] generator using the default Herwig tune and the NNPDF3.0LO PDF set [65]. Differences in the shapes of the signal distributions predicted by the PYTHIA and Herwig samples are considered as an uncertainty.

Detailed information about the simulation of the background processes can be found in Ref. [66]. A brief description is given below. The NNPDF3.0 [65] PDF sets are used in all matrix element calculations. The WZ process, where both the W and Z bosons decay leptonically, is simulated with the SHERPA [2.2.12] generator [67] using matrix elements that contain all diagrams with four electroweak (EW) vertices. This process is calculated for up to one additional parton at next-to-LO (NLO) in perturbative QCD and up to three additional partons at LO using COMIX [68] and OPENLOOPS [69], and merged with the SHERPA parton shower based on the Catani-Seymour dipole factorization [70].

² ATLAS uses a right-handed coordinate system with its origin at the nominal interaction point (IP) in the center of the detector and the z -axis along the beam pipe. The x -axis points from the IP to the center of the LHC ring, and the y -axis points upwards. Polar coordinates (r, ϕ) are used in the transverse plane, ϕ being the azimuthal angle around the z -axis. The pseudorapidity is defined in terms of the polar angle θ as $\eta = -\ln \tan(\theta/2)$ and is equal to the rapidity $y = \frac{1}{2} \ln \left(\frac{E+p_z}{E-p_z} \right)$ in the relativistic limit. Transverse momentum (p_T) is defined relative to the beam axis and is calculated as $p_T = p \sin \theta$ where p is the momentum. Angular distance is measured in units of $\Delta R = \sqrt{(\Delta y)^2 + (\Delta \phi)^2}$.

The WZ production in association with two jets involving only EW vertices as well as the interference between the EW and strong contributions are simulated using MADGRAPH5_AMC@NLO [2.6.2] [71] at LO interfaced to PYTHIA [8.235] [72] for modeling the parton shower in the dipole recoil scheme [73].

The production of the SPS $W^\pm W^\pm$ processes at LO has contributions both from processes that involve only EW interaction vertices, referred to as EW $W^\pm W^\pm$ and from processes that involve strong interaction vertices, referred to as QCD $W^\pm W^\pm$. The SPS $W^\pm W^\pm$ contributions are simulated with MADGRAPH5_AMC@NLO [2.6.7] at LO. The samples corresponding to the EW $W^\pm W^\pm$ production and decay are simulated with diagrams including exactly six orders of the EW coupling [66]. The simulation of the QCD $W^\pm W^\pm$ process and the interference between EW and QCD contributions includes diagrams with exactly four and five EW vertices, respectively.

The diboson ZZ production is simulated using the SHERPA [2.2.2] generator. The $W\gamma$ and $Z\gamma$ processes are simulated with SHERPA [2.2.11] with all off-shell contributions included. The NLO matrix elements with up to one additional parton and LO matrix elements with up to three partons are merged with the parton shower using an MEPS@NLO merging scale [74–77] of $Q = 20$ GeV.

Additional samples are used to model minor backgrounds. The production of $t\bar{t}V$ and tZq events are simulated at NLO and LO in QCD, respectively, using the MADGRAPH5_AMC@NLO [2.3.3] generator interfaced to PYTHIA [8.210] for parton showering. The production of $t\bar{t}$ and single-top-quark events is simulated using the POWHEGBOXv2 [78–81] generator at NLO in QCD and the production of V +jets events [82] is simulated with the MADGRAPH5_AMC@NLO [2.3.2] generator. PYTHIA [8.230] with the A14 set of tuned parameters is used for the parton shower. The production of triboson (VVV) events is simulated with the SHERPA [2.2.2] generator, accurate at NLO in QCD for the inclusive process and at LO for up to two additional parton emissions, using factorized gauge-boson decays. These background samples are normalized to the highest-order theory predictions available as described in Ref. [66].

4. Object reconstruction and event selection

Events are selected online by a set of single-electron [83] or single-muon triggers [84], with lepton p_T lowest thresholds ranging from 20 to 26 GeV, depending on the lepton flavor and data-taking period. Only data taken from stable beam collisions that satisfy a standard set of data-quality requirements, ensuring that all the ATLAS subdetectors were functioning correctly, are considered [85]. Events are required to have at least one collision vertex reconstructed from at least two ID tracks with $p_T > 500$ MeV. For events with several collision vertices, the one with the largest sum of the squared transverse momenta of the associated tracks is taken as the hard-scatter vertex [86].

Electrons are reconstructed from isolated electromagnetic calorimeter clusters, which are matched to tracks in the ID [87]. “Baseline” electrons are required to satisfy a likelihood-based identification criterion with $p_T > 4.5$ GeV and $|\eta| < 2.47$ with an average efficiency of 93%, referred to as “Loose” working point in Ref. [87]. The electrons must be outside the barrel/endcap transition region ($1.37 < |\eta| < 1.52$) of the calorimeter. The transverse impact parameter significance³ is required to satisfy $|d_0|/\sigma(d_0) < 5$. The longitudinal impact parameter⁴ is required to satisfy $|z_0 \sin(\theta)| < 0.5$ mm. “Signal” electrons have the same requirements as baseline electrons but with $p_T > 27$ GeV and must additionally satisfy a more restrictive (“Tight”) likelihood-based identification

³ The transverse impact parameter significance is defined as $|d_0|/\sigma(d_0)$, where d_0 is the distance of closest approach of the e or μ track to the z -axis in the transverse plane and $\sigma(d_0)$ is its uncertainty.

⁴ The longitudinal impact parameter is equal to $|z_0 \sin(\theta)|$, where z_0 is the difference between the value of the z coordinate of the point on the track at which d_0 is defined, and the longitudinal position of the primary vertex.

with an average efficiency of 80% and “Gradient” isolation requirements [87]. A charge selector tool based on boosted decision trees uses shower shape and track-to-cluster matching variables [87] to reject electron candidates where the charge is likely misidentified. “Background” electrons, used to estimate the background processes with non-prompt electrons, are required to pass “Medium” likelihood-based identification with an average efficiency of 88% [87], with no requirements on the isolation criteria. Background electrons are required to fail the signal electron selection criteria to ensure that the samples of signal and background electrons are statistically independent.

Muons are reconstructed [88] from tracks in the MS, matched to a corresponding track in the ID where possible. Baseline muons are required to have $p_T > 3$ GeV and $|\eta| < 2.7$ with $|d_0|/\sigma(d_0) < 15$ and $|z_0 \sin(\theta)| < 1.5$ mm. Baseline muon candidates must satisfy the “Loose” cut-based identification criteria with an average efficiency of 99% [88]. Signal muons must satisfy a more restrictive identification criteria (“Medium”) with an average efficiency of 97% with the “PflowTight” isolation requirement [88]. The signal muons must have $p_T > 27$ GeV and are restricted to the range $|\eta| < 2.5$ with $|d_0|/\sigma(d_0) < 3$ and $|z_0 \sin(\theta)| < 0.5$ mm. The isolation requirement for background muons, used to estimate the background processes with non-prompt muons, is changed to a less restrictive working point (“PflowLoose”), with an efficiency of 99%, with $|d_0|/\sigma(d_0) < 10$ [88]. Background muons are required to fail the signal muon selection to ensure that the samples of signal and background muons are statistically independent. The muon charge misidentification rate is found to be negligible [89].

Jets are reconstructed using the anti- k_r algorithm [90,91], with a radius parameter of $R = 0.4$, using particle-flow objects [92] as inputs. Contamination from jets originating from pileup is reduced by using the jet-vertex-tagger algorithm [93]. The jets are calibrated as described in Ref. [94] and required to have $p_T > 30$ GeV and $|\eta| \leq 4.5$. In order to suppress contributions from background processes that involve top quarks or leptonic b -hadron decays, the DL1r classification algorithm based on recurrent neural networks [95] is used to identify jets originating from b -quarks, referred to as “ b -jets”. The b -jets with $p_T > 20$ GeV and $|\eta| < 2.5$ have an identification efficiency of 85% in $t\bar{t}$ events with an expected rejection factor (defined as the inverse of the efficiency) of about 40 for light-flavor jets, and about 2.9 for jets originating from charm quarks [96–98].

An object overlap removal procedure is applied to baseline leptons and jets to avoid ambiguities in detector reconstruction. This procedure prevents cases where the detector response to a single physical object is reconstructed as two different final state objects. First, this procedure removes any electron if it shares an ID track with another higher p_T electron. Second, electrons sharing their tracks with a muon candidate are removed. Third, a jet is removed if it overlaps with an electron within a ΔR distance of 0.2, unless it is a b -jet and the electron p_T is below 100 GeV, in which case the electron is removed, and any electrons within $\Delta R = 0.4$ of a remaining jet are removed. Any jet that is within $\Delta R = 0.2$ of a muon and has less than three associated tracks is removed, unless it is a b -jet. Lastly, the remaining muons are removed if their track is within $\Delta R = 0.4$ of a remaining jet.

The missing transverse momentum, with magnitude E_T^{miss} , is calculated from the negative vector sum of the transverse momenta of all of the selected and calibrated objects in the event including a track-based soft term [99].

Candidate events in the signal region (SR) are required to have a same-sign signal lepton pair, with an invariant mass $m_{\ell\ell}$ greater than 20 GeV to reduce the non-prompt lepton background contribution. One of the leptons must be matched to the lepton that fired a single-lepton trigger. Events with an additional baseline muon or electron are vetoed to reduce the contributions from the WZ and ZZ background processes. Events with b -jets are discarded, reducing the non-prompt lepton background and signal contributions by 36% and 4%, respectively. The E_T^{miss} must be larger than 30 GeV to exploit the presence of neutrinos in the final state and to reduce the contribution of $Z/\gamma^* \rightarrow ee$ events where the

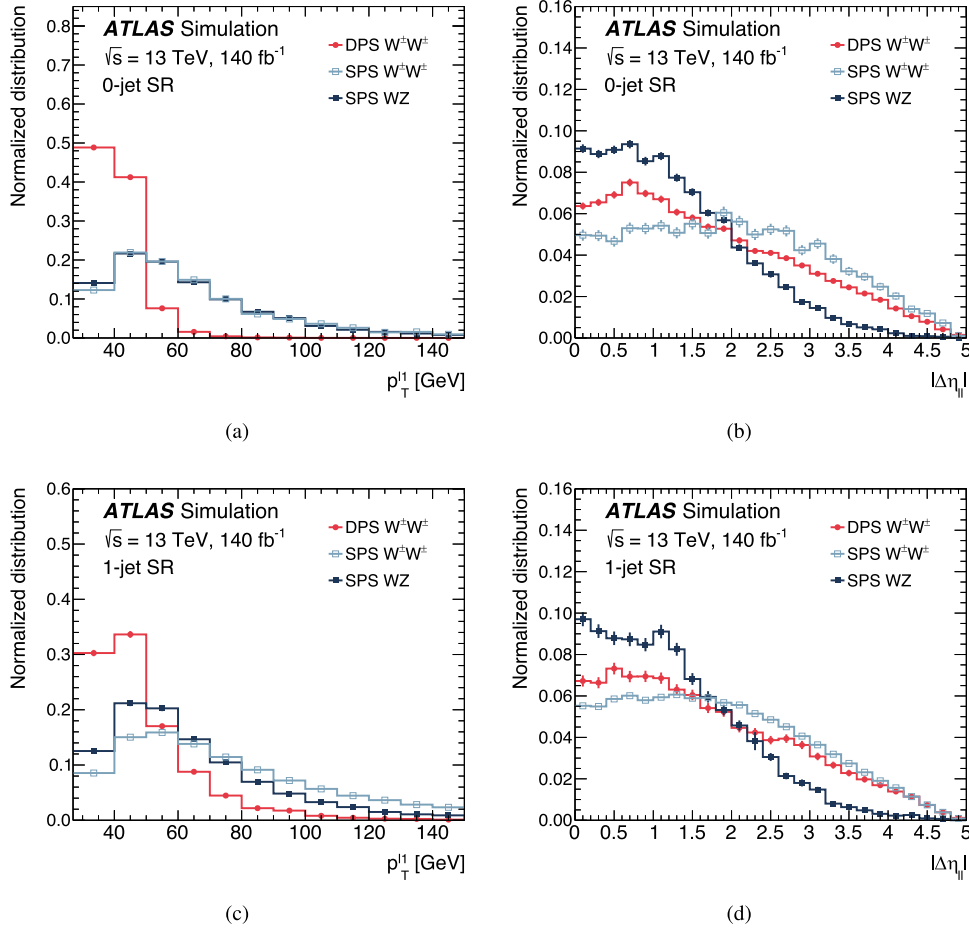


Fig. 2. Distributions of (a and c) p_T^1 and (b and d) $|\Delta\eta_{\ell\ell}|$ in the SR (a and b) 0-jet category and (c and d) 1-jet category for the DPS $W^\pm W^\pm$, SPS $W^\pm W^\pm$, and WZ processes. The error bars represent the statistical uncertainties due to the limited number of simulated events.

charge of the electron is misidentified. For the ee final state, both electrons are required to be in the barrel region with $|\eta| < 1.37$, to further reduce backgrounds with electron charge misidentification. In addition, if a third baseline lepton does not pass the overlap removal requirement, but the $m_{\ell\ell}$ of a same-flavor opposite-charge signal lepton and the third lepton is compatible with the Z boson mass, $|m_{\ell\ell} - m_Z| < 15$ GeV, the event is also rejected. Events with two or more selected jets are vetoed to suppress the contribution of the SPS $W^\pm W^\pm$ background.

The normalization of the WZ process is constrained in a dedicated signal-depleted CR defined closely following the SR selection but requiring three charged leptons in the final state, two of which have opposite charge in order to be compatible with a Z boson decay. The third lepton is required to satisfy $p_T > 15$ GeV. Events containing a fourth baseline electron or muon are removed to reject events from the ZZ background process. The trilepton invariant mass is required to be greater than 106 GeV.

5. Analysis strategy

The predicted DPS $W^\pm W^\pm$ contribution changes significantly depending on the number of exclusive jets in the SR. Therefore, the events in the SR are categorized according to the number of jets in the final state, in exclusive 0-jet and 1-jet categories, where the expected signal contribution in the 0-jet category is approximately 70% of the overall expected signal yield. The composition of the non-prompt and charge misidentification background processes is lepton- p_T and flavor dependent. The SR in each jet category is further split into four categories depending on the flavors of the leading- and subleading- p_T leptons: ee ,

$e\mu$, μe , $\mu\mu$, to explore the different signal-to-background ratios and to enable better constraint on the background uncertainties.

To extract the DPS $W^\pm W^\pm$ production, two independent deep neural networks (DNNs) are trained on MC simulated events in the 0-jet and 1-jet categories, aiming to separate the DPS signal from the dominant WZ background process. Dedicated optimizations of the model structures and hyperparameters are performed for each DNN with 3 hidden layers and up to 127 neurons in the first layer. The kinematic variables showing the best discrimination, evaluated by removing each variable and retraining the network, are retained. The variable importance is also evaluated with the SHAP framework [100]. Only lepton kinematic variables are considered to avoid potential biases in the modeling of jet-related variables, as the LO DPS $W^\pm W^\pm$ MC simulation models jets via parton showering. Eight such kinematic variables are retained from a larger set as summarized in Table 1. The $p_T^{\ell 1}$ and $|\Delta\eta_{\ell\ell}|$ variables provide the strongest discrimination for the signal DNNs. The simulated distributions of these variables in the SR 0-jet and 1-jet categories for the DPS $W^\pm W^\pm$, SPS $W^\pm W^\pm$, and WZ processes are shown in Fig. 2.

The non-prompt background contribution, where either a hadron or a lepton from a hadron decay satisfies the signal lepton selection criteria, is estimated using the data-driven fake-factor method [101]. Fake factors are determined as functions of electron or muon p_T and η in a dedicated region enriched in non-prompt leptons. This region is selected from collision data by requiring events in which jets recoil against a non-prompt lepton candidates [66]. A back-to-back topology between the jet and lepton is enforced by imposing a minimum azimuthal angle separation between the lepton and the jet, $\Delta\phi_{\ell j} > 2.8$. Contributions from prompt leptons produced in W , Z , or top-quark decays, as well as from

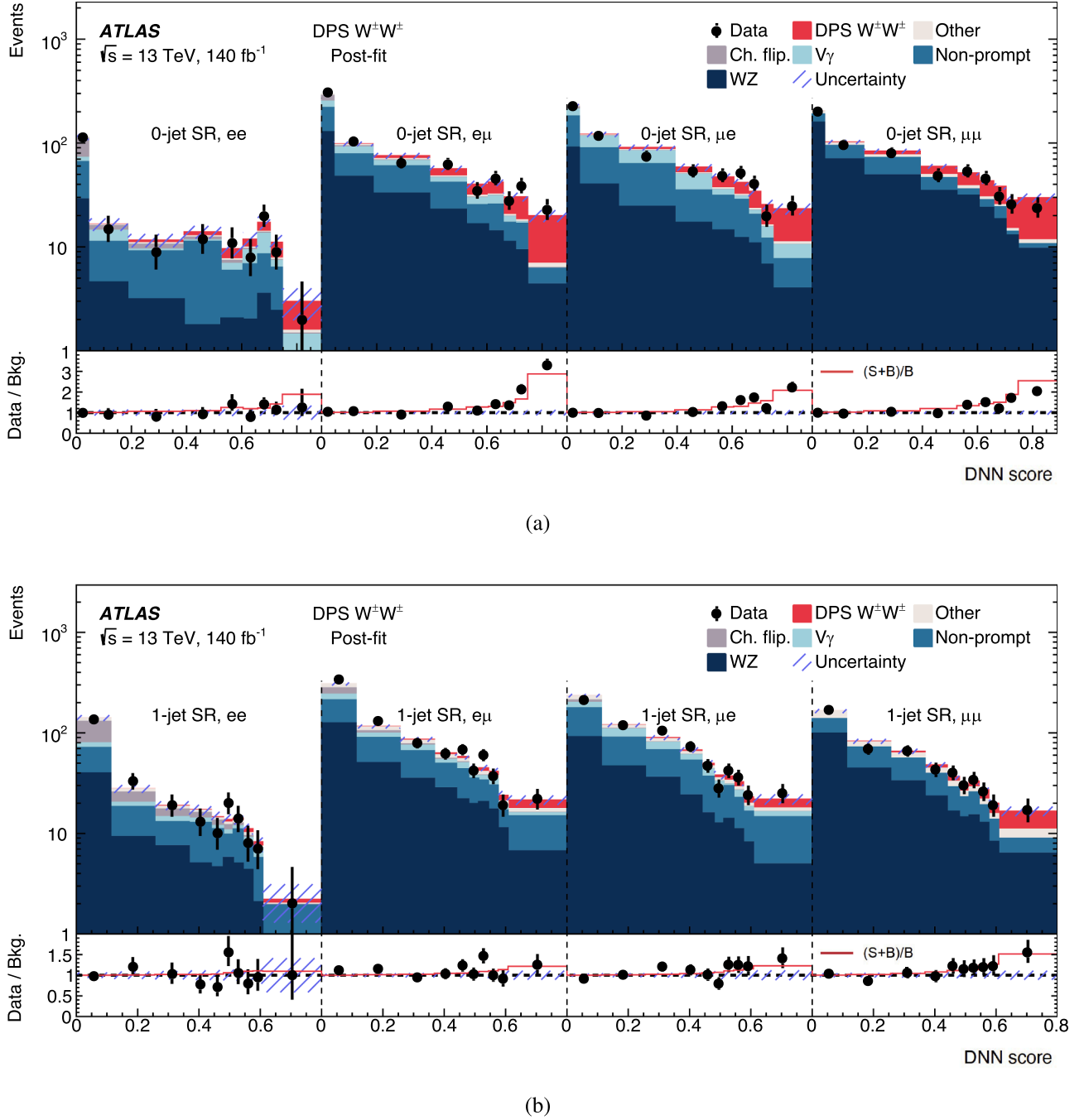


Fig. 3. Distributions of the DNN scores in the SR for each four dilepton final states in the (a) 0-jet and (b) 1-jet categories. The predicted yields are shown with their best-fit normalization and shape. The shaded area surrounding the expectation represents the total uncertainties in the predicted yields. The ratios of the observed yields to the total background predictions are shown by the points in the bottom panels. The solid line in the bottom panel represents the signal-to-background ratio $(1 + S/B)$. The shaded area in the bottom panels represents the relative uncertainties in the predicted yields. The “Other” category in the legend combines SPS $W^\pm W^\pm$, ZZ , VVV , top quark, and pileup background processes.

photon conversions in $\gamma + \text{jet}$ events, are subtracted in this region using MC simulation. The region is designed to closely match the composition of non-prompt lepton sources present in the SR, ensuring the validity of the fake factors when estimating the background contribution in the SR. The fake factors for electrons and muons are evaluated independently as the ratio of events where the non-prompt lepton passes the signal lepton selection to those where it passes the background lepton selection. The final estimate of the non-prompt background in the SR is obtained by re-scaling data from the same SR event selection but with background leptons by the corresponding fake factors [101].

Another significant background source arises from opposite-sign lepton pair events in which one of the two lepton charges has been misidentified. This effect is more prevalent for electrons due to bremsstrahlung radiation followed by electron-positron pair production. This background, referred to as *charge flip*, is estimated by re-weighting opposite-sign events in data with a factor representing the probability of charge misidentification in electrons [87]. The charge misidentification rate is determined as a function of electron p_T and η , using simulated $Z \rightarrow e^+e^-$ events that are corrected to match the misidentification rate in data through dedicated scale factors [66]. The uncertainty in this background

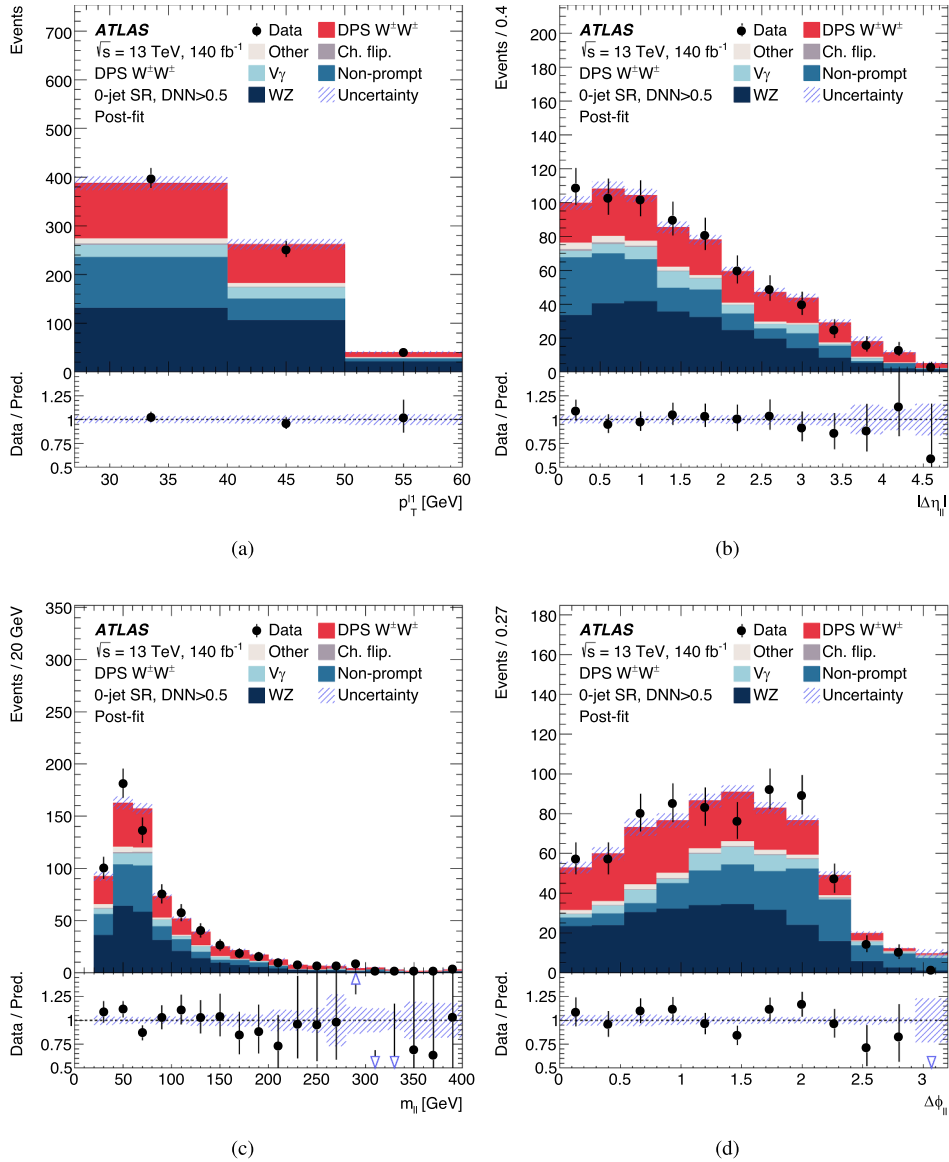


Fig. 4. Post-fit distributions of (a) p_T^1 , (b) $|\Delta\eta_{\ell\ell}|$, (c) $m_{\ell\ell}$, and (d) $\Delta\phi_{\ell\ell}$ in the 0-jet category in a region with the signal DNN score greater than 0.5. The distributions for the combined four dilepton final states are shown. The predicted yields are shown with their best-fit normalization and shape. The shaded area around the expectation represents the total uncertainty in the predicted yields. The ratios of the observed yields to the total predictions are shown by the points in the bottom panels. The “Other” category in the legend combines SPS $W^\pm W^\pm$, ZZ , VVV , top quark, and pileup background processes.

contribution is 40%, mainly driven by uncertainties in the scale factors used to calibrate the charge-selector tool, which are derived from $Z \rightarrow e^+e^-$ events [87].

The background from $\ell\gamma$ events, where the prompt photon γ is misidentified as an electron, is modeled using the $W\gamma$ simulated sample, and is further suppressed by the electron charge-selector tool. This background is assigned an overall normalization uncertainty of 40%, motivated by the scale factor uncertainties of the charge-selector tool, following the approach used in Ref. [102]. The small contributions of prompt lepton backgrounds from the SPS $W^\pm W^\pm$, ZZ , VVV , and top quark processes are modeled using MC samples.

The contribution to the signal yield from the production of two overlapping same-sign W bosons originating from separate pp interactions within the same bunch crossing, referred to as pileup background, is largely reduced by the requirements on $|z_0 \sin(\theta)|$. This background contribution is estimated using a toy study based on the average number of pp interactions per bunch crossing, the longitudinal size of the beam

spot, and the number of expected W^+ and W^- events in the fiducial region, following the method described in Ref. [103]. The resulting contribution in the SR is estimated to be approximately 4.5% of the total signal yield. A signal template normalized to this contribution is used to model this background, which constitutes less than 1% of the total background in the SR. Further reduction of this background by an application of a more restrictive requirement on $|z_0 \sin(\theta)|$ is not considered as the contribution is sufficiently small.

Systematic uncertainties in this measurement arise from experimental and theory sources. The results are driven by the statistical uncertainty of the data in the SR and none of the considered systematic uncertainties have a significant impact on the sensitivity of this result. Experimental systematic uncertainties are related to the trigger, lepton reconstruction, identification and isolation efficiencies [87,88], lepton energy (momentum) scale and resolution [87,88], jet energy scale and resolution [94], b -jet identification [96], modeling of E_T^{miss} [99], and integrated luminosity [50,51]. The uncertainty in the pileup reweighting

Table 1

Lepton kinematic variables used in the training and optimization of the DNNs.

Description	Variable
p_T of the leading lepton	p_T^1
p_T of the subleading lepton	p_T^2
Invariant mass of the dilepton system	$m_{\ell\ell}$
Pseudorapidity of the dilepton system	$\eta_{\ell\ell}$
Difference in azimuthal angle between the leading and subleading leptons	$\Delta\phi_{\ell\ell}$
Difference in pseudorapidity between the leading and subleading leptons	$ \Delta\eta_{\ell\ell} $
Distance ΔR between the leading and subleading leptons	$\Delta R_{\ell\ell}$
Difference in azimuthal angle between the missing transverse momentum and subleading lepton	$\Delta\phi_{\ell_2, E_T^{\text{miss}}}$

procedure is considered by varying the average number of pp collisions in simulated events to cover the uncertainty in the measured inelastic pp cross-section [104]. The uncertainties related to the non-prompt lepton background is studied in detail. Three sources of systematic uncertainty are considered including the statistical error on the fake factors, uncertainties in the composition of the fake factor CR obtained by varying the b -jet requirement in this region, and uncertainties related to the prompt lepton contribution in the fake-factor CR [66]. Uncertainties in the data-driven charge flip background are described in Ref. [87]. The theory uncertainties in the physics modeling of the background processes are estimated by varying the factorization and renormalization scales, the strong coupling constant α_S , and the choice of the PDF [105]. The theory uncertainties in the modeling of the DPS $W^\pm W^\pm$ signal include scale

variations and an uncertainty related to the difference in the shapes of the signal distributions predicted by the PYTHIA and Herwig samples. The systematic uncertainties with the largest impact on the result are related to the jet and E_T^{miss} scale and resolution and the non-prompt lepton background estimation.

6. Results

A binned maximum-likelihood fit is performed for the DPS $W^\pm W^\pm$ process using the DNN score distributions in the 0-jet and 1-jet categories. The DNN score boundaries are chosen independently in the two exclusive jet categories to maximize the expected significance of the DPS $W^\pm W^\pm$ process. The total number of events in the WZ CR and the four dilepton final states in the SR are fitted simultaneously in the two exclusive jet categories with the DPS $W^\pm W^\pm$ normalization and the two normalizations of the WZ production (in association with 0-jet and 1-jet) kept as floating parameters. The WZ production cross section is scaled based on jet multiplicity at particle level. This procedure accounts for possible different effects in the SR and WZ CR of the bin-to-bin migration between the reconstructed and particle level distributions. Contributions of DPS $W^\pm W^\pm$ events with τ -leptons from at least one of the W boson decays, with the τ -lepton decaying leptonically to an electron or a muon, are scaled with the DPS $W^\pm W^\pm$ normalization assuming lepton universality in W decays and correspond to approximately 5% of the total signal yield in the SR. The systematic uncertainties are included as nuisance parameters [106] with Gaussian priors. The nuisance parameters are adjusted in the fit with the shape and normalization of each distribution varying within the specified constraints.

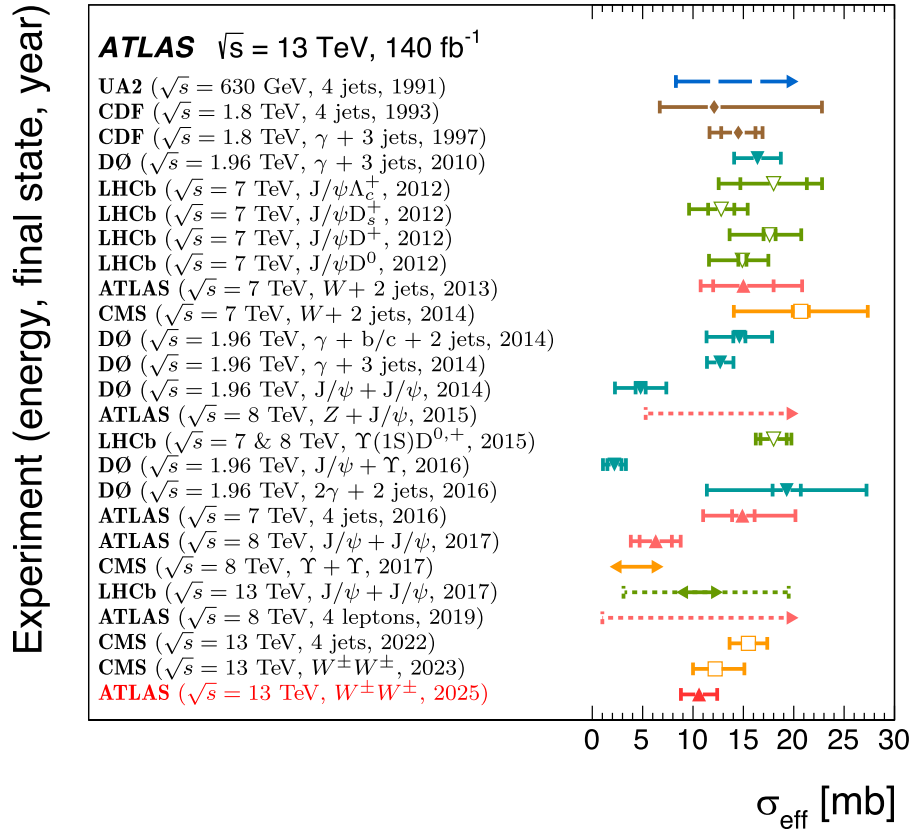


Fig. 5. Summary of measurements and limits on σ_{eff} , determined in different experiments [16–40], sorted chronologically. The measurements that were made by different experiments are denoted by different symbols and colors. The inner error bars represent statistical uncertainties and the outer error bars correspond to the total uncertainty. Dashed arrows indicate lower limits. Lines with arrows on both ends represent ranges of the σ_{eff} values, determined within a single publication. In the case of the double J/ψ measurement by LHCb [40], the dashed line denotes the upper and lower uncertainties. The AFS measurement of $\sigma_{\text{eff}} = 5$ mb at $\sqrt{s} = 63$ GeV [25] was published without uncertainties and is not included in the plot.

Table 2

Post-fit expected signal and background yields and observed data events in the SR 0–jet category. The yields are shown for the four dilepton final states. The total uncertainties in the predicted yields are shown. The uncertainties in the “Combined” result take into account correlations of systematic uncertainties across the final states. The “Other” category in the legend combines SPS $W^\pm W^\pm$, ZZ , VVV , top quark, and pileup background processes.

Process	ee	$e\mu$	μe	$\mu\mu$	Combined
DPS $W^\pm W^\pm$	13.7 ± 2.0	68 ± 9	66 ± 9	90 ± 12	237 ± 32
WZ	48.9 ± 2.9	288 ± 12	221 ± 9	409 ± 13	968 ± 31
Non-prompt	78 ± 10	204 ± 15	248 ± 18	108 ± 14	640 ± 50
Charge flip	43 ± 10	39 ± 6	13.0 ± 1.9	—	95 ± 17
$V\gamma$	20 ± 5	70 ± 15	107 ± 23	—	200 ± 40
Other	5.6 ± 0.8	18.7 ± 2.5	14.8 ± 1.8	31 ± 5	71 ± 9
Total	209 ± 10	688 ± 17	670 ± 19	639 ± 17	2210 ± 40
Data	201	716	665	612	2194

Table 3

Post-fit expected signal and background yields and observed data events in the SR 1–jet category. The yields are shown for the four dilepton final states. The total uncertainties in the predicted yields are shown. The uncertainties in the “Combined” result take into account correlations of systematic uncertainties across the final states. The “Other” category combines SPS $W^\pm W^\pm$, ZZ , VVV , top quark, and pileup background processes.

Process	ee	$e\mu$	μe	$\mu\mu$	Combined
DPS $W^\pm W^\pm$	4.8 ± 0.8	26 ± 4	25 ± 4	35 ± 5	91 ± 14
WZ	84 ± 4	337 ± 12	265 ± 10	275 ± 11	959 ± 33
Non-prompt	79 ± 10	257 ± 19	271 ± 19	152 ± 19	760 ± 60
Charge flip	65 ± 15	49 ± 7	14.5 ± 2.1	—	128 ± 24
$V\gamma$	18 ± 4	73 ± 17	84 ± 18	—	170 ± 40
Other	17.8 ± 1.4	63 ± 5	54 ± 4	64 ± 4	199 ± 14
Total	269 ± 13	806 ± 18	714 ± 18	525 ± 17	2310 ± 40
Data	262	860	711	513	2346

The particle level jets used for the jet multiplicity normalization of the WZ process are reconstructed from stable particles with a lifetime of $\tau > 30$ ps in the simulation after parton showering, hadronization, and decay of particles with $\tau < 30$ ps. The anti- k_r algorithm with a radius parameter of $R = 0.4$ is used where muons, electrons, neutrinos, and photons associated with the W and Z boson decays excluded. The particle level jets with $|\eta| < 4.5$ and $p_T > 30$ GeV are considered. The small contribution of the WZ production in association with two or more jets is normalized to the SM prediction and allowed to vary within the uncertainty. The simulated WZ SHERPA samples are used to account for bin-to-bin migration effects between the reconstructed and particle level distributions.

The signal DNN score distributions in each category are shown in Fig. 3 with the normalizations and nuisance parameters adjusted by the fit. A good separation between signal and background is achieved. The post-fit yields in the 0–jet and 1–jet categories are shown in Tables 2 and 3, respectively. The normalization factors for the WZ production in association with 0–jet and 1–jet are 0.96 ± 0.05 and 0.94 ± 0.05 , respectively, consistent with the values reported in Ref. [102]. No uncertainties are significantly constrained or pulled in the simultaneous fit. The post-fit distributions of the $m_{\ell\ell}$, $|\Delta\eta_{\ell\ell}|$, $\Delta\phi_{\ell\ell}$, and $p_T^{\ell 1}$ in the 0–jet SR category in a region with the signal DNN score greater than 0.5 are shown in Fig. 4.

The visible excess in the DNN score distributions is quantified by calculating the corresponding p -value using a profile likelihood-ratio test statistic in the asymptotic approximation [107]. The background-only hypothesis is rejected with an observed significance of 8.8 standard deviations. The fiducial cross section times branching fraction for the DPS $W^\pm W^\pm$ process ($\sigma_B(W^\pm W^\pm)$) is extracted in the fiducial region defined to be as close as possible to the data event selection requirements. The fiducial phase space definition requires two prompt

Table 4

The fractional uncertainty of different components in the DPS $\sigma_B(W^\pm W^\pm)$ measurement. The contribution of a systematic uncertainty (uncertainty group) to the total uncertainty is evaluated by fixing the respective nuisance parameter(s) to its (their) best-fit value(s), redoing the fit, and subtracting the uncertainties in the cross section in quadrature. The procedure is implemented incrementally such that the sum in quadrature of the grouped systematic and statistical uncertainties corresponds to the total cross section uncertainty by construction. Lepton uncertainties encompass the effects of the calibration of lepton energy or momentum scale and resolution, as well as the lepton trigger, reconstruction, identification, and isolation efficiencies. The “DPS $W^\pm W^\pm$ model” uncertainty is related to the differences in the shapes of the signal distributions predicted by the PYTHIA and Herwig samples. The “Model statistical” is related to the effect of a finite number of data events used for data-driven background estimates and of MC events.

Source	Uncertainty [%]
Experimental	4.7
Electrons	0.4
Muons	0.8
Jets	3.1
E_T^{miss}	1.5
Flavor tagging	0.3
Non-prompt leptons	2.6
Charge flip	0.6
Pileup reweighting	1.3
Luminosity	0.8
Modeling	1.5
DPS $W^\pm W^\pm$ scale	0.2
DPS $W^\pm W^\pm$ model	0.3
SPS $W^\pm W^\pm$ scale, PDF & α_S	0.2
WZ scale, PDF & α_S	0.8
WZ normalization	0.1
Other background normalizations	1.1
Model statistical	0.6
Experimental and modeling	5.0
Data statistical	13
Total	14

leptons at particle level (e or μ) with $p_T > 27$ GeV and $|\eta| < 2.5$, dressed by adding the four-momenta of nearby prompt photons within a small cone of $\Delta R < 0.1$, with $m_{\ell\ell} > 20$ GeV. Contributions of events with τ -leptons from at least one of the W boson decays are not included in the fiducial region definition. The number of particle level jets, as defined above, is required to be less than 2. The electrons in the dielectron final state are required to have $|\eta|$ less than 1.37. Events with the dielectron invariant mass in the range $|m_{ee} - m_Z| < 15$ GeV are rejected. The particle-level E_T^{miss} is reconstructed from the visible final-state objects and must be greater than 30 GeV. The fraction of signal events generated outside the fiducial region but satisfying the SR selection at detector level is approximately 14%. The measured DPS $\sigma_B(W^\pm W^\pm)$ is 4.59 ± 0.64 fb. This value cannot be directly compared to the corresponding DPS $\sigma_B(W^\pm W^\pm)$ CMS measurement [47] as the definitions of the fiducial regions differ. A summary of the fractional uncertainties in the DPS $\sigma_B(W^\pm W^\pm)$ measurement is shown in Table 4. The results are driven by the statistical uncertainty of the data. Excluding the $|\eta| < 1.37$ requirement for the dielectron final state in the fiducial region definition yields a DPS $\sigma_B(W^\pm W^\pm)$ of 5.52 ± 0.77 fb. The DPS $\sigma_B(W^\pm W^\pm)$ in this fiducial region is approximately 20% larger than in the nominal fiducial region, as the charged leptons tend to have large $|\eta|$ values.

The DPS $\sigma_B(W^\pm W^\pm)$ measurement is used to extract the value of σ_{eff} using Eq. (1). A common fiducial region for the cross sections of the W^+ , W^- , and DPS $W^\pm W^\pm$ processes needs to be defined for the correct determination of σ_{eff} . Therefore, the measured $\sigma_B(W^\pm W^\pm)$

value is extrapolated to a region having the same requirements as the analysis fiducial region but removing the particle-level requirements on $m_{\ell\ell}$ and E_T^{miss} , and the requirements on electron $|\eta| < 1.37$ and $|m_{ee} - m_Z| < 15$ GeV in the dielectron final state. The extrapolation is performed using the PYTHIA signal samples. The extrapolation factor obtained with PYTHIA is 1.75 ± 0.04 , where the uncertainty includes the QCD scale variations. The extrapolation factor obtained with the Herwig sample is in excellent agreement with this value. The cross sections of the W^+ and W^- processes in this common fiducial region are calculated using the SHERPA [2.2.11] event generator at NLO in QCD. The predicted cross sections times the per-flavor leptonic branching fractions are $\sigma_{W^+} = 5.23 \pm 0.34$ nb and $\sigma_{W^-} = 4.00 \pm 0.22$ nb where the uncertainties include the QCD scale variations and are propagated in the determination of σ_{eff} . The contributions of events with two SPS $W + 1$ -jet processes are not included in the numerator of Eq. (1) as the number of particle level jets is required to be less than 2 for the DPS $\sigma_B(W^\pm W^\pm)$. The resulting value of σ_{eff} is 10.6 ± 1.8 mb consistent with the corresponding CMS measurement of $12.2^{+2.9}_{-2.2}$ mb [47] and with previous determinations at hadron colliders as shown in Fig. 5.

7. Conclusion

This letter reports the measurement of double parton scattering in same-sign W boson pair production with the ATLAS detector. The dataset used corresponds to an integrated luminosity of 140 fb^{-1} of proton–proton collisions at a center-of-mass energy of 13 TeV, collected during Run 2 of the Large Hadron Collider. The study is performed in final states including two same-charge leptons, electron or muon, missing transverse momentum, and up to one jet. An excess of events over the expected background contributions is reported with a significance of 8.8 standard deviations. The measured fiducial cross section times leptonic branching fraction is 4.59 ± 0.64 fb. The measurement corresponds to a double parton scattering effective cross section of 10.6 ± 1.8 mb.

Data availability

The public release of data supporting the findings of this article will follow the CERN Open Data Policy [109]. Inquiries about plots and tables associated with this article can be addressed to atlas.publications@cern.ch.

Declaration of competing interest

The authors declare that they have no known competing financial interests or personal relationships that could have appeared to influence the work reported in this paper.

Acknowledgements

We thank CERN for the very successful operation of the LHC and its injectors, as well as the support staff at CERN and at our institutions worldwide without whom ATLAS could not be operated efficiently.

The crucial computing support from all WLCG partners is acknowledged gratefully, in particular from CERN, the ATLAS Tier-1 facilities at TRIUMF/SFU (Canada), NDFG (Denmark, Norway, Sweden), CC-IN2P3 (France), KIT/GridKA (Germany), INFN-CNAF (Italy), NL-T1 (Netherlands), PIC (Spain), RAL (UK) and BNL (USA), the Tier-2 facilities worldwide and large non-WLCG resource providers. Major contributors of computing resources are listed in Ref. [108].

We gratefully acknowledge the support of ANPCyT, Argentina; YerPhI, Armenia; ARC, Australia; BMWFW and FWF, Austria; ANAS, Azerbaijan; CNPq and FAPESP, Brazil; NSERC, NRC and CFI, Canada; CERN; ANID, Chile; CAS, MOST and NSFC, China; Minciencias, Colombia; MEYS CR, Czech Republic; DNRF and DNSRC, Denmark; IN2P3-CNRS and CEA-DRF/IRFU, France; SRNSFG, Georgia; BMFTR, HGF and MPG,

Germany; GSRI, Greece; RGC and Hong Kong SAR, China; ICHEP and Academy of Sciences and Humanities, Israel; INFN, Italy; MEXT and JSPS, Japan; CNRST, Morocco; NWO, Netherlands; RCN, Norway; MNiSW, Poland; FCT, Portugal; MNE/IFA, Romania; MSTDI, Serbia; MSSR, Slovakia; ARIS and MVZI, Slovenia; DSI/NRF, South Africa; MICIU/AEI, Spain; SRC and Wallenberg Foundation, Sweden; SERI, SNSF and Cantons of Bern and Geneva, Switzerland; NSTC, Taipei; TENMAK, Türkiye; STFC/UKRI, United Kingdom; DOE and NSF, United States of America.

Individual groups and members have received support from BCKDF, CANARIE, CRC and DRAC, Canada; CERN-CZ, FORTE and PRIMUS, Czech Republic; COST, ERC, ERDF, Horizon 2020, ICSC-NextGenerationEU and Marie Skłodowska-Curie Actions, European Union; Investissements d’Avenir Labex, Investissements d’Avenir Idex and ANR, France; DFG and AvH Foundation, Germany; Herakleitos, Thales and Aristeia programmes co-financed by EU-ESF and the Greek NSRF, Greece; BSF-NSF and MINERVA, Israel; NCN and NAWA, Poland; La Caixa Banking Foundation, CERCA Programme Generalitat de Catalunya and PROMETEO and GenT Programmes Generalitat Valenciana, Spain; Göran Gustafssons Stiftelse, Sweden; The Royal Society and Leverhulme Trust, United Kingdom.

In addition, individual members wish to acknowledge support from CERN: European Organization for Nuclear Research (CERN DOCT); Chile: [Agencia Nacional de Investigación y Desarrollo](#) (FONDECYT 1230812, FONDECYT 1240864, Fondecyt 3240661); China: Chinese Ministry of Science and Technology (MOST-2023YFA1605700, MOST-2023YFA1609300), [National Natural Science Foundation of China](#) (NSFC - 12175119, NSFC 12275265); Czech Republic: Czech Science Foundation (GACR - 24-11373S), Ministry of Education Youth and Sports (ERC-CZ-LL2327, FORTE CZ.02.01.01/00/22_008/0004632), PRIMUS Research Programme (PRIMUS/21/SCI/017); EU: H2020 [European Research Council](#) (ERC - 101002463); European Union: European Research Council (BARD No. 101116429, ERC - 948254, ERC 101089007), European Regional Development Fund (SMASH CO-FUND 101081355, SLO ERDF), Horizon 2020 Framework Programme (MUCCA - CHIST-ERA-19-XAI-00), European Union, Future Artificial Intelligence Research (FAIR-NextGenerationEU PE00000013), Italian Center for High Performance Computing, Big Data and Quantum Computing (ICSC, NextGenerationEU); France: Agence Nationale de la Recherche (ANR-21-CE31-0022, ANR-22-EDIR-0002); Germany: Baden-Württemberg Stiftung (BW Stiftung-Postdoc Eliteprogramme), Deutsche Forschungsgemeinschaft (DFG - 469666862, DFG - CR 312/5-2); China: Research Grants Council (GRF); Italy: Istituto Nazionale di Fisica Nucleare (ICSC, NextGenerationEU), Ministero dell’Università e della Ricerca (NextGenEU 153D23001490006 M4C2.1.1, NextGenEU 153D23000820006 M4C2.1.1, NextGenEU 153D23001490006 M4C2.1.1, SOE2024_0000023); Japan: [Japan Society for the Promotion of Science](#) (JSPS KAKENHI JP22H01227, JSPS KAKENHI JP22H04944, JSPS KAKENHI JP22KK0227, JSPS KAKENHI JP24K23939, JSPS KAKENHI JP25H00650, JSPS KAKENHI JP25H01291, JSPS KAKENHI JP25K01023); Norway: Research Council of Norway (RCN-314472); Poland: Ministry of Science and Higher Education (IDUB AGH, POB8, D4 no 9722), Polish National Science Centre (NCN 2021/42/E/ST2/00350, NCN OPUS 2023/51/B/ST2/02507, NCN OPUS nr 2022/47/B/ST2/03059, NCN UMO-2019/34/E/ST2/00393, UMO-2022/47/O/ST2/00148, UMO-2023/49/B/ST2/04085, UMO-2023/51/B/ST2/00920, UMO-2024/53/N/ST2/00869); Portugal: Foundation for Science and Technology (FCT); Spain: Ministry of Science and Innovation (MCIN & NextGenEU PCI2022-135018-2, MICIN & FEDER PID2021-125273NB, RYC2019-028510-I, RYC2020-030254-I, RYC2021-031273-I, RYC2022-038164-I); Sweden: Carl Trygger Foundation (Carl Trygger Foundation CTS 22:2312), Swedish Research Council (Swedish Research Council 2023-04654, VR 2021-03651, VR 2022-03845, VR 2022-04683, VR 2023-03403, VR 2024-05451), Knut and Alice Wallenberg Foundation (KAW 2018.0458, KAW 2022.0358, KAW 2023.0366); Switzerland:

Swiss National Science Foundation (SNSF - PCEFP2_194658); United Kingdom: Leverhulme Trust (Leverhulme Trust RPG-2020-004), Royal Society (NIF-R1-231091); United States of America: U.S. Department of Energy (ECA DE-AC02-76SF00515), Neubauer Family Foundation.

Appendix

The ATLAS Collaboration

G. Aad¹⁰⁴, E. Aakvaag¹⁷, B. Abbott¹²³, S. Abdelhameed^{119a}, K. Abeling⁵³, N.J. Abicht⁴⁹, S.H. Abidi³⁰, M. Aboelela⁴⁵, A. Aboulhorma^{36e}, H. Abramowicz¹⁵⁷, Y. Abulaiti¹²⁰, B.S. Acharya^{69a,69b,m}, A. Ackermann^{63a}, C. Adam Bourdarios⁴, L. Adamczyk^{87a}, S.V. Addepalli¹⁴⁹, M.J. Addison¹⁰³, J. Adelman¹¹⁸, A. Adiguzel^{22c}, T. Adye¹³⁷, A.A. Affolder¹³⁹, Y. Afik⁴⁰, M.N. Agaras¹³, A. Aggarwal¹⁰², C. Agheorghiesei^{28c}, F. Ahmadov^{39,ad}, S. Ahuja⁹⁷, X. Ai^{143b}, G. Aielli^{76a,76b}, A. Aikot¹⁶⁹, M. Ait Tamlilhat^{36e}, B. Aitbenchikh^{36a}, M. Akbiyik¹⁰², T.P.A. Åkesson¹⁰⁰, A.V. Akimov¹⁵¹, D. Akiyama¹⁷⁴, N.N. Akolkar²⁵, S. Aktas^{22a}, G.L. Alberghi^{24b}, J. Albert¹⁷¹, U. Alberti²⁰, P. Albicocco⁵³, G.L. Albouy⁶⁰, S. Alderweireldt⁵², Z.L. Alegria¹²⁴, M. Aleksa³⁷, I.N. Aleksandrov³⁹, C. Alexa^{28b}, T. Alexopoulos¹⁰, F. Alfonsi^{24b}, M. Algren⁵⁶, M. Alhroob¹⁷³, B. Ali¹³⁵, H.M.J. Ali^{93,u}, S. Ali³², S.W. Alibocus⁹⁴, M. Aliev^{34c}, G. Alimonti^{71a}, W. Alkhalaf⁵⁵, C. Allaire⁶⁶, B.M.M. Allbrooke¹⁵², J.S. Allen¹⁰³, J.F. Allen⁵², P.P. Allport²¹, A. Aloisio^{72a,72b}, F. Alonso⁹², C. Alpigiani¹⁴², Z.M.K. Alsolami⁹³, A. Alvarez Fernandez¹⁰², M. Alves Cardoso⁵⁶, M.G. Alviggi^{72a,72b}, M. Aly¹⁰³, Y. Amaral Coutinho^{83b}, A. Ambler¹⁰⁶, C. Amelung³⁷, M. Ameri¹⁰³, C.G. Ames¹¹¹, T. Amezza¹³⁰, D. Amidei¹⁰⁸, B. Amini⁵⁴, K. Amirie¹⁶¹, A. Amirkhanov³⁹, S.P. Amor Dos Santos^{133a}, K.R. Amos¹⁶⁹, D. Amperiadou¹⁵⁸, S. An⁸⁴, C. Anastopoulos¹⁴⁵, T. Andeen¹¹, J.K. Anders⁹⁴, A.C. Anderson⁵⁹, A. Andreazza^{71a,71b}, S. Angelidakis⁹, A. Angerami⁴², A.V. Anisenkov³⁹, A. Annovi^{74a}, C. Antel³⁷, E. Antipov¹⁵¹, M. Antonelli⁵³, F. Anulli^{75a}, M. Aoki⁸⁴, T. Aoki¹⁵⁹, M.A. Aparo¹⁵², L. Aperio Bella⁴⁸, M. Apicella³¹, C. Appelt¹⁵⁷, A. Apyan²⁷, M. Arampatzis¹⁰, S.J. Arbiol Val⁸⁸, C. Arcangeletti⁵³, A.T.H. Arce⁵¹, J.-F. Arguin¹¹⁰, S. Argyropoulos¹⁵⁸, J.-H. Arling⁴⁸, O. Arnaez⁴, H. Arnold¹⁵¹, G. Artoni^{75a,75b}, H. Asada¹¹³, K. Asai¹²¹, S. Asatryan¹⁷⁹, N.A. Asbah³⁷, R.A. Ashby Pickering¹⁷³, A.M. Aslam⁹⁷, K. Assamagan³⁰, R. Astalos^{29a}, K.S.V. Astrand¹⁰⁰, S. Atashi¹⁶⁵, R.J. Atkin^{34a}, H. Atmani^{36f}, P.A. Atlasdihda¹³¹, K. Augsten¹³⁵, A.D. Aurio⁴¹, V.A. Austrup¹⁰³, G. Avolio³⁷, K. Axiotis⁵⁶, A. Azzam¹³, D. Babal^{29b}, H. Bachacou¹³⁸, K. Bachas^{158,q}, A. Bachi³⁵, E. Bachmann⁵⁰, M.J. Backes^{63a}, A. Badae⁴⁰, T.M. Baer¹⁰⁸, P. Bagnaia^{75a,75b}, M. Bahmani¹⁹, D. Bahner⁵⁴, K. Bai¹²⁶, J.T. Baines¹³⁷, L. Baines⁹⁶, O.K. Baker¹⁷⁸, E. Bakos¹⁶, D. Bakshi Gupta⁸, L.E. Balabram Filho^{83b}, V. Balakrishnan¹²³, R. Balasubramanian⁴, E.M. Baldwin³⁸, P. Bales^{87a}, E. Ballabene^{24b,24a}, F. Balli¹³⁸, L.M. Baltes^{63a}, W.K. Balunas³³, J. Balz¹⁰², I. Bamwidhi^{119b}, E. Banas⁸⁸, M. Bandieramonte¹³², A. Bandyopadhyay²⁵, S. Bansal²⁵, L. Barak¹⁵⁷, M. Barakat⁴⁸, E.L. Barberio¹⁰⁷, D. Barberis^{18b}, M. Barbero¹⁰⁴, M.Z. Barel¹¹⁷, T. Barillari¹¹², M.-S. Barisits³⁷, T. Barklow¹⁴⁹, P. Baron¹³⁶, D.A. Baron Moreno¹⁰³, A. Baroncelli⁶², A.J. Barr¹²⁹, J.D. Barr⁹⁸, F. Barreiro¹⁰¹, J. Barreiro Guimarães da Costa¹⁴, M.G. Barros Teixeira^{133a}, S. Barsov³⁸, F. Bartels^{63a}, R. Bartoldus¹⁴⁹, A.E. Barton⁹³, P. Bartos^{29a}, A. Basan¹⁰², M. Baselga⁴⁹, S. Bashiri⁸⁸, A. Bassalat^{66,b}, M.J. Basso^{162a}, S. Bataju⁴⁵, R. Bate¹⁷⁰, R.L. Bates⁵⁹, S. Batlamous¹⁰¹, M. Battaglia¹³⁹, D. Battulga¹⁹, M. Bauge^{75a,75b}, M. Bauer⁷⁹, P. Bauer²⁵, L.T. Bayer⁴⁸, L.T. Bazzano Hurrell³¹, J.B. Beacham¹¹², T. Beau¹³⁰, J.Y. Beauchamp⁹², P.H. Beauchemin¹⁶⁴, P. Bechtel²⁵, H.P. Beck^{20,p}, K. Becker¹⁷³, A.J. Beddall⁸², V.A. Bednyakov³⁹, C.P. Bee¹⁵¹, L.J. Beemster¹⁶, M. Begalli^{83d}, M. Begel³⁰, J.K. Behr⁴⁸, J.F. Beirer³⁷, E. Beisiegel²⁵, M. Belfkir^{119b}, G. Bella¹⁵⁷, L. Bellagamba^{24b}, A. Bellerive³⁵, C.D.

Bellgraph⁶⁸, P. Bellos²¹, K. Beloborodov³⁸, D. Benčekroun^{36a}, F. Bendebba^{36a}, Y. Benhammou¹⁵⁷, K.C. Benkendorfer⁶¹, L. Beresford⁴⁸, M. Beretta⁵³, E. Bergeas Kuutmann¹⁶⁷, N. Berger⁴, B. Bergmann¹³⁵, J. Beringer^{18a}, G. Bernardi⁵, C. Bernius¹⁴⁹, F.U. Bernlochner²⁵, F. Bernon³⁷, A. Berrocal Guardia¹³, T. Berry⁹⁷, P. Berta¹³⁶, A. Berthold⁵⁰, A. Berti^{133a}, R. Bertrand¹⁰⁴, S. Bethke¹¹², A. Betti^{75a,75b}, A.J. Bevan⁹⁶, L. Bezio⁵⁶, N.K. Bhalla⁵⁴, S. Bharthuar¹¹², S. Bhatta¹⁵¹, P. Bhattarai¹⁴⁹, Z.M. Bhatti¹²⁰, K.D. Bhide⁵⁴, V.S. Bhopatkar¹²⁴, R.M. Bianchi¹³², G. Bianco^{24b,24a}, O. Biebel¹¹¹, M. Biglietti^{77a}, C.S. Billingsley⁴⁵, Y. Bimgdi^{36f}, M. Bindi⁵⁵, A. Bingham¹⁷⁷, A. Bingul^{22b}, C. Bini^{75a,75b}, G.A. Bird³³, M. Birman¹⁷⁵, M. Biros¹³⁶, S. Biryukov¹⁵², T. Bisanz⁴⁹, E. Bisceglie^{24b,24a}, J.P. Biswal¹³⁷, D. Biswas¹⁴⁷, I. Bloch⁴⁸, A. Blue⁵⁹, U. Blumenschein⁹⁶, J. Blumenthal¹⁰², V.S. Bobrovnikov³⁹, L. Boccardo^{57b,57a}, M. Boehler⁵⁴, B. Boehm¹⁷², D. Bogavac¹³, A.G. Bogdanchikov³⁸, L.S. Boggia¹³⁰, V. Boisvert⁹⁷, P. Bokan³⁷, T. Bold^{87a}, M. Bomben⁵, M. Bona⁹⁶, M. Boonekamp¹³⁸, A.G. Borbély⁵⁹, I.S. Bordulev³⁸, G. Borissov⁹³, D. Bortoletto¹²⁹, D. Boscherini^{24b}, M. Bosman¹³, K. Bouaouda^{36a}, N. Bouchhar¹⁶⁹, L. Boudet⁴, J. Boudreau¹³², E.V. Bouhova-Thacker⁹³, D. Boumediene⁴¹, R. Bouquet^{57b,57a}, A. Boveia¹²², J. Boyd³⁷, D. Boye³⁰, I.R. Boyko³⁹, L. Bozianu⁵⁶, J. Bracinik²¹, N. Brahimi⁴, G. Brandt¹⁷⁷, O. Brandt³³, B. Brau¹⁰⁵, J.E. Brau¹²⁶, R. Brenner¹⁷⁵, L. Brenner¹¹⁷, R. Brenner¹⁶⁷, S. Bressler¹⁷⁵, G. Brianti^{78a,78b}, D. Britton⁵⁹, D. Britzger¹¹², I. Brock²⁵, R. Brock¹⁰⁹, G. Brooijmans⁴², A.J. Brooks⁶⁸, E.M. Brooks^{162b}, E. Brost³⁰, L.M. Brown^{171,162a}, L.E. Bruce⁶¹, T.L. Bruckler¹²⁹, P.A. Bruckman de Renstrom⁸⁸, B. Brüers⁴⁸, A. Bruni^{24b}, G. Bruni^{24b}, D. Brunner^{47a,47b}, M. Bruschi^{24b}, N. Bruscinò^{75a,75b}, T. Buanes¹⁷, Q. Buat¹⁴², D. Buchin¹¹², A.G. Buckley⁵⁹, O. Bulekov⁸², B.A. Bullard¹⁴⁹, S. Burdin⁹⁴, C.D. Burgard⁴⁹, A.M. Burger⁹¹, B. Burghgrave⁸, O. Burlayenko⁵⁴, J. Burleson¹⁶⁸, J.C. Burzynski¹⁴⁸, E.L. Busch⁴², V. Büscher¹⁰², P.J. Bussey⁵⁹, J.M. Butler²⁶, C.M. Buttar⁵⁹, J.M. Butterworth⁹⁸, W. Buttinger¹³⁷, C.J. Buxo Vazquez¹⁰⁹, A.R. Buzykaev³⁹, S. Cabrera Urbán¹⁶⁹, L. Cadamuro⁶⁶, H. Cai¹³², Y. Cai^{24b,114c,24a}, Y. Cai^{114a}, V.M.M. Cairo³⁷, O. Cakir^{3a}, N. Calace³⁷, P. Calafiura^{18a}, G. Calderini¹³⁰, P. Calfayan³⁵, L. Calic¹⁰⁰, G. Callea⁵⁹, L.P. Caloba^{83b}, D. Calvet⁴¹, S. Calvet⁴¹, R. Camacho Toro¹³⁰, S. Camarda³⁷, D. Camarero Munoz²⁷, P. Camarri^{76a,76b}, C. Camincher¹⁷¹, M. Campanelli⁹⁸, A. Camplani⁴³, V. Canale^{72a,72b}, A.C. Cancay^{3a}, E. Canonero⁹⁷, J. Cantero¹⁶⁹, Y. Cao¹⁶⁸, F. Capocasa²⁷, M. Capua^{44b,44a}, A. Carbone^{71a,71b}, R. Cardarelli^{76a}, J.C.J. Cardenas⁸, M.P. Cardiff²⁷, G. Carducci^{44b,44a}, T. Carli³⁷, G. Carlino^{72a}, J.I. Carlotto¹³, B.T. Carlson^{132,1}, E.M. Carlson¹⁷¹, J. Carmignani⁹⁴, L. Carminati^{71a,71b}, A. Carnelli⁴, M. Carnesale³⁷, S. Caron¹¹⁶, E. Carquin^{140g}, I.B. Carr¹⁰⁷, S. Carrá^{73a,73b}, G. Carratta^{24b,24a}, C. Carrion Martinez¹⁶⁹, A.M. Carroll¹²⁶, M.P. Casado¹³, P. Casolaro^{72a,72b}, M. Caspar⁴⁸, F.L. Castillo⁴, L. Castillo Garcia¹³, V. Castillo Gimenez¹⁶⁹, N.F. Castro^{133a,133e}, A. Catinaccio³⁷, J.R. Catmore¹²⁸, T. Cavaliere⁴, V. Cavaliere³⁰, L.J. Caviedes Betancourt^{23b}, E. Celebi⁸², S. Cella³⁷, V. Cepaitis⁵⁶, K. Cerny¹²⁵, A.S. Cerqueira^{83a}, A. Cerrí^{74a,74b,ak}, L. Cerrito^{76a,76b}, F. Cerutti^{18a}, B. Cervato^{71a,71b}, A. Cervelli^{24b}, G. Cesarini⁵³, S.A. Cetin⁸², P.M. Chabrilat¹³⁰, R. Chakkappal¹⁶⁶, S. Chakraborty¹⁷³, A. Chambers⁶¹, J. Chan^{18a}, W.Y. Chan¹⁵⁹, J.D. Chapman³³, E. Chapon¹³⁸, B. Chargeishvili^{155b}, D.G. Charlton²¹, C. Chauhan¹³⁶, Y. Che^{114a}, S. Chekanov⁶, S.V. Chekulaev^{162a}, G.A. Chelkov^{39a}, B. Chen¹⁵⁷, B. Chen¹⁷¹, H. Chen^{114a}, H. Chen³⁰, J. Chen^{144a}, J. Chen¹⁴⁸, M. Chen¹²⁹, S. Chen⁸⁹, S.J. Chen^{114a}, X. Chen^{144a}, X. Chen^{15,ag}, Z. Chen⁶², C.L. Cheng¹⁷⁶, H.C. Cheng^{64a}, S. Cheong¹⁴⁹, A. Cheplakov³⁹, E. Cherepanova¹¹⁷, R. Cherkaoui El Moursli^{36e}, E. Cheu⁷, K. Cheung⁶⁵, L. Chevalier¹³⁸, V. Chiarella⁵³, G. Chiarelli^{74a}, G. Chiodini^{70a}, A.S. Chisholm²¹, A. Chitan^{28b}, M. Chitshvili¹⁶⁹, M.V. Chizhov^{39,s}, K. Choi¹¹, Y. Chou¹⁴², E.Y.S. Chow¹¹⁶, K.L. Chu¹⁷⁵, M.C. Chu^{64a}, X. Chu^{14,114c}, Z. Chubinidze⁵³, J.

Chudoba¹³⁴, J.J. Chwastowski⁸⁸, D. Cieri¹¹², K.M. Ciesla^{87a}, V. Cindro⁹⁵, A. Ciocio^{18a}, F. Ciroto^{72a,72b}, Z.H. Citron¹⁷⁵, M. Citterio^{71a}, D.A. Ciubotaru^{28b}, A. Clark⁵⁶, P.J. Clark⁵², N. Clarke Hall⁹⁸, C. Clarry¹⁶¹, S.E. Clawson⁴⁸, C. Clement^{47a,47b}, Y. Coadou¹⁰⁴, M. Cobal^{69a,69c}, A. Coccaro^{57b}, R.F. Coelho Barrue^{133a}, R. Coelho Lopes De Sa¹⁰⁵, S. Coelli^{71a}, L.S. Colangeli¹⁶¹, B. Cole⁴², P. Collado Soto¹⁰¹, J. Collot⁶⁰, R. Coluccia^{70a,70b}, P. Conde Muiño^{133a,133g}, M.P. Connell^{34c}, S.H. Connell^{34c}, E.I. Conroy¹²⁹, M. Contreras Cossio¹¹, F. Conventi^{72a,ai}, A.M. Cooper-Sarkar¹²⁹, L. Corazzina^{75a,75b}, F.A. Corchia^{24b,24a}, A. Cordeiro Oudot Choi¹⁴², L.D. Corpe⁴¹, M. Corradi^{75a,75b}, F. Corriveau^{106,ab}, A. Cortes-Gonzalez¹⁵⁹, M.J. Costa¹⁶⁹, F. Costanza⁴, D. Costanzo¹⁴⁵, B.M. Cote¹²², J. Couthures⁴, G. Cowan⁹⁷, K. Cranmer¹⁷⁶, L. Cremer⁴⁹, D. Cremonini^{24b,24a}, S. Crépe-Renaudin⁶⁰, F. Crescioli¹³⁰, T. Cresta^{73a,73b}, M. Cristinziani¹⁴⁷, M. Cristoforetti^{78a,78b}, V. Croft¹¹⁷, J.E. Crosby¹²⁴, G. Crosetti^{44b,44a}, A. Cueto¹⁰¹, H. Cui⁹⁸, Z. Cui⁷, B.M. Cunnett¹⁵², W.R. Cunningham⁵⁹, F. Curcio¹⁶⁹, J.R. Curran⁵², M.J. Da Cunha Sargedas De Sousa^{57b,57a}, J.V. Da Fonseca Pinto^{83b}, C. Da Via¹⁰³, W. Dabrowski^{87a}, T. Dado³⁷, S. Dahbi¹⁵⁴, T. Dai¹⁰⁸, D. Dal Santo²⁰, C. Dallapiccola¹⁰⁵, M. Dam⁴³, G. D'amen³⁰, V. D'Amico¹¹¹, J. Damp¹⁰², J.R. Dandoy³⁵, M. D'Andrea^{57b,57a}, D. Dannheim³⁷, G. D'anniballe^{74a,74b}, M. Danninger¹⁴⁸, V. Dao¹⁵¹, G. Darbo^{57b}, S.J. Das³⁰, F. Dattola⁴⁸, S. D'Auria^{71a,71b}, A. D'Avanzo^{72a,72b}, T. Davidek¹³⁶, J. Davidson¹⁷³, I. Dawson⁹⁶, K. De⁸, C. De Almeida Rossi¹⁶¹, R. De Asmundis^{72a}, N. De Biase⁴⁸, S. De Castro^{24b,24a}, N. De Groot¹¹⁶, P. de Jong¹¹⁷, H. De la Torre¹¹⁸, A. De Maria^{114a}, A. De Salvo^{75a}, U. De Sanctis^{76a,76b}, F. De Santis^{70a,70b}, A. De Santo¹⁵², J.B. De Vivie De Regie⁶⁰, J. Debeve⁹⁵, D.V. Dedovich³⁹, J. Degens⁹⁴, A.M. Deiana⁴⁵, J. Del Peso¹⁰¹, L. Delagrangé¹³⁰, F. Deliot¹³⁸, C.M. Delitzsch⁴⁹, M. Della Pietra^{72a,72b}, D. Della Volpe⁵⁶, A. Dell'Acqua³⁷, L. Dell'Asta^{71a,71b}, M. Delmastro⁴, C.C. Delogu¹⁰², P.A. Delsart⁶⁰, S. Demers¹⁷⁸, M. Demichev³⁹, S.P. Denisov³⁸, H. Denizli^{22a,i}, L. D'Eramo⁴¹, D. Derendarz⁸⁸, F. Derue¹³⁰, P. Dervan⁹⁴, A.M. Desai¹, K. Desch²⁵, F.A. Di Bello^{57b,57a}, A. Di Ciaccio^{76a,76b}, L. Di Ciaccio⁴, A. Di Domenico^{75a,75b}, C. Di Donato^{72a,72b}, A. Di Girolamo³⁷, G. Di Gregorio³⁷, A. Di Luca^{78a,78b}, B. Di Micco^{77a,77b}, R. Di Nardo^{77a,77b}, K.F. Di Petrillo⁴⁰, M. Diamantopoulou³⁵, F.A. Dias¹¹⁷, M.A. Diaz^{140a,140b}, A.R. Didenko³⁹, M. Didenko¹⁶⁹, S.D. Diefenbacher^{18a}, E.B. Diehl¹⁰⁸, S. Díez Cornell⁴⁸, C. Diez Pardos¹⁴⁷, C. Dimitriadis¹⁵⁰, A. Dimitrievska²¹, A. Dimri¹⁵¹, Y. Ding⁶², J. Dingfelder²⁵, T. Dingley¹²⁹, I.-M. Dinu^{28b}, S.J. Dittmeier^{63b}, F. Dittus³⁷, M. Divisek¹³⁶, B. Dixit⁹⁴, F. Djama¹⁰⁴, T. Djobava^{155b}, C. Doglioni^{103,100}, A. Dohnalova^{29a}, Z. Dolezal¹³⁶, K. Domijan^{87a}, K.M. Dona⁴⁰, M. Donadelli^{83d}, B. Dong¹⁰⁹, J. Donini⁴¹, A. D'Onofrio^{72a,72b}, M. D'Onofrio⁹⁴, J. Dopke¹³⁷, A. Doria^{72a}, N. Dos Santos Fernandes^{133a}, I.A. Dos Santos Luz^{83e}, P. Dougan¹⁰³, M.T. Dova⁹², A.T. Doyle⁵⁹, M.P. Drescher⁵⁵, E. Dreyer¹⁷⁵, I. Drivas-koulouris¹⁰, M. Drnevich¹²⁰, D. Du⁶², T.A. du Pree¹¹⁷, Z. Duan^{114a}, M. Dubau⁴, F. Dubinin³⁹, M. Dubovsky^{29a}, E. Duchovni¹⁷⁵, G. Duckeck¹¹¹, P.K. Duckett⁹⁸, O.A. Ducu^{28b}, D. Duda⁵², A. Dudarev³⁷, E.R. Duden²⁷, M. D'uffizi¹⁰³, L. Duflot⁶⁶, M. Dührssen³⁷, I. Dumina^{28g}, A.E. Dumitriu^{28b}, M. Dunford^{63a}, K. Dunne^{47a,47b}, A. Duperrin¹⁰⁴, H. Duran Yildiz^{3a}, A. Durglishvili^{155b}, D. Duvnjak³⁵, G.I. Dyckes^{18a}, M. Dyndal^{87a}, B.S. Dziejczak³⁷, Z.O. Earnshaw¹⁵², G.H. Eberwein¹²⁹, B. Eckerova^{29a}, S. Eggbrecht⁵⁵, E. Egidio Purcino De Souza^{83e}, G. Eigen¹⁷, K. Einsweiler^{18a}, T. Ekelof¹⁶⁷, P.A. Ekman¹⁰⁰, S. El Farkh^{36b}, Y. El Ghazali⁶², H. El Jarrari³⁷, A. El Moussaouy^{36a}, M. Ellert¹⁶⁷, F. Ellinghaus¹⁷⁷, T.A. Elliot⁹⁷, N. Ellis³⁷, J. Elmsheuser³⁰, M. Elsayy^{119a}, M. Elsing³⁷, D. Emelianov¹³⁷, Y. Enari⁸⁴, I. Ene^{18a}, S. Epari¹¹⁰, D. Ernani Martins Neto⁸⁸, F. Ernst³⁷, M. Errenst¹⁷⁷, M. Escalier⁶⁶, C. Escobar¹⁶⁹, E. Etzion¹⁵⁷, G. Evans^{133a,133b}, H. Evans⁶⁸, L.S. Evans⁹⁷, A. Ezhilov³⁸, S. Ezzarqtouni^{36a}, F. Fabbri^{24b,24a}, L. Fabbri^{24b,24a}, G. Facini⁹⁸, V. Fadeyev¹³⁹, R.M. Fakhruddinov³⁸, D. Fakoudis¹⁰², S. Falciano^{75a}, L.F. Falda Ulhoa

Coelho^{133a}, F. Fallavollita¹¹², G. Falsetti^{44b,44a}, J. Faltova¹³⁶, C. Fan¹⁶⁸, K.Y. Fan^{64b}, Y. Fan¹⁴, Y. Fang^{14,114c}, M. Fantì^{71a,71b}, M. Faraj^{69a,69b}, Z. Farazpay⁹⁹, A. Farbin⁸, A. Farilla^{77a}, K. Farman¹⁵⁴, T. Farooque¹⁰⁹, J.N. Farr¹⁷⁸, S.M. Farrington^{137,52}, F. Fassi^{36e}, D. Fassouliotis⁹, L. Fayard⁶⁶, P. Federic¹³⁶, P. Federicova¹³⁴, O.L. Fedin^{38a}, M. Feickert¹⁷⁶, L. Feligioni¹⁰⁴, D.E. Fellers^{18a}, C. Feng^{143a}, Y. Feng¹⁴, Z. Feng¹¹⁷, M.J. Fenton¹⁶⁵, L. Ferencz⁴⁸, B. Fernandez Barbadillo⁹³, P. Fernandez Martinez⁶⁷, M.J.V. Fernoux¹⁰⁴, J. Ferrando⁹³, A. Ferrari¹⁶⁷, P. Ferrari^{117,116}, R. Ferrari^{73a}, D. Ferrere⁵⁶, C. Ferretti¹⁰⁸, M.P. Fewell¹¹, D. Fiacco^{75a,75b}, F. Fiedler¹⁰², P. Fiedler¹³⁵, S. Filimonov³⁹, M.S. Filip^{28b,i}, A. Filipčić⁹⁵, E.K. Filmer^{162a}, F. Filthaut¹¹⁶, M.C.N. Fiolhais^{133a,133c,c}, L. Fiorini¹⁶⁹, W.C. Fisher¹⁰⁹, T. Fitschen¹⁰³, P.M. Fitzhugh¹³⁸, I. Fleck¹⁴⁷, P. Fleischmann¹⁰⁸, T. Flick¹⁷⁷, M. Flores^{34d,af}, L.R. Flores Castillo^{64a}, L. Flores Sanz De Acedo³⁷, F.M. Follega^{78a,78b}, N. Fomin³³, J.H. Foo¹⁶¹, A. Formica¹³⁸, A.C. Forti¹⁰³, E. Fortin³⁷, A.W. Fortman^{18a}, L. Foster^{18a}, L. Fountas^{9,i}, D. Fournier⁶⁶, H. Fox⁹³, P. Francavilla^{74a,74b}, S. Francescato⁶¹, S. Franchellucci⁵⁶, M. Franchini^{24b,24a}, S. Franchino^{63a}, D. Francis³⁷, L. Franco¹¹⁶, V. Franco Lima³⁷, L. Franconi⁴⁸, M. Franklin⁶¹, G. Frattari²⁷, Y.Y. Frid¹⁵⁷, J. Friend⁵⁹, N. Fritzsche³⁷, A. Froch⁵⁶, D. Froidevaux³⁷, J.A. Frost¹²⁹, Y. Fu¹⁰⁹, S. Fuenzalida Garrido^{140g}, M. Fujimoto¹⁰⁴, K.Y. Fung^{64a}, E. Furtado De Simas Filho^{83e}, M. Furukawa¹⁵⁹, J. Fuster¹⁶⁹, A. Gaa⁵⁵, A. Gabrielli^{24b,24a}, A. Gabrielli¹⁶¹, P. Gadow³⁷, G. Gagliardi^{57b,57a}, L.G. Gagnon^{18a}, S. Gaid^{85b}, S. Galantzan¹⁵⁷, J. Gallagher¹, E.J. Gallas¹²⁹, A.L. Gallen¹⁶⁷, B.J. Gallop¹³⁷, K.K. Gan¹²², S. Ganguly¹⁵⁹, Y. Gao⁵², A. Garabaglu¹⁴², F.M. Garay Walls^{140a,140b}, C. García¹⁶⁹, A. Garcia Alonso¹¹⁷, A.G. Garcia Caffaro¹⁷⁸, J.E. García Navarro¹⁶⁹, M.A. Garcia Ruiz^{23b}, M. Garcia-Sciveres^{18a}, G.L. Gardner¹³¹, R.W. Gardner⁴⁰, N. Garelli¹⁶⁴, R.B. Garg¹⁴⁹, J.M. Gargan⁵², C.A. Garner¹⁶¹, C.M. Garvey^{34a}, V.K. Gassmann¹⁶⁴, G. Gaudio^{73a}, V. Gautam¹³, P. Gauzzi^{75a,75b}, J. Gavranovic⁹⁵, I.L. Gavrilenko^{133a}, A. Gavriluk³⁸, C. Gay¹⁷⁰, G. Gaycken¹²⁶, E.N. Gazis¹⁰, A. Gekow¹²², C. Gemme^{57b}, M.H. Genest⁶⁰, A.D. Gentry¹¹⁵, S. George⁹⁷, T. Gerasis⁴⁶, A.A. Gerwin¹²³, P. Gessinger-Befurt³⁷, M.E. Geyik¹⁷⁷, M. Ghani¹⁷³, K. Ghorbanian⁹⁶, A. Ghosal¹⁴⁷, A. Ghosh¹⁶⁵, A. Ghosh⁷, B. Giacobbe^{24b}, S. Giagu^{75a,75b}, T. Gian¹¹⁷, A. Giannini⁶², S.M. Gibson⁹⁷, M. Gignac¹³⁹, D.T. Gil^{87b}, A.K. Gilbert^{87a}, B.J. Gilbert⁴², D. Gillberg³⁵, G. Gilles¹¹⁷, D.M. Gingrich^{2,ah}, M.P. Giordan^{69a,69c}, P.F. Giraud¹³⁸, G. Giudliarelli^{69a,69c}, D. Giugni^{71a}, F. Giuli^{76a,76b}, I. Gkiyas^{9,i}, L.K. Gladilin³⁸, C. Glasman¹⁰¹, M. Glazewska²⁰, R.M. Gleason¹⁶⁵, G. Glemža⁴⁸, M. Glisic¹²⁶, I. Gnesi^{44b}, Y. Go³⁰, M. Goblirsch-Kolb³⁷, B. Gocke⁴⁹, D. Godin¹¹⁰, B. Gokturk^{22a}, S. Goldfarb¹⁰⁷, T. Golling⁵⁶, M.G.D. Gololo^{34c}, D. Golubkov³⁸, J.P. Gombas¹⁰⁹, A. Gomes^{133a,133b}, G. Gomes Da Silva¹⁴⁷, A.J. Gomez Delegido³⁷, R. Gonçalo^{133a}, L. Gonella²¹, A. Gongadze^{155c}, F. Gonnella²¹, J.L. Gonski¹⁴⁹, R.Y. González Andana⁵², S. González de la Hoz¹⁶⁹, M.V. Gonzalez Rodrigues⁴⁸, R. Gonzalez Suarez¹⁶⁷, S. Gonzalez-Sevilla⁵⁶, L. Goossens³⁷, B. Gorini³⁷, E. Gorini^{70a,70b}, A. Gorišek⁹⁵, T.C. Gosart¹³¹, A.T. Goshaw⁵¹, M.I. Gostkin³⁹, S. Goswami¹²⁴, C.A. Gottardo³⁷, S.A. Gotz¹¹¹, M. Gouighri^{36b}, A.G. Goussiou¹⁴², N. Govender^{34c}, R.P. Grabarczyk¹²⁹, I. Grabowska-Bold^{87a}, K. Graham³⁵, E. Gramstad¹²⁸, S. Grancagnolo^{70a,70b}, C.M. Grant¹, P.M. Gravila^{28f}, F.G. Gravili^{70a,70b}, H.M. Gray^{18a}, M. Greco¹¹², M.J. Green¹, C. Grefe²⁵, A.S. Grefsrud¹⁷, I.M. Gregor⁴⁸, K.T. Greif¹⁶⁵, P. Grenier¹⁴⁹, S.G. Grewe¹¹², A.A. Grillo¹³⁹, K. Grimm³², S. Grinstein^{13,x}, J.-F. Grivaz⁶⁶, E. Gross¹⁷⁵, J. Grosse-Knetter⁵⁵, L. Guan¹⁰⁸, G. Guerrieri³⁷, R. Guevara¹²⁸, R. Gugel¹⁰², J. A. M. Guhit¹⁰⁸, A. Guida¹⁹, E. Guilloton¹⁷³, S. Guindon³⁷, F. Guo^{14,114c}, J. Guo^{144a}, L. Guo⁴⁸, L. Guo^{114b,v}, Y. Guo¹⁰⁸, A. Gupta⁴⁹, R. Gupta¹³², S. Gupta²⁷, S. Gurbuz²⁵, S.S. Gurdasani⁴⁸, G. Gustavino^{75a,75b}, P. Gutierrez¹²³, L.F. Gutierrez Zagazeta¹³¹, M. Gutsche⁵⁰, C. Gutschow⁹⁸, C. Gwenlan¹²⁹, C.B. Gwilliam⁹⁴, E.S. Haaland¹²⁸, A. Haas¹²⁰, M. Habedank⁵⁹, C. Haber^{18a},

H.K. Hadavand⁸, A. Haddad⁴¹, A. Hade⁵⁰, A.I. Hagan⁹³, J.J. Hahn¹⁴⁷, E.H. Haines⁹⁸, M. Haleem¹⁷², J. Haley¹²⁴, G.D. Hallowell¹⁰⁴, K. Hamano¹⁷¹, H. Hamdaoui¹⁶⁷, M. Hamer²⁵, S.E.D. Hammoud⁶⁶, E.J. Hampshire⁹⁷, J. Han^{143a}, L. Han^{114a}, L. Han⁶², S. Han¹⁴, K. Hanagaki⁸⁴, M. Hance¹³⁹, D.A. Hangal⁴², H. Hanif¹⁴⁸, M.D. Hank¹³¹, J.B. Hansen⁴³, P.H. Hansen⁴³, D. Harada⁵⁶, T. Harenberg¹⁷⁷, S. Harkusha¹⁷⁹, M.L. Harris¹⁰⁵, Y.T. Harris²⁵, J. Harrison¹³, N.M. Harrison¹²², P.F. Harrison¹⁷³, M.L.E. Hart⁹⁸, N.M. Hartman¹¹², N.M. Hartmann¹¹¹, R.Z. Hasan^{97,137}, Y. Hasegawa¹⁴⁶, F. Haslbeck¹²⁹, S. Hassan¹⁷, R. Hauser¹⁰⁹, M. Haviernik¹³⁶, C.M. Hawkes²¹, R.J. Hawkings³⁷, Y. Hayashi¹⁵⁹, D. Hayden¹⁰⁹, C. Hayes¹⁰⁸, R.L. Hayes¹¹⁷, C.P. Hays¹²⁹, J.M. Hays⁹⁶, H.S. Hayward⁹⁴, M. He^{14,114c}, Y. He⁴⁸, Y. He⁹⁸, N.B. Heatley⁹⁶, V. Hedberg¹⁰⁰, C. Heidegger⁵⁴, K.K. Heidegger⁵⁴, J. Heilman³⁵, S. Heim⁴⁸, T. Heim^{18a}, J.G. Heinlein¹³¹, J.J. Heinrich¹²⁶, L. Heinrich¹¹², J. Hejbal¹³⁴, M. Helbig⁵⁰, A. Held¹⁷⁶, S. Hellesund¹⁷, C.M. Helling¹⁷⁰, S. Hellman^{47a,47b}, A.M. Henriques Correia³⁷, H. Herde¹⁰⁰, Y. Hernández Jiménez¹⁵¹, L.M. Herrmann²⁵, T. Herrmann⁵⁰, G. Herten⁵⁴, R. Hertenberger¹¹¹, L. Hervas³⁷, M.E. Hespinoza¹⁰², N.P. Hessey^{162a}, J. Hessler¹¹², M. Hidaoui^{36b}, N. Hidic¹³⁶, E. Hill¹⁶¹, T.S. Hillersoy¹⁷, S.J. Hillier²¹, J.R. Hinds¹⁰⁹, F. Hinterkeuser²⁵, M. Hirose¹²⁷, S. Hirose¹⁶³, D. Hirschebuehl¹⁷⁷, T.G. Hitchings¹⁰³, B. Hiti⁹⁵, J. Hobbs¹⁵¹, R. Hobincu^{28e}, N. Hod¹⁷⁵, A.M. Hodges¹⁶⁸, M.C. Hodgkinson¹⁴⁵, B.H. Hodgkinson¹²⁹, A. Hoercker³⁷, D.D. Hofer¹⁰⁸, J. Hofer¹⁶⁹, M. Holzbock³⁷, L.B.A.H. Hommels³³, V. Homsak¹²⁹, B.P. Honan¹⁰³, J.J. Hong⁶⁸, T.M. Hong¹³², B.H. Hooberman¹⁶⁸, W.H. Hopkins⁶, M.C. Hoppesch¹⁶⁸, Y. Horii¹¹³, M.E. Horstmann¹¹², S. Hou¹⁵⁴, M.R. Housenga¹⁶⁸, J. Howarth⁵⁹, J. Hoya⁶, M. Hrabovsky¹²⁵, T. Hryn'ova⁴, P.J. Hsu⁶⁵, S.-C. Hsu¹⁴², T. Hsu⁶⁶, M. Hu^{18a}, Q. Hu⁶², S. Huang³³, X. Huang^{14,114c}, Y. Huang¹³⁶, Y. Huang^{114b}, Y. Huang¹⁰², Y. Huang¹⁴, Z. Huang⁶⁶, Z. Hubacek¹³⁵, F. Huegging²⁵, T.B. Huffman¹²⁹, M. Hufnagel¹²⁹, M. Hufnagel^{83a}, C.A. Hugli⁴⁸, M. Huhtinen³⁷, S.K. Huiberts¹⁷, R. Hulsken¹⁰⁶, C.E. Hultquist^{18a}, D.L. Humphreys¹⁰⁵, N. Huseynov¹², J. Huston¹⁰⁹, J. Huth⁶¹, R. Hyneman⁷, G. Iacobucci⁵⁶, G. Iakovidis³⁰, L. Iconomidou-Fayard⁶⁶, J.P. Iddon³⁷, P. Iengo^{72a,72b}, R. Iguchi¹⁵⁹, Y. Iiyama¹⁵⁹, T. Iizawa¹⁵⁹, Y. Ikegami⁸⁴, D. Iliadis¹⁵⁸, N. Ilic¹⁶¹, H. Imam^{36a}, G. Inacio Goncalves^{83d}, S.A. Infante Cabanas^{140c}, T. Ingebreten Carlson^{47a,47b}, J.M. Inglis⁹⁶, G. Introzzi^{73a,73b}, M. Iodice^{77a}, V. Ippolito^{75a,75b}, R.K. Irwin⁹⁴, M. Ishino¹⁵⁹, W. Islam¹⁷⁶, C. Issever¹⁹, S. Istin^{22a,am}, K. Itabashi⁸⁴, H. Ito¹⁷⁴, R. Iuppa^{78a,78b}, A. Ivina¹⁷⁵, V. Izzo^{72a}, P. Jacka¹³⁵, P. Jackson¹, P. Jain⁴⁸, K. Jakobs⁵⁴, T. Jakoubek¹⁷⁵, J. Jamieson⁵⁹, W. Jang¹⁵⁹, S. Jankovych¹³⁶, M. Javurkova¹⁰⁵, P. Jawahar¹⁰³, L. Jeanty¹²⁶, J. Jejelava^{155a,ae}, P. Jenni^{54,f}, C.E. Jessiman³⁵, C. Jia^{143a}, H. Jia¹⁷⁰, J. Jia¹⁵¹, X. Jia^{112,114c}, Z. Jia^{114a}, C. Jiang⁵², Q. Jiang^{64b}, S. Jiggins⁴⁸, M. Jimenez Ortega¹⁶⁹, J. Jimenez Pena¹³, S. Jin^{114a}, A. Jinaru^{28b}, O. Jinnouchi¹⁴¹, P. Johansson¹⁴⁵, K.A. Johns⁷, J.W. Johnson¹³⁹, F.A. Jolly⁴⁸, D.M. Jones¹⁵², E. Jones⁴⁸, K.S. Jones⁸, P. Jones³³, R.W.L. Jones⁹³, T.J. Jones⁹⁴, H.L. Joos⁵⁵, R. Joshi¹²², J. Jovicevic¹⁶, X. Ju^{18a}, J.J. Jungbuth³⁷, T. Junkermann^{63a}, A. Juste Rozas^{13,c}, M.K. Juzek⁸⁸, S. Kabana^{140f}, A. Kaczmarska⁸⁸, S.A. Kadir¹⁴⁹, M. Kado¹¹², H. Kagan¹²², M. Kagan¹⁴⁹, A. Kahn¹³¹, C. Kahra¹⁰², T. Kaji¹⁵⁹, E. Kajomovit¹⁵⁶, N. Kakati¹⁷⁵, N. Kakoty¹³, I. Kalaitzidou⁵⁴, S. Kandel¹⁸, N.J. Kang¹³⁹, D. Kar^{34h}, E. Karentzos²⁵, O. Karkout¹¹⁷, S.N. Karpov³⁹, Z.M. Karpova³⁹, V. Kartvelishvili⁹³, A.N. Karyukhin³⁸, E. Kasimi¹⁵⁸, J. Katzy⁴⁸, S. Kaur³⁵, K. Kawade¹⁴⁶, M.P. Kawale¹²³, C. Kawamoto⁸⁹, T. Kawamoto⁶², E.F. Kay³⁷, F.I. Kaya¹⁶⁴, S. Kazakos¹⁰⁹, V.F. Kazanin³⁸, J.M. Keaveney^{34a}, R. Keeler¹⁷¹, G.V. Kehris⁶¹, J.S. Keller³⁵, J.M. Kelly¹⁷¹, J.J. Kempster¹⁵², O. Kepka¹³⁴, J. Kerr^{162b}, B.P. Kerridge¹³⁷, B.P. Kersevan⁹⁵, L. Keszeghova^{29a}, R.A. Khan¹³², A. Khanov¹²⁴, A.G. Kharlamov³⁸, T. Kharlamov³⁸, E.E. Khoda¹⁴², M. Kholodenko^{133a}, T.J. Khoo¹⁹, G. Khoraiuli¹⁷², Y. Khouli^{36a}, J. Khubua^{155b,†}, Y.A.R. Khwairam¹³⁰, B. Kibirige^{34h}, D. Kim⁶, D.W. Kim^{47a,47b}, Y.K. Kim⁴⁰, N. Kimura⁹⁸, M.K. Kingston⁵⁵, A. Kirchoff⁵⁵, C. Kirfel²⁵, F. Kirfel²⁵, J. Kirk¹³⁷, A.E. Kiryunin¹¹², S. Kita¹⁶³, O. Kivernyk²⁵, M. Klassen¹⁶⁴, C. Klein³⁵, L. Klein¹⁷², M.H. Klein⁴⁵, S.B. Klein⁵⁶, U. Klein⁹⁴, A. Klimentov³⁰, T. Klioutchnikova³⁷, P. Kluit¹¹⁷, S. Kluth¹¹², E. Kneringer⁷⁹, T.M. Knight¹⁶¹, A. Knue⁴⁹, M. Kobel⁵⁰, D. Kobylanski¹⁷⁵, S.F. Koch¹²⁹, M. Kocian¹⁴⁹, P. Kodyš¹³⁶, D.M. Koeck¹²⁶, T. Koffas³⁵, O. Kolay⁵⁰, I. Koletsou⁴, T. Komarek⁸⁸, K. Köneke⁵⁵, A.X.Y. Kong¹, T. Kono¹²¹, N. Konstantinidis⁹⁸, P. Kontaxakis⁵⁶, B. Konya¹⁰⁰, R. Kopeliansky⁴², S. Koperny^{87a}, K. Korcyl⁸⁸, K. Kordas^{158,d}, A. Korn⁹⁸, S. Korn⁵⁵, I. Korolkov¹³, N. Korotkov³⁸, B. Kortman¹¹⁷, O. Kortner¹¹², S. Kortner¹¹², W.H. Kostecka¹¹⁸, M. Kostov^{29a}, V.V. Kostyukhin¹⁴⁷, A. Kotskechagia³⁷, A. Kotwal⁵¹, A. Koulouris³⁷, A. Kourkumeli-Charalampidi^{73a,73b}, C. Kourkumelis⁹, E. Kourlitis¹¹², O. Kovanda¹²⁶, R. Kowalewski¹⁷¹, W. Kozański¹²⁶, A.S. Kozhin³⁸, V.A. Kramarenko³⁸, G. Kramberger⁹⁵, P. Kramer²⁵, M.W. Krasny¹³⁰, A. Krasznahorkay¹⁰⁵, A.C. Kraus¹¹⁸, J.W. Kraus¹⁷⁷, J.A. Kremer⁴⁸, N.B. Krenkel¹⁴⁷, T. Kresse⁵⁰, L. Kretschmann¹⁷⁷, J. Kretschmar⁹⁴, P. Krieger¹⁶¹, K. Krizka²¹, K. Kroening⁴⁹, H. Kroha¹¹², J. Kroll¹³⁴, J. Kroll¹³¹, K.S. Krowpman¹⁰⁹, U. Kruchonak³⁹, H. Krüger²⁵, N. Krumnack⁸¹, M.C. Kruse⁵¹, O. Kuchinskaia³⁹, S. Kудay^{3a}, S. Kuehn³⁷, R. Kuesters⁵⁴, T. Kuhl⁴⁸, V. Kukhtin³⁹, Y. Kulchitsky³⁹, S. Kuleshov^{140d,140b}, J. Kull¹, E.V. Kumar¹¹¹, M. Kumar^{34h}, N. Kumari⁴⁸, P. Kumari^{162b}, A. Kupco¹³⁴, T. Kupfer⁴⁹, A. Kupich³⁸, O. Kuprash⁵⁴, H. Kurashige⁸⁶, L.L. Kurchaninov^{162a}, O. Kurdysh⁴, Y.A. Kurochkin³⁸, A. Kurova³⁸, M. Kuze¹⁴¹, A.K. Kvam¹⁰⁵, J. Kvita¹²⁵, N.G. Kyriacou¹⁰⁸, C. Lacasta¹⁶⁹, F. Lacava^{75a,75b}, H. Lacker¹⁹, D. Lacour¹³⁰, N.N. Lad⁹⁸, E. Ladygin³⁹, A. Lafarge⁴¹, B. Laforge¹³⁰, T. Lagouri¹⁷⁸, F.Z. Lahbabi^{36a}, S. Lai⁵⁵, W.S. Lai⁹⁸, J.E. Lambert¹⁷¹, S. Lammers⁶⁸, W. Lampl⁷, C. Lampoudis^{158,d}, G. Lamprinouidis¹⁰², A.N. Lancaster¹¹⁸, E. Lançon³⁰, U. Landgraf⁶⁴, M.P.J. Landon⁹⁶, V.S. Lang⁵⁴, O.K.B. Langrekken¹²⁸, A.J. Lankford¹⁶⁵, F. Lanni³⁷, K. Lantzsch²⁵, A. Lanza^{73a}, M. Lanzani¹⁶⁹, J.F. Laporte¹³⁸, T. Lari^{71a}, D. Larsen¹⁷, L. Larson¹¹, F. Lasagni Manghi^{24b}, M. Lassnig³⁷, S.D. Lawlor¹⁴⁵, R. Lazaridou¹⁶⁵, M. Lazzaroni^{71a,71b}, H.D.M. Le¹⁰⁹, E.M. Le Boulicaut¹⁷⁸, L.T. Le Pottier^{18a}, B. Leban^{24b,24c}, F. Ledroit-Guillon⁶⁰, T.F. Lee^{162b}, L.L. Leeuw^{34c}, M. Lefebvre¹⁷¹, C. Leggett^{18a}, G. Lehmann Miotto³⁷, M. Leigh⁵⁶, W.A. Light¹⁰⁵, W. Leinonen¹¹⁶, A. Leisos^{158,u}, M.A.L. Leite^{83c}, C.E. Leitgeb¹⁹, R. Leitner¹³⁶, K.J.C. Leney⁴⁵, T. Lenz²⁵, S. Leone^{74a}, C. Leonidopoulos⁵², A. Leopold¹⁵⁰, J.H. Lepage Bourbonnais³⁵, R. Les¹⁰⁹, C.G. Lester³³, M. Levchenko³⁸, J. Levêque⁴, L.J. Levinson¹⁷⁵, G. Levrini^{24b,24a}, M.P. Lewicki⁸⁸, C. Lewis¹⁴², D.J. Lewis⁴, L. Lewitt¹⁴⁵, A. Li³⁰, B. Li^{143a}, C. Li¹⁰⁸, C.-Q. Li¹¹², H. Li^{143a}, H. Li¹⁰³, H. Li¹⁵, H. Li⁶², H. Li^{143a}, J. Li^{144a}, K. Li¹⁴, L. Li^{144a}, R. Li¹⁷⁸, S. Li^{14,114c}, S. Li^{144b,144a}, T. Li⁵, X. Li¹⁰⁶, Y. Li¹⁴, Z. Li¹⁵⁹, Z. Li^{14,114c}, Z. Li⁶², S. Liang^{14,114c}, Z. Liang¹⁴, M. Liberatore¹³⁸, B. Libertini^{76a}, K. Lie^{64c}, J. Lieber Marin^{83e}, H. Lien⁶⁸, H. Lin¹⁰⁸, S.F. Lin¹⁵¹, L. Linden¹¹¹, R.E. Lindley⁷, J.H. Lindon³⁷, J. Ling⁶¹, E. Lipeles¹³¹, A. Lipniacka¹⁷, A. Lister¹⁷⁰, J.D. Little⁶⁸, B. Liu¹⁴, B.X. Liu^{114b}, D. Liu^{144b,144a}, D. Liu¹³⁹, E.H.L. Liu²¹, J.K.K. Liu¹²⁰, K. Liu^{144b}, K. Liu^{144b,144a}, M. Liu⁶², M.Y. Liu⁶², P. Liu¹⁴, Q. Liu^{144b,142,144a}, X. Liu⁶², X. Liu^{143a}, Y. Liu^{114b,114c}, Y.L. Liu^{143a}, Y.W. Liu⁶², Z. Liu^{66,k}, S.L. Lloyd⁹⁶, E.M. Lobodzinska⁴⁸, P. Loch⁷, E. Lodhi¹⁶¹, K. Lohwasser¹⁴⁵, E. Loiacono⁴⁸, J.D. Lomas²¹, J.D. Long⁴², I. Longhini¹⁶⁵, R. Longo¹⁶⁸, A. Lopez Solis¹³, N.A. Lopez-canelas⁷, N. Lorenzo Martinez⁴, A.M. Lory¹¹¹, M. Losada^{119a}, G. Lösckce Centeno¹⁵², X. Lou^{47a,47b}, X. Lou^{14,114c}, A. Lounis⁶⁶, P.A. Love⁹³, M. Lu⁶⁶, S. Lu¹³¹, Y.J. Lu¹⁵⁴, H.J. Lubatti¹⁴², C. Luci^{75a,75b}, F.L. Lucio Alves^{114a}, F. Luehring⁶⁸, B.S. Lunday¹³¹, O. Lundberg¹⁵⁰, J. Lunde³⁷, N.A. Luongo⁶, M.S. Lutz³⁷, A.B. Lux²⁶, D. Lynn³⁰, R. Lysak¹³⁴, V. Lysenko¹³⁵, E. Lytken¹⁰⁰, V. Lyubushkin³⁹, T. Lyubushkina³⁹, M.M. Lyukova¹⁵¹, M. Firdaus M. Sober⁵², H. Ma³⁰, K. Ma⁶², L.L. Ma^{143a}, W. Ma⁶², Y. Ma¹²⁴, J.C. MacDonald¹⁰²,

P.C. Machado De Abreu Farias^{83e}, R. Madar⁴¹, T. Madula⁹⁸, J. Maeda⁸⁶, T. Maeno³⁰, P.T. Mafa^{34c,j}, H. Maguire¹⁴⁵, M. Maheshwari³³, V. Maiboroda⁶⁶, A. Maio^{133a,133b,133d}, K. Maj^{87a}, O. Majersky⁴⁸, S. Majewski¹²⁶, R. Makhmanazarov³⁸, N. Makovec⁶⁶, V. Maksimovic¹⁶, B. Malaescu¹³⁰, J. Malamant¹²⁸, Pa. Malecki⁸⁸, V.P. Maleev³⁸, F. Malek^{60,o}, M. Mali⁹⁵, D. Malito⁹⁷, U. Mallik^{80,t}, A. Maloizel⁵, S. Maltezos¹⁰, A. Malvezzi Lopes^{83d}, S. Malyukov³⁹, J. Mamuzic⁹⁵, G. Mancini⁵³, M.N. Mancini²⁷, G. Manco^{73a,73b}, J.P. Mandalia⁹⁶, S.S. Mandarri¹⁵², I. Mandić⁹⁵, L. Manhaes de Andrade Filho^{83a}, I.M. Maniatis¹⁷⁵, J. Manjarres Ramos⁹¹, D.C. Mankad¹⁷⁵, A. Mann¹¹¹, T. Manoussos³⁷, M.N. Mantinan⁴⁰, S. Manzoni³⁷, L. Mao^{144a}, X. Mapekula^{34c}, A. Marantis¹⁵⁸, R.R. Marcelo Gregorio⁹⁶, G. Marchiori⁵, C. Marcon^{71a}, E. Maricic¹³⁸, M. Marinescu⁴⁸, S. Marium⁴⁸, M. Marjanovic¹²³, A. Markhoos⁵⁴, M. Markovitch⁶⁶, M.K. Maroun¹⁰⁵, M.C. Marr¹⁴⁸, G.T. Marsden¹⁰³, E.J. Marshall⁹³, Z. Marshall^{18a}, S. Marti-Garcia¹⁶⁹, J. Martin⁹⁸, T.A. Martin¹³⁷, V.J. Martin⁵², B. Martin dit Latour¹⁷, L. Martinelli^{75a,75b}, M. Martinez^{13,x}, P. Martinez Agullo¹⁶⁹, V.I. Martinez Outschoorn¹⁰⁵, P. Martinez Suarez³⁷, S. Martin-Haugh¹³⁷, G. Martinovicova¹³⁶, V.S. Martou^{28b}, A.C. Martyniuk⁹⁸, A. Marzin³⁷, D. Mascione^{78a,78b}, L. Masetti¹⁰², J. Masik¹⁰³, A.L. Maslennikov³⁹, S.L. Mason⁴², P. Massarotti^{72a,72b}, P. Mastrandrea^{74a,74b}, A. Mastroberardino^{44b,44a}, T. Masubuchi¹²⁷, T.T. Mathew¹²⁶, J. Matousek¹³⁶, D.M. Mattern⁴⁹, J. Maurer^{28b}, T. Maurin⁵⁹, A.J. Maury⁶⁶, B. Maček⁹⁵, C. Mavungu Tsava¹⁰⁴, D.A. Maximov³⁸, A.E. May¹⁰³, E. Mayer⁴¹, R. Mazini^{34h}, I. Maznas¹¹⁸, S.M. Mazza¹³⁹, E. Mazzeo³⁷, J.P. Mc Gowan¹⁷¹, S.P. Mc Kee¹⁰⁸, C.A. Mc Lean⁶, C.C. McCracken¹⁷⁰, E.F. McDonald¹⁰⁷, A.E. McDougall¹¹⁷, L.F. Mcelhinney⁹³, J.A. MCFayden¹⁵², R.P. McGovern¹³¹, R.P. Mckenzie^{34h}, T.C. Mclachlan⁴⁸, D.J. Mclaughlin⁹⁸, S.J. McMahon¹³⁷, C.M. Mcpartland⁹⁴, R.A. McPherson^{171,ab}, S. Mehlhase¹¹¹, A. Mehta⁹⁴, D. Melini¹⁶⁹, B. R. Mellado Garcia^{34h}, A. H. Melo⁵⁵, F. Meloni⁴⁸, A.M. Mendes Jacques Da Costa¹⁰³, L. Meng⁹³, S. Menke¹¹², M. Mentink³⁷, E. Meoni^{44b,44a}, G. Mercado¹¹⁸, S. Merianos¹⁵⁸, C. Merlassino^{69a,69c}, C. Meroni^{71a,71b}, J. Metcalfe⁶, A.S. Mete⁶, E. Meuser¹⁰², C. Meyer⁶⁸, J.-P. Meyer¹³⁸, Y. Miao^{114a}, R.P. Middleton¹³⁷, M. Mihovilovic⁶⁶, L. Mijović⁵², G. Mikenberg¹⁷⁵, M. Mikestikova¹³⁴, M. Mikuz⁹⁵, H. Mildner¹⁰², A. Milic³⁷, D.W. Miller⁴⁰, E.H. Miller¹⁴⁹, A. Milov¹⁷⁵, D.A. Milstead^{47a,47b}, T. Min^{114a}, A.A. Minaenko³⁸, I.A. Minashvili^{155b}, A.I. Mincer¹²⁰, B. Mindur^{87a}, M. Mineev³⁹, Y. Mino⁸⁹, L. M. Mir¹³, M. Miralles Lopez⁵⁹, M. Mironova^{18a}, M. Missio¹¹⁶, A. Mitra¹⁷³, V.A. Mitsou¹⁶⁹, Y. Mitsumori¹¹³, O. Miu¹⁶¹, P.S. Miyagawa⁹⁶, T. Mkrtychyan^{63a}, M. Mlinarevic⁹⁸, T. Mlinarevic⁹⁸, M. Mlynarikova¹³⁶, L. Mlynarska^{87a}, S. Mobius²⁰, M.H. Mohamed Farook¹¹⁵, S. Mohapatra⁴², S. Mohiuddin¹²⁴, G. Mokgatitswane^{34h}, L. Moleri¹⁷⁵, U. Molinatti¹²⁹, L.G. Mollier²⁰, B. Mondal¹³⁴, S. Mondal¹³⁵, K. Mönig⁴⁸, E. Monnier¹⁰⁴, L. Monsonis Romero¹⁶⁹, J. Montejo Berlingen¹³, A. Montella^{47a,47b}, M. Montella¹²², F. Montecelli^{77a,77b}, F. Monticelli⁹², S. Monzani^{69a,69c}, A. Morancho Tarda⁴³, N. Morange⁶⁶, A.L. Moreira De Carvalho⁴⁸, M. Moreno Llácer¹⁶⁹, C. Moreno Martinez⁵⁶, J.M. Moreno Perez^{23b}, P. Morettini^{57b}, S. Morgenstern³⁷, M. Morii⁶¹, M. Morinaga¹⁵⁹, M. Moritsu⁹⁰, F. Morodei^{75a,75b}, P. Moschovakos³⁷, B. Moser⁵⁴, M. Mosidze^{155b}, T. Moskalets⁴⁵, P. Moskvitina¹¹⁶, J. Moss³², P. Moszkowicz^{87a}, A. Moussa^{36d}, Y. Moyal¹⁷⁵, H. Moyano Gomez¹³, E.J.W. Moyses¹⁰⁵, T.G. Mroz⁸⁸, O. Mtintsilana^{34h}, S. Muanza¹⁰⁴, M. Mucha²⁵, J. Mueller¹³², R. Müller³⁷, G.A. Mullier¹⁶⁷, A.J. Mullin³³, J.J. Mullin⁵¹, A.C. Mullins⁴⁵, A.E. Mulski⁶¹, D.P. Mungo¹⁶¹, D. Munoz Perez¹⁶⁹, F.J. Munoz Sanchez¹⁰³, W.J. Murray^{173,137}, M. Muškinja⁹⁵, C. Mwewa⁴⁸, A.G. Myagkov^{38a}, A.J. Myers⁸, G. Myers¹⁰⁸, M. Myska¹³⁵, B.P. Nachman^{18a}, K.Nagai¹²⁹, K.Nagano⁸⁴, R. Nagasaka¹⁵⁹, J.L. Nagle^{30,aj}, E. Nagy¹⁰⁴, A.M. Nairz³⁷, Y. Nakahama⁸⁴, K. Nakamura⁸⁴, K. Nakkali⁵, A. Nandi^{63b}, H. Nanjo¹²⁷, E.A. Narayanan⁴⁵, Y. Narukawa¹⁵⁹, I. Naryshkin³⁸, L. Nasella^{71a,71b}, S. Nasri^{119b}, C. Nass²⁵, G. Navarro^{23a}, J. Navarro-Gonzalez¹⁶⁹, A. Nayaz¹⁹, P.Y. Nechaeva³⁸, S. Nechaeva^{24b,24a}, F. Nechansky¹³⁴, L. Nedic¹²⁹, T.J. Neepe²¹, A. Negri^{73a,73b}, M. Negrini^{24b}, C. Nellist¹¹⁷, C. Nelson¹⁰⁶, K. Nelson¹⁰⁸, S. Nemecek¹³⁴, M. Nessi^{37,g}, M.S. Neubauer¹⁶⁸, J. Newell⁹⁴, P.R. Newman²¹, Y.W.Y. Ng¹⁶⁸, B. Ngair^{119a}, H.D.N. Nguyen¹¹⁰, J.D. Nichols¹²³, R.B. Nickerson¹²⁹, R. Nicolaidou¹³⁸, J. Nielsen¹³⁹, M. Niemeyer⁵⁵, J. Niermann³⁷, N. Nikiforov³⁷, V. Nikolaenko^{38,a}, I. Nikolic-Audit¹³⁰, P. Nilsson³⁰, I. Ninca⁴⁸, G. Ninio¹⁵⁷, A. Nisati^{75a}, R. Nisius¹¹², N. Nitika^{69a,69c}, J.-E. Nitschke⁵⁰, E.K. Nkdimeng^{34b}, T. Nobe¹⁵⁷, D. Noll^{18a}, T. Nommensen¹⁵³, M.B. Norfolk¹⁴⁵, B.J. Norman³⁵, M. Noury^{36a}, J. Novak⁹⁵, T. Novak⁹⁵, R. Novotny¹³⁵, L. Nozka¹²⁵, K. Ntekas¹⁶⁵, N.M.J. Nunes De Moura Junior^{83b}, J. Ocariz¹³⁰, A. Ochi⁸⁶, I. Ochoa^{133a}, S. Oerdek^{48,y}, J.T. Offermann⁴⁰, A. Ogrodnik¹³⁶, A. Oh¹⁰³, C.C. Ohm¹⁵⁰, H. Oide⁸⁴, M.L. Ojeda³⁷, Y. Okumura¹⁵⁹, L.F. Oleiro Seabra^{133a}, I. Oleksiyuk⁵⁶, G. Oliveira Correa¹³, D. Oliveira Damazio³⁰, J.L. Oliver¹⁶⁵, R. Omar⁶⁸, Ö. Öncel⁵⁴, A.P. O'Neill²⁰, A. Onofre^{133a,133e}, P.U.E. Onyisi¹¹, M.J. Oreglia⁴⁰, D. Orestano^{77a,77b}, R. Orlandini^{77a,77b}, R.S. Orr¹⁶¹, L.M. Osojnak¹³¹, Y. Osumi¹¹³, G. Otero y Garzon³¹, H. Otono⁹⁰, M. Ouchrif^{56d}, F. Ould-Saada¹²⁸, T. Ovsiannikova¹⁴², M. Owen⁵⁹, R.E. Owen¹³⁷, V.E. Ozcan^{22a}, F. Ozturk⁸⁸, N. Ozturk⁸, S. Ozturk⁸², H.A. Pacey¹²⁹, K. Pachal^{162a}, A. Pacheco Pages¹³, C. Padilla Aranda¹³, G. Padovano^{75a,75b}, S. Pagan Griso^{18a}, G. Palacino⁶⁸, A. Palazzo^{70a,70b}, J. Pampel²⁵, J. Pan¹⁷⁸, T. Pan^{64a}, D.K. Panchal¹¹, C.E. Pandini⁶⁰, J.G. Panduro Vazquez¹³⁷, H.D. Pandya¹, H. Pang¹³⁸, P. Pani⁴⁸, G. Panizzo^{69a,69c}, L. Panwar¹³⁰, L. Paolozzi⁵⁶, S. Parajuli¹⁶⁸, A. Paramonov⁶, C. Paraskevopoulos⁵³, D. Paredes Hernandez^{64b}, A. Pareti^{73a,73b}, K.R. Park⁴², T.H. Park¹¹², F. Parodi^{57b,57a}, J.A. Parsons⁴², U. Parzefall⁵⁴, B. Pascual Dias⁴¹, L. Pascual Dominguez¹⁰¹, E. Pasqualucci^{75a}, S. Passaggio^{57b}, F. Pastore⁹⁷, P. Patel⁸⁸, U.M. Patel⁵¹, J.R. Pater¹⁰³, T. Pauly³⁷, F. Pauwels¹³⁶, C.I. Pazos¹⁶⁴, M. Pedersen¹²⁸, R. Pedro^{133a}, S.V. Peleganchuk³⁸, O. Penc¹³⁴, E.A. Pender⁵², S. Peng¹⁵, G.D. Penn¹⁷⁸, K.E. Pensi¹¹¹, M. Penzin³⁸, B.S. Peralva^{83d}, A.P. Pereira Peixoto¹⁴², L. Pereira Sanchez¹⁴⁹, D.V. Perepelitsa^{30,aj}, G. Perera¹⁰⁵, E. Perez Codina³⁷, M. Perganti¹⁰, H. Pernegger³⁷, S. Perrella^{75a,75b}, K. Peters⁴⁸, R.F.Y. Peters¹⁰³, B.A. Petersen³⁷, T.C. Petersen⁴³, E. Petit¹⁰⁴, V. Petousis¹³⁵, A.R. Petri^{71a,71b}, C. Petridou^{158,d}, T. Petru¹³⁶, A. Petrukhin¹⁴⁷, M. Pettee^{18a}, A. Petukhov⁸², K. Petukhova³⁷, R. Pezoa^{140g}, L. Pezzotti^{24b,24a}, G. Pezzullo¹⁷⁸, L. Pfaffenbichler³⁷, A.J. Pflieger⁷⁹, T.M. Pham¹⁷⁶, T. Pham¹⁰⁷, P.W. Phillips¹³⁷, G. Piacquadio¹⁵¹, E. Pianori^{18a}, F. Piazza¹²⁶, R. Piegaia³¹, D. Pietreanu^{28b}, A.D. Pilkington¹⁰³, M. Pinamonti^{69a,69c}, J.L. Pinfold², B.C. Pinheiro Pereira^{133a}, J. Pinol Bel¹³, A.E. Pinto Pinoargote¹³⁰, L. Pintucci^{69a,69c}, K.M. Piper¹⁵², A. Pirttikoski⁵⁶, D.A. Pizzi³⁵, L. Pizzimento^{64b}, A. Plebani³³, M.-A. Pleier³⁰, V. Pleskot¹³⁶, E. Plotnikova³⁹, G. Poddar⁹⁶, R. Poettgen¹⁰⁰, L. Poggioli¹³⁰, S. Polacek¹³⁶, G. Polesello^{73a}, A. Poley¹⁴⁸, A. Polini^{24b}, C.S. Pollard¹⁷³, Z.B. Pollock¹²², E. Pompa Pacchi¹²³, N.I. Pond⁹⁸, D. Ponomarenko⁶⁸, L. Pontecorvo³⁷, S. Popa^{28a}, G.A. Popeneciu^{28d}, A. Poreba³⁷, D.M. Portillo Quintero^{162a}, S. Pospisil¹³⁵, M.A. Postill¹⁴⁵, P. Postolache^{28c}, K. Potamianos¹⁷³, P.A. Potepa^{87a}, I.N. Potrap³⁹, C.J. Potter³³, H. Potti¹⁵³, J. Poveda¹⁶⁹, M.E. Pozo Astigarraga³⁷, R. Pozzi³⁷, A. Prades Ibanez^{76a,76b}, S.R. Pradhan¹⁴⁵, J. Pretel¹⁷¹, D. Price¹⁰³, M. Primavera^{70a}, L. Primomo^{69a,69c}, M.A. Principe Martin¹⁰¹, R. Privara¹²⁵, T. Procter^{87b}, M.L. Proffitt¹⁴², N. Proklova¹³¹, K. Prokofiev^{64c}, G. Proto¹¹², J. Proudfoot⁶, M. Przybycien^{87a}, W.W. Przygoda^{87b}, A. Psallidas⁴⁶, J.E. Pudefoot¹⁴⁵, D. Pudza⁵³, H.I. Purnell², D. Pyatizbyantseva¹¹⁶, J. Qian¹⁰⁸, R. Qian¹⁰⁹, D. Qichen¹²⁹, Y. Qin¹³, T. Qiu⁵², A. Quadt⁵⁵, M. Queitsch-Maitland¹⁰³, G. Quetant⁵⁶, R.P. Quinn¹⁷⁰, G. Rabanal Bolanos⁶¹, D. Rafanoharana¹², F. Raffaelli^{76a,76b}, F. Ragusa^{71a,71b}, J.L. Rainbolt⁴⁰, S. Rajagopalan³⁰, E. Ramakoti³⁹, L. Rambelli^{57b,57a}, I.A. Ramirez-Berend³⁵, K. Ran^{48,114c}, D.S. Rankin¹³¹, N.P.

Rapheeha^{34h}, H. Rasheed^{28b}, D.F. Rassloff^{63a}, A. Rastogi^{18a}, S. Rave¹⁰², S. Ravera^{57b,57a}, B. Ravina³⁷, I. Ravinovich¹⁷⁵, M. Raymond³⁷, A.L. Read¹²⁸, N.P. Readioff¹⁴⁵, D.M. Rebuffi^{73a,73b}, A.S. Reed⁵⁹, K. Reeves²⁷, J.A. Reidelsturz¹⁷⁷, D. Reikher¹²⁶, A. Rej⁴⁹, C. Rembser³⁷, H. Ren⁶², M. Renda^{28b}, F. Renner⁴⁸, A.G. Rennie⁵⁹, A.L. Rescia^{57b,57a}, S. Resconi^{71a}, M. Ressegotti^{57b,57a}, S. Rettie³⁷, W.F. Rettie³⁵, M.M. Revering³³, E. Reynolds^{18a}, O.L. Rezanova³⁹, P. Reznicek¹³⁶, H. Riani^{36d}, N. Ribaric⁵¹, B. Ricci^{69a,69c}, E. Ricci^{78a,78b}, R. Richter¹¹², S. Richter^{47a,47b}, E. Richter-Was^{87b}, M. Ridel¹³⁰, S. Ridouani^{36d}, P. Rieck¹²⁰, P. Riedler³⁷, E.M. Riefel^{47a,47b}, J.O. Rieger¹¹⁷, M. Rijssenbeek¹⁵¹, M. Rimoldi³⁷, L. Rinaldi^{24b,24a}, P. Rincke^{167,55}, G. Ripellino¹⁶⁷, I. Riu¹³, J.C. Rivera Vergara¹⁷¹, F. Rizatdinova¹²⁴, E. Rizvi⁹⁶, B.R. Roberts^{18a}, S.S. Roberts¹³⁹, D. Robinson³³, M. Robles Manzano¹⁰², A. Robson⁵⁹, A. Rocchi^{76a,76b}, C. Roda^{74a,74b}, S. Rodriguez Bosca³⁷, Y. Rodriguez Garcia^{23a}, A.M. Rodríguez Vera¹¹⁸, S. Roe³⁷, J.T. Roemer³⁷, O. Røhne¹²⁸, R.A. Rojas³⁷, C.P.A. Roland¹³⁰, A. Romaniouk⁷⁹, E. Romano^{73a,73b}, M. Romano^{24b}, A.C. Romero Hernandez¹⁶⁸, N. Rompotis⁹⁴, L. Roos¹³⁰, S. Rosati^{75a}, B.J. Rosser⁴⁰, E. Rossi¹²⁹, E. Rossi^{72a,72b}, L.P. Rossi⁶¹, L. Rossini⁵⁴, R. Rosten¹²², M. Rotaru^{28b}, B. Rottler⁵⁴, D. Rousseau⁶⁶, D. Rousso⁴⁸, S. Roy-Garand¹⁶¹, A. Rozanov¹⁰⁴, Z.M.A. Rozario⁵⁹, Y. Rozen¹⁵⁶, A. Rubio Jimenez¹⁶⁹, V.H. Ruelas Rivera¹⁹, T.A. Ruggeri¹, A. Ruggiero¹²⁹, A. Ruiz-Martinez¹⁶⁹, A. Rummler³⁷, Z. Rurikova⁵⁴, N.A. Rusakovich³⁹, S. Rusciller⁴⁹, H.L. Russell¹⁷¹, G. Russo^{75a,75b}, J.P. Rutherford⁷, S. Rutherford Colmenares³³, M. Rybar¹³⁶, P. Rybczynski^{87a}, A. Ryzhov⁴⁵, J.A. Sabater Iglesias⁵⁶, H.F.-W. Sadrozinski¹³⁹, F. Safai Tehrani^{75a}, S. Saha¹, M. Sahinsoy⁸², B. Sahoo¹⁷⁵, A. Saibel¹⁶⁹, B.T. Saifuddin¹²³, M. Saimpert¹³⁸, G.T. Saito^{83c}, M. Saito¹⁵⁹, T. Saito¹⁵⁹, A. Sala^{71a,71b}, A. Salnikov¹⁴⁹, J. Salt¹⁶⁹, A. Salvador Salas¹⁵⁷, F. Salvatore¹⁵², A. Salzburger³⁷, D. Sammel⁵⁴, E. Sampson⁹³, D. Sampsonidis^{158,d}, D. Sampsonidou¹²⁶, J. Sánchez¹⁶⁹, V. Sanchez Sebastian¹⁶⁹, H. Sandaker¹²⁸, C.O. Sander⁴⁸, J.A. Sandesara¹⁷⁶, M. Sandhoff¹⁷⁷, C. Sandoval^{23b}, L. Sanfilippo^{63a}, D.P.C. Sankey¹³⁷, T. Sano⁸⁹, A. Sansoni⁵³, M. Santana Queiroz^{18b}, L. Santi³⁷, C. Santoni⁴¹, H. Santos^{133a,133b}, A. Santra¹⁷⁵, E. Sanzani^{24b,24a}, K.A. Saoucha^{85b}, J.G. Saraiva^{133a,133d}, J. Sardain⁷, O. Sasaki⁸⁴, K. Sato¹⁶³, C. Sauer³⁷, E. Sauvan⁴, P. Savard^{161,ah}, R. Sawada¹⁵⁹, C. Sawyer¹³⁷, L. Sawyer⁹⁹, C. Sbarra^{24b}, A. Sbrizzi^{24b,24a}, T. Scanlon⁹⁸, J. Schaarschmidt¹⁴², U. Schäfer¹⁰², A.C. Schaffer^{66,45}, D. Schaille¹¹¹, R.D. Schamberger¹⁵¹, C. Scharf¹⁹, M.M. Schefer²⁰, V.A. Schegelsky³⁸, D. Scheirich¹³⁶, M. Schernau^{140f}, C. Scheulen⁵⁶, C. Schiavi^{57b,57a}, M. Schioppa^{44b,44a}, B. Schlag¹⁴⁹, S. Schlenker³⁷, J. Schmeing¹⁷⁷, E. Schmidt¹¹², M.A. Schmidt¹⁷⁷, K. Schmieden¹⁰², C. Schmitt¹⁰², N. Schmitt¹⁰², S. Schmitt⁴⁸, N.A. Schneider¹¹¹, L. Schoeffel¹³⁸, A. Schoening^{63b}, P.G. Scholer³⁵, E. Schopf¹⁴⁷, M. Schott²⁵, S. Schramm⁵⁶, T. Schroer⁵⁶, H.-C. Schultz-Coulon¹³⁸, M. Schumacher⁵⁴, B.A. Schumm¹³⁹, Ph. Schune¹³⁸, H.R. Schwartz⁷, A. Schwartzman¹⁴⁹, T.A. Schwarz¹⁰⁸, Ph. Schwemling¹³⁸, R. Schwienhorst¹⁰⁹, F.G. Sciacca²⁰, A. Sciandra³⁰, G. Sciolla²⁷, F. Scuri^{74a}, C.D. Sebastiani³⁷, K. Sedlaczek¹¹⁸, S.C. Seidel¹¹⁵, A. Seiden¹³⁹, B.D. Seidlitz⁴², C. Seitz⁴⁸, J.M. Seixas^{83b}, G. Sekhniaidze^{72a}, L. Selem⁶⁰, N. Semprini-Cesari^{24b,24a}, A. Semushin¹⁷⁹, D. Sengupta⁵⁶, V. Senthilkumar¹⁶⁹, L. Serin⁶⁶, M. Sessa^{72a,72b}, H. Severini¹²³, F. Sforza^{57b,57a}, A. Sfyrla⁵⁶, Q. Sha¹⁴, E. Shabalina⁵⁵, H. Shaddix¹¹⁸, A.H. Shah³³, R. Shaheen¹⁵⁰, J.D. Shahinian¹³¹, M. Shamim³⁷, L.Y. Shan¹⁴, M. Shapiro^{18a}, A. Sharma³⁷, A.S. Sharma¹⁷⁰, P. Sharma³⁰, P.B. Shatalov³⁸, K. Shaw¹⁵², S.M. Shaw¹⁰³, Q. Shen¹⁴, D.J. Sheppard¹⁴⁸, P. Sherwood⁹⁸, L. Shi⁹⁸, X. Shi¹⁴, S. Shimizu⁸⁴, C.O. Shimmin¹⁷⁸, I.P.J. Shipsey^{129,†}, S. Shirabe⁹⁰, M. Shiyakova^{39,z}, M.J. Shochet⁴⁰, D.R. Shope¹²⁸, B. Shrestha¹²³, S. Shrestha^{122,al}, I. Shreyber³⁹, M.J. Shroff¹⁷¹, P. Sicho¹³⁴, A.M. Sickles¹⁶⁸, E. Sideras Haddad^{34h,166}, A.C. Sidley¹¹⁷, A. Sidoti^{24b}, F. Siegert⁵⁰, Dj. Sijacki¹⁶, F. Sili⁹², J.M. Silva⁵², I. Silva Ferreira^{83b}, M.V. Silva Oliveira³⁰, S.B. Silverstein^{47a}, S. Simion⁶⁶, R. Simoniello³⁷, E.L. Simpson¹⁰³, H. Simpson¹⁵², L.R. Simpson⁶, S. Simsek⁸², S. Sindhu⁵⁵, P. Sinervo¹⁶¹, S.N. Singh²⁷, S. Singh³⁰, S. Sinha⁴⁸, S. Sinha¹⁰³, M. Sioli^{24b,24a}, K. Sioulas⁹, I. Siral³⁷, E. Sitnikova⁴⁸, J. Sjölin^{47a,47b}, A. Skaf⁵⁵, E. Skorda²¹, P. Skubic¹²³, M. Slawinska⁸⁸, I. Slazyk¹⁷, I. Sliusar¹²⁸, V. Smakhtin¹⁷⁵, B.H. Smart¹³⁷, S.Yu. Smirnov^{140b}, Y. Smirnov⁸², L.N. Smirnova^{38,a}, O. Smirnova¹⁰⁰, A.C. Smith⁴², D.R. Smith¹⁶⁵, J.L. Smith¹⁰³, M.B. Smith³⁵, R. Smith¹⁴⁹, H. Smitmans¹⁰², M. Smizanska⁹³, K. Smolek¹³⁵, P. Smolyanskiy¹³⁵, A.A. Snesarev³⁹, H.L. Snoek¹¹⁷, S. Snyder³⁰, R. Sobie^{171,ab}, A. Soffer¹⁵⁷, C.A. Solans Sanchez³⁷, E.Yu. Soldatov³⁹, U. Soldevila¹⁶⁹, A.A. Solodkov^{34h}, S. Solomon²⁷, E. Soloshenko³⁹, K. Solovieva⁵⁴, O.V. Solovyanov⁴¹, P. Sommer⁵⁰, A. Sonay¹³, A. Sopczak¹³⁵, A.L. Soppio⁵², F. Sopkova^{29b}, J.D. Sorenson¹¹⁵, I.R. Sotarriva Alvarez¹⁴¹, V. Sotilingam^{63a}, O.J. Soto Sandoval^{140c,140b}, S. Sottocornola⁶⁸, R. Soualah^{85a}, Z. Soumami^{36c}, D. South⁴⁸, N. Soybelman¹⁷⁵, S. Spagnolo^{70a,70b}, M. Spalla¹¹², D. Sperlich⁵⁴, B. Spisso^{72a,72b}, D.P. Spiteri⁵⁹, L. Splendori¹⁰⁴, M. Spusta¹³⁶, E.J. Staats³⁵, R. Stamen^{63a}, E. Stanecka⁸⁸, W. Stanek-Maslouska⁴⁸, M.V. Stange⁵⁰, B. Stanislaus^{18a}, M.M. Stanitzki⁴⁸, B. Stapf⁴⁸, E.A. Starchenko³⁸, G.H. Stark¹³⁹, J. Stark⁹¹, P. Staroba¹³⁴, P. Starovoitov^{85b}, R. Staszewski⁸⁸, C. Stauch¹¹¹, G. Stavropoulos⁴⁶, A. Steff³⁷, A. Stein¹⁰², P. Steinberg³⁰, B. Stelzer^{148,162a}, H.J. Stelzer¹³², O. Stelzer^{162a}, H. Stenzel⁵⁸, T.J. Stevenson¹⁵², G.A. Stewart³⁷, J.R. Stewart¹²⁴, G. Stoica^{28b}, M. Stolarski^{133a}, S. Stonjek¹¹², A. Straessner⁵⁰, J. Strandberg¹⁵⁰, S. Strandberg^{47a,47b}, M. Stratmann¹⁷⁷, M. Strauss¹²³, T. Streblner¹⁰⁴, P. Strizenecek^{29b}, R. Ströhmer¹⁷², D.M. Strom¹²⁶, R. Stroynowski⁴⁵, A. Strubig^{47a,47b}, S.A. Stucci³⁰, B. Stugu¹⁷, J. Stupak¹²³, N.A. Styles⁴⁸, D. Su¹⁴⁹, S. Su⁶², X. Su⁶², D. Suchy^{29a}, K. Sugizaki¹³¹, V.V. Sulim³⁸, D.M.S. Sultan¹²⁹, L. Sultanaliyeva²⁵, S. Sultansoy^{3b}, S. Sun¹⁷⁶, W. Sun¹⁴, O. Sunneborn Gudnadottir¹⁶⁷, N. Sur¹⁰⁰, M.R. Sutton¹⁵², M. Svatos¹³⁴, P.N. Swallow³³, M. Swiatlowski^{162a}, T. Swirski¹⁷², A. Swoboda³⁷, I. Sykora^{29a}, M. Sykora¹³⁶, T. Sykora¹³⁶, D. Ta¹⁰², K. Tackmann^{48,y}, A. Taffard¹⁶⁵, R. Tafirout^{162a}, Y. Takubo⁸⁴, M. Talby¹⁰⁴, A.A. Talyshev³⁸, K.C. Tam^{64b}, N.M. Tamir¹⁵⁷, A. Tanaka¹⁵⁹, J. Tanaka¹⁵⁹, R. Tanaka⁶⁶, M. Tanasini¹⁵¹, Z. Tao¹⁷⁰, S. Tapia Araya^{140g}, S. Tapprogge¹⁰², A. Tarek Bouelfadl Mohamed¹⁰⁹, S. Tarem¹⁵⁶, K. Tariq¹⁴, G. Tarna³⁷, G.F. Tartarelli^{71a}, M.J. Tartarini⁹¹, P. Tas¹³⁶, M. Tasevsky¹³⁴, E. Tassi^{44b,44a}, A.C. Tate¹⁶⁸, Y. Tayalati^{36e,aa}, G.N. Taylor¹⁰⁷, W. Taylor^{162b}, R.J. Taylor Vara¹⁶⁹, A.S. Tegetmeier⁹¹, P. Teixeira-Dias⁹⁷, J.J. Teoh¹⁶¹, K. Terashi¹⁵⁹, J. Terron¹⁰¹, S. Terzo¹³, M. Testa⁵³, R.J. Teuscher^{161,ab}, A. Thaler⁷⁹, O. Theiner⁵⁶, T. Thevenaux-Pelzer¹⁰⁴, D.W. Thomas⁹⁷, J.P. Thomas²¹, E.A. Thompson^{18a}, P.D. Thompson²¹, E. Thomson¹³¹, R.E. Thornberry⁴⁵, C. Tian⁶², Y. Tian⁵⁶, V. Tikhomirov⁸², Yu.A. Tikhonov³⁹, S. Timoshenko³⁸, D. Timoshyn¹³⁶, E.X.L. Ting¹, P. Tipton¹⁷⁸, A. Tishelman-Charny³⁰, K. Todome¹⁴¹, S. Todorova-Nova¹³⁶, L. Toffolin^{69a,69c}, M. Togawa⁸⁴, J. Tojo⁹⁰, S. Tokár^{29a}, O. Toldaiev⁶⁸, G. Tolkachev¹⁰⁴, M. Tomoto⁸⁴, L. Tompkins^{149,n}, E. Torrence¹²⁶, H. Torres⁹¹, E. Torró Pastor¹⁶⁹, M. Toscani³¹, C. Toscin⁴⁰, M. Tost¹¹, D.R. Tovey¹⁴⁵, T. Trefzger¹⁷², P.M. Tricarico¹³, A. Tricoli³⁰, I.M. Trigger^{162a}, S. Trincaz-Duvold¹³⁰, D.A. Trischuk²⁷, A. Tropina³⁹, L. Truong^{34c}, M. Trzebinski⁸⁸, A. Trzupek⁸⁸, F. Tsai¹⁵¹, M. Tsai¹⁰⁸, A. Tsiamsi¹⁵⁸, P.V. Tsiarashka³⁹, S. Tsigaridas^{162a}, A. Tsigiridis^{158,u}, V. Tiskaridze^{155a}, E.G. Tskhadadze^{155a}, M. Tsopoulou¹⁵⁸, Y. Tsujikawa⁸⁹, I.I. Tsukerman³⁸, V. Tsulaia^{18a}, S. Tsuno⁸⁴, K. Tsuru¹²¹, D. Tsybychev¹⁵¹, Y. Tu^{64b}, A. Tudorache^{28b}, V. Tudorache^{28b}, S.B. Tuncay¹²⁹, S. Turchikhin^{57b,57a}, I. Turk Cakir^{3a}, R. Turra^{71a}, T. Turtuvshin^{39,ac}, P.M. Tuts⁴², S. Tzamarias^{158,d}, E. Tzovara¹⁰², Y. Uematsu⁸⁴, F. Ukegawa¹⁶³, P.A. Ulloa Poblete^{140c,140b}, E.N. Umaka³⁰, G. Unal³⁷, A. Undrus³⁰, G. Unel¹⁶⁵, J. Urban^{29b}, P. Urrejola^{140a}, G. Usai⁸, R. Ushioda¹⁶⁰, M. Usman¹¹⁰, F. Ustuner⁵², Z. Uysal⁸², V. Vacek¹³⁵, B. Vachon¹⁰⁶, T. Vafeiadis³⁷, A. Vaitkus⁹⁸, C. Valderanis¹¹¹, E. Valdes Santurio^{47a,47b}, M.

Valente³⁷, S. Valentineti^{24b,24a}, A. Valero¹⁶⁹, E. Valiente Moreno¹⁶⁹, A. Vallier⁹¹, J.A. Valls Ferrer¹⁶⁹, D.R. Van Arneinan¹¹⁷, A. Van Der Graaf⁴⁹, H.Z. Van Der Schyf^{34h}, P. Van Gemmeren⁶, M. Van Rijnbach³⁷, S. Van Stroud⁹⁸, I. Van Vulpen¹¹⁷, P. Vana¹³⁶, M. Vanadia^{76a,76b}, U.M. Vande Voorde¹⁵⁰, W. Vandelli³⁷, E.R. Vandewall¹²⁴, D. Vannicola¹⁵⁷, L. Vannoli⁵³, R. Vari^{75a}, M. Varma¹⁷⁸, E.W. Varnes⁷, C. Varni¹¹⁸, D. Varouchas⁶⁶, L. Varriale¹⁶⁹, K.E. Varvell¹⁵³, M.E. Vasile^{28b}, L. Vasilin⁸⁴, M.D. Vassilev¹⁴⁹, A. Vasyukov³⁹, L.M. Vaughan¹²⁴, R. Vavricka¹³⁶, T. Vazquez Schroeder¹³, J. Veatch³², V. Vecchio¹⁰³, M.J. Veen¹⁰⁵, I. Veliscek³⁰, I. Velkovska⁹⁵, L.M. Veloce¹⁶¹, F. Veloso^{133a,133c}, S. Veneziano^{75a}, A. Ventura^{70a,70b}, A. Verbitskiy¹¹², M. Verducci^{74a,74b}, C. Vergis⁹⁶, M. Verissimo De Araujo^{83b}, W. Verkerke¹¹⁷, J.C. Vermeulen¹¹⁷, C. Vernieri¹⁴⁹, M. Vessella¹⁶⁵, M.C. Vetterli^{148,ah}, A. Vgenopoulos¹⁰², N. Viaux Maira^{140g}, T. Vickey¹⁴⁵, O.E. Vickey Boeriu¹⁴⁵, G.H.A. Viehhauser¹²⁹, L. Viganì^{63b}, M. Vigi¹¹², M. Villa^{24b,24a}, M. Villaplana Perez¹⁶⁹, E.M. Villhauer⁴⁰, E. Vilucchi⁵³, M. Vincent¹⁶⁹, M.G. Vincker³⁵, A. Visibile¹¹⁷, C. Vittori³⁷, I. Vivarelli^{24b,24a}, E. Voevodina¹¹², F. Vogel¹¹¹, J.C. Voigt⁵⁰, P. Vokac¹³⁵, Yu. Volkotrub^{87b}, L. Vomberg²⁵, E. Von Toerne²⁵, B. Vormwald³⁷, K. Vorobev⁵¹, M. Vos¹⁶⁹, K. Voss¹⁴⁷, M. Vozak³⁷, L. Vozdecky¹²³, N. Vranjes¹⁶, M. Vranjes Milosavljevic¹⁶, M. Vreeswijk¹¹⁷, N.K. Vu^{144b,144a}, R. Vuillermet³⁷, O. Vujanovic¹⁰², I. Vukotic⁴⁰, I.K. Vyas³⁵, J.F. Wack³³, S. Wada¹⁶³, C. Wagner¹⁴⁹, J.M. Wagner^{18a}, W. Wagner¹⁷⁷, S. Wahdan¹⁷⁷, H. Wahlberg⁹², C.H. Waits¹²³, J. Walder¹³⁷, R. Walker¹¹¹, K. Walkingshaw Pass⁵⁹, W. Walkowiak¹⁴⁷, A. Wall¹³¹, E.J. Wallin¹⁰⁰, T. Wamorkar^{18a}, K. Wandall-Christensen¹⁶⁹, A. Wang⁶², A.Z. Wang¹³⁹, C. Wang¹⁰², C. Wang¹¹, H. Wang^{18a}, J. Wang^{64c}, P. Wang¹⁰³, P. Wang⁹⁸, R. Wang⁶¹, R. Wang⁶, S.M. Wang¹⁵⁴, S. Wang¹⁴, T. Wang¹¹⁶, T. Wang⁶², W.T. Wang⁸⁰, W. Wang¹⁴, X. Wang¹⁶⁸, X. Wang^{144a}, X. Wang⁴⁸, Y. Wang^{114a}, Y. Wang⁶², Z. Wang¹⁰⁸, Z. Wang^{144b}, Z. Wang¹⁰⁸, C. Wanotayaroj⁸⁴, A. Warburton¹⁰⁶, A.L. Warnerbring¹⁴⁷, S. Waterhouse⁹⁷, A.T. Watson²¹, H. Watson⁵², M.F. Watson²¹, E. Watton⁵⁹, G. Watts¹⁴², B.M. Waugh⁹⁸, J.M. Webb⁵⁴, C. Weber³⁰, H.A. Weber¹⁹, M.S. Weber²⁰, S.M. Weber^{63a}, C. Wei⁶², Y. Wei⁵⁴, A.R. Weidberg¹²⁹, E.J. Weik¹²⁰, J. Weingarten⁴⁹, C. Weiser⁵⁴, C.J. Wells⁴⁸, T. Wenaus³⁰, T. Wengler³⁷, N.S. Wenke¹¹², N. Wermes²⁵, M. Wessels^{63a}, A.M. Wharton⁹³, A.S. White⁶¹, A. White⁸, M.J. White¹, D. Whiteson¹⁶⁵, L. Wickremasinghe¹²⁷, W. Wiedenmann¹⁷⁶, M. Wieler¹³⁷, R. Wierda¹⁵⁰, C. Wiglesworth⁴³, H.G. Wilkens³⁷, J.J.H. Wilkinson³³, D.M. Williams⁴², H.H. Williams¹³¹, S. Williams³³, S. Willocq¹⁰⁵, B.J. Wilson¹⁰³, D.J. Wilson¹⁰³, P.J. Windischhofer⁴⁰, F.I. Winkel³¹, F. Winklmeier¹²⁶, B.T. Winter⁵⁴, M. Wittgen¹⁴⁹, M. Wobisch⁹⁹, T. Wojtkowski⁶⁰, Z. Wolffs¹¹⁷, J. Wollrath³⁷, M.W. Wolter⁸⁸, H. Wolters^{133a,133c}, M.C. Wong¹³⁹, E.L. Woodward⁴², S.D. Worm⁴⁸, B.K. Wosiek⁸⁸, K.W. Woźniak⁸⁸, S. Wozniowski⁵⁵, K. Wraight⁵⁹, C. Wu¹⁶¹, C. Wu²¹, J. Wu¹⁵⁹, M. Wu^{114b}, M. Wu¹¹⁶, S.L. Wu¹⁷⁶, S. Wu¹⁴, X. Wu⁶², Y. Wu⁶², Z. Wu⁴, Z. Wu^{114a}, J. Wuerzinger¹¹², T.R. Wyatt¹⁰³, B.M. Wynne⁵², S. Xella⁴³, L. Xia^{114a}, M. Xia¹⁵, M. Xie⁶², A. Xiong¹²⁶, J. Xiong^{18a}, D. Xu¹⁴, H. Xu⁶², L. Xu⁶², R. Xu¹³¹, T. Xu¹⁰⁸, Y. Xu¹⁴², Z. Xu⁵², R. Xue¹³², B. Yabsley¹⁵³, S. Yacoob^{34a}, Y. Yamaguchi⁸⁴, E. Yamashita¹⁵⁹, H. Yamauchi¹⁶³, T. Yamazaki^{18a}, Y. Yamazaki⁸⁶, S. Yan⁵⁹, Z. Yan¹⁰⁵, H.J. Yang^{144a,144b}, H.T. Yang⁶², S. Yang⁶², T. Yang^{64c}, X. Yang³⁷, X. Yang¹⁴, Y. Yang¹⁵⁹, Y. Yang⁶², W.-M. Yao^{18a}, C.L. Yardley¹⁵², J. Ye¹⁴, S. Ye³⁰, X. Ye⁶², Y. Yeh⁹⁸, I. Yeletsikh³⁹, B. Yeo^{18b}, M.R. Yexley⁹⁸, T.P. Yildirim¹²⁹, K. Yorita¹⁷⁴, C.J.S. Young³⁷, C. Young¹⁴⁹, N.D. Young¹²⁶, Y. Yu⁶², J. Yuan^{14,114c}, M. Yuan¹⁰⁸, R. Yuan^{144b,144a}, L. Yue⁹⁸, M. Zaazoua⁶², B. Zabinski⁸⁸, I. Zahir^{36a}, A. Zaiō^{57b,57a}, Z.K. Zak⁸⁸, T. Zakareishvili¹⁶⁹, S. Zambito⁵⁶, J.A. Zamora Saa^{140d}, J. Zang¹⁵⁹, R. Zanzottera^{71a,71b}, O. Zaplatilek¹³⁵, C. Zeitnitz¹⁷⁷, H. Zeng¹⁴, J.C. Zeng¹⁶⁸, D.T. Zenger Jr²⁷, O. Zenin³⁸, T. Ženiš^{29a}, S. Zenz⁹⁶, D. Zerwas⁶⁶, M. Zhai^{14,114c}, D.F.

Zhang¹⁴⁵, G. Zhang¹⁴, J. Zhang^{143a}, J. Zhang⁶, K. Zhang^{14,114c}, L. Zhang⁶², L. Zhang^{114a}, P. Zhang^{14,114c}, R. Zhang^{114a}, S. Zhang⁹¹, T. Zhang¹⁵⁹, Y. Zhang¹⁴², Y. Zhang⁹⁸, Y. Zhang⁶², Y. Zhang^{114a}, Z. Zhang^{143a}, Z. Zhang⁶⁶, H. Zhao¹⁴², T. Zhao^{143a}, Y. Zhao³⁵, Z. Zhao⁶², Z. Zhao⁶², A. Zhemchugov³⁹, J. Zheng^{114a}, K. Zheng¹⁶⁸, X. Zheng⁶², Z. Zheng¹⁴⁹, D. Zhong¹⁶⁸, B. Zhou¹⁰⁸, H. Zhou⁷, N. Zhou^{144a}, Y. Zhou¹⁵, Y. Zhou^{114a}, Y. Zhou⁷, C.G. Zhu^{143a}, J. Zhu¹⁰⁸, X. Zhu^{144b}, Y. Zhu^{144a}, Y. Zhu⁶², X. Zhuang¹⁴, K. Zhukov⁶⁸, N.I. Zimine³⁹, J. Zinsser^{63b}, M. Ziolkowski¹⁴⁷, L. Živković¹⁶, A. Zoccoli^{24b,24a}, K. Zoch⁶¹, A. Zografos³⁷, T.G. Zorbas¹⁴⁵, O. Zormpa⁴⁶, L. Zwalinski³⁷,

¹ Department of Physics, University of Adelaide, Adelaide, Australia

² Department of Physics, University of Alberta, Edmonton, AB, Canada

^{3a} Department of Physics, Ankara University, Ankara

^{3b} Division of Physics, TOBB University of Economics and Technology, Ankara, Türkiye

⁴ LAPP, Université Savoie Mont Blanc, CNRS/IN2P3, Annecy, France

⁵ APC, Université Paris Cité, CNRS/IN2P3, Paris, France

⁶ High Energy Physics Division, Argonne National Laboratory, Argonne, IL, United States of America

⁷ Department of Physics, University of Arizona, Tucson, AZ, United States of America

⁸ Department of Physics, University of Texas at Arlington, Arlington, TX, United States of America

⁹ Physics Department, National and Kapodistrian University of Athens, Athens, Greece

¹⁰ Physics Department, National Technical University of Athens, Zografou, Greece

¹¹ Department of Physics, University of Texas at Austin, Austin, TX, United States of America

¹² Institute of Physics, Azerbaijan Academy of Sciences, Baku, Azerbaijan

¹³ Institut de Física d'Altes Energies (IFAE), Barcelona Institute of Science and Technology, Barcelona, Spain

¹⁴ Institute of High Energy Physics, Chinese Academy of Sciences, Beijing, China

¹⁵ Physics Department, Tsinghua University, Beijing, China

¹⁶ Institute of Physics, University of Belgrade, Belgrade, Serbia

¹⁷ Department for Physics and Technology, University of Bergen, Bergen, Norway

^{18a} Physics Division, Lawrence Berkeley National Laboratory, Berkeley, CA

^{18b} University of California, Berkeley, CA, United States of America

¹⁹ Institut für Physik, Humboldt Universität zu Berlin, Berlin, Germany

²⁰ Albert Einstein Center for Fundamental Physics and Laboratory for High Energy Physics, University of Bern, Bern, Switzerland

²¹ School of Physics and Astronomy, University of Birmingham, Birmingham, United Kingdom

^{22a} Department of Physics, Bogazici University, Istanbul

^{22b} Department of Physics Engineering, Gaziantep University, Gaziantep

^{22c} Department of Physics, Istanbul University, Istanbul, Türkiye

^{23a} Facultad de Ciencias y Centro de Investigaciones, Universidad Antonio Nariño, Bogotá

^{23b} Departamento de Física, Universidad Nacional de Colombia, Bogotá, Colombia

^{24a} Dipartimento di Fisica e Astronomia A. Righi, Università di Bologna, Bologna

^{24b} INFN Sezione di Bologna, Italy

²⁵ Physikalisches Institut, Universität Bonn, Bonn, Germany

²⁶ Department of Physics, Boston University, Boston, MA, United States of America

²⁷ Department of Physics, Brandeis University, Waltham, MA, United States of America

^{28a} Transilvania University of Brasov, Brasov

- ^{28b} Horia Hulubei National Institute of Physics and Nuclear Engineering, Bucharest
- ^{28c} Department of Physics, Alexandru Ioan Cuza University of Iasi, Iasi
- ^{28d} National Institute for Research and Development of Isotopic and Molecular Technologies, Physics Department, Cluj-Napoca
- ^{28e} National University of Science and Technology Politehnica, Bucharest
- ^{28f} West University in Timisoara, Timisoara
- ^{28g} Faculty of Physics, University of Bucharest, Bucharest, Romania
- ^{29a} Faculty of Mathematics, Physics and Informatics, Comenius University, Bratislava
- ^{29b} Department of Subnuclear Physics, Institute of Experimental Physics, Slovak Academy of Sciences, Kosice, Slovak Republic
- ³⁰ Physics Department, Brookhaven National Laboratory, Upton, NY, United States of America
- ³¹ Universidad de Buenos Aires, Facultad de Ciencias Exactas y Naturales, Departamento de Física, y CONICET, Instituto de Física de Buenos Aires (IFIBA), Buenos Aires, Argentina
- ³² California State University, CA, United States of America
- ³³ Cavendish Laboratory, University of Cambridge, Cambridge, United Kingdom
- ^{34a} Department of Physics, University of Cape Town, Cape Town
- ^{34b} iThemba Labs, Western Cape
- ^{34c} Department of Mechanical Engineering Science, University of Johannesburg, Johannesburg
- ^{34d} National Institute of Physics, University of the Philippines Diliman, Philippines
- ^{34e} Department of Physics, Stellenbosch University, Matieland
- ^{34f} Department of Physics, University of South Africa, Pretoria
- ^{34g} University of Zululand, KwaDlangezwa
- ^{34h} School of Physics, University of the Witwatersrand, Johannesburg, South Africa
- ³⁵ Department of Physics, Carleton University, Ottawa, ON, Canada
- ^{36a} Faculté des Sciences Ain Chock, Université Hassan II de Casablanca
- ^{36b} Faculté des Sciences, Université Ibn-Tofail, Kénitra
- ^{36c} Faculté des Sciences Semlalia, Université Cadi Ayyad, LPHEA-Marrakech
- ^{36d} LPMR, Faculté des Sciences, Université Mohamed Premier, Oujda
- ^{36e} Faculté des sciences, Université Mohammed V, Rabat
- ^{36f} Institute of Applied Physics, Mohammed VI Polytechnic University, Ben Guerir, Morocco
- ³⁷ CERN, Geneva, Switzerland
- ³⁸ Affiliated with an institute formerly covered by a cooperation agreement with CERN
- ³⁹ Affiliated with an international laboratory covered by a cooperation agreement with CERN
- ⁴⁰ Enrico Fermi Institute, University of Chicago, Chicago, IL, United States of America
- ⁴¹ LPC, Université Clermont Auvergne, CNRS/IN2P3, Clermont-Ferrand, France
- ⁴² Nevis Laboratory, Columbia University, Irvington, NY, United States of America
- ⁴³ Niels Bohr Institute, University of Copenhagen, Copenhagen, Denmark
- ^{44a} Dipartimento di Fisica, Università della Calabria, Rende
- ^{44b} INFN Gruppo Collegato di Cosenza, Laboratori Nazionali di Frascati, Italy
- ⁴⁵ Physics Department, Southern Methodist University, Dallas, TX, United States of America
- ⁴⁶ National Centre for Scientific Research “Demokritos”, Agia Paraskevi, Greece
- ^{47a} Department of Physics, Stockholm University
- ^{47b} Oskar Klein Centre, Stockholm, Sweden
- ⁴⁸ Deutsches Elektronen-Synchrotron DESY, Hamburg and Zeuthen, Germany
- ⁴⁹ Fakultät Physik, Technische Universität Dortmund, Dortmund, Germany
- ⁵⁰ Institut für Kern- und Teilchenphysik, Technische Universität Dresden, Dresden, Germany
- ⁵¹ Department of Physics, Duke University, Durham, NC, United States of America
- ⁵² SUPA - School of Physics and Astronomy, University of Edinburgh, Edinburgh, United Kingdom
- ⁵³ INFN e Laboratori Nazionali di Frascati, Frascati, Italy
- ⁵⁴ Physikalisches Institut, Albert-Ludwigs-Universität Freiburg, Freiburg, Germany
- ⁵⁵ II. Physikalisches Institut, Georg-August-Universität Göttingen, Göttingen, Germany
- ⁵⁶ Département de Physique Nucléaire et Corpusculaire, Université de Genève, Genève, Switzerland
- ^{57a} Dipartimento di Fisica, Università di Genova, Genova
- ^{57b} INFN Sezione di Genova, Italy
- ⁵⁸ II. Physikalisches Institut, Justus-Liebig-Universität Giessen, Giessen, Germany
- ⁵⁹ SUPA - School of Physics and Astronomy, University of Glasgow, Glasgow, United Kingdom
- ⁶⁰ LPSC, Université Grenoble Alpes, CNRS/IN2P3, Grenoble INP, Grenoble, France
- ⁶¹ Laboratory for Particle Physics and Cosmology, Harvard University, Cambridge, MA, United States of America
- ⁶² Department of Modern Physics and State Key Laboratory of Particle Detection and Electronics, University of Science and Technology of China, Hefei, China
- ^{63a} Kirchhoff-Institut für Physik, Ruprecht-Karls-Universität Heidelberg, Heidelberg
- ^{63b} Physikalisches Institut, Ruprecht-Karls-Universität Heidelberg, Heidelberg, Germany
- ^{64a} Department of Physics, Chinese University of Hong Kong, Shatin, N.T., Hong Kong
- ^{64b} Department of Physics, University of Hong Kong, Hong Kong
- ^{64c} Department of Physics and Institute for Advanced Study, Hong Kong University of Science and Technology, Clear Water Bay, Kowloon, Hong Kong, China
- ⁶⁵ Department of Physics, National Tsing Hua University, Hsinchu, Taiwan
- ⁶⁶ IJCLab, Université Paris-Saclay, CNRS/IN2P3, 91405, Orsay, France
- ⁶⁷ Centro Nacional de Microelectrónica (IMB-CNM-CSIC), Barcelona, Spain
- ⁶⁸ Department of Physics, Indiana University, Bloomington, IN, United States of America
- ^{69a} INFN Gruppo Collegato di Udine, Sezione di Trieste, Udine
- ^{69b} ICTP, Trieste
- ^{69c} Dipartimento Politecnico di Ingegneria e Architettura, Università di Udine, Udine, Italy
- ^{70a} INFN Sezione di Lecce
- ^{70b} Dipartimento di Matematica e Fisica, Università del Salento, Lecce, Italy
- ^{71a} INFN Sezione di Milano
- ^{71b} Dipartimento di Fisica, Università di Milano, Milano, Italy
- ^{72a} INFN Sezione di Napoli
- ^{72b} Dipartimento di Fisica, Università di Napoli, Napoli, Italy
- ^{73a} INFN Sezione di Pavia
- ^{73b} Dipartimento di Fisica, Università di Pavia, Pavia, Italy
- ^{74a} INFN Sezione di Pisa
- ^{74b} Dipartimento di Fisica E. Fermi, Università di Pisa, Pisa, Italy
- ^{75a} INFN Sezione di Roma
- ^{75b} Dipartimento di Fisica, Sapienza Università di Roma, Roma, Italy
- ^{76a} INFN Sezione di Roma Tor Vergata
- ^{76b} Dipartimento di Fisica, Università di Roma Tor Vergata, Roma, Italy
- ^{77a} INFN Sezione di Roma Tre

- ^{77b} Dipartimento di Matematica e Fisica, Università Roma Tre, Roma, Italy
- ^{78a} INFN-TIFPA
- ^{78b} Università degli Studi di Trento, Trento, Italy
- ⁷⁹ Universität Innsbruck, Department of Astro and Particle Physics, Innsbruck, Austria
- ⁸⁰ University of Iowa, Iowa City, IA, United States of America
- ⁸¹ Department of Physics and Astronomy, Iowa State University, Ames, IA, United States of America
- ⁸² Istinye University, Sariyer, Istanbul, Türkiye
- ^{83a} Departamento de Engenharia Elétrica, Universidade Federal de Juiz de Fora (UFJF), Juiz de Fora
- ^{83b} Universidade Federal do Rio De Janeiro COPPE/EE/IF, Rio de Janeiro
- ^{83c} Instituto de Física, Universidade de São Paulo, São Paulo
- ^{83d} Rio de Janeiro State University, Rio de Janeiro
- ^{83e} Federal University of Bahia, Bahia, Brazil
- ⁸⁴ KEK, High Energy Accelerator Research Organization, Tsukuba, Japan
- ^{85a} Khalifa University of Science and Technology, Abu Dhabi
- ^{85b} University of Sharjah, Sharjah, United Arab Emirates
- ⁸⁶ Graduate School of Science, Kobe University, Kobe, Japan
- ^{87a} Faculty of Physics and Applied Computer Science, AGH University of Krakow, Krakow
- ^{87b} Marian Smoluchowski Institute of Physics, Jagiellonian University, Krakow, Poland
- ⁸⁸ Institute of Nuclear Physics, Polish Academy of Sciences, Krakow, Poland
- ⁸⁹ Faculty of Science, Kyoto University, Kyoto, Japan
- ⁹⁰ Research Center for Advanced Particle Physics and Department of Physics, Kyushu University, Fukuoka, Japan
- ⁹¹ L2IT, Université de Toulouse, CNRS/IN2P3, UPS, Toulouse, France
- ⁹² Instituto de Física La Plata, Universidad Nacional de La Plata and CONICET, La Plata, Argentina
- ⁹³ Physics Department, Lancaster University, Lancaster, United Kingdom
- ⁹⁴ Oliver Lodge Laboratory, University of Liverpool, Liverpool, United Kingdom
- ⁹⁵ Department of Experimental Particle Physics, Jožef Stefan Institute and Department of Physics, University of Ljubljana, Ljubljana, Slovenia
- ⁹⁶ Department of Physics and Astronomy, Queen Mary University of London, London, United Kingdom
- ⁹⁷ Department of Physics, Royal Holloway University of London, Egham, United Kingdom
- ⁹⁸ Department of Physics and Astronomy, University College London, London, United Kingdom
- ⁹⁹ Louisiana Tech University, Ruston, LA, United States of America
- ¹⁰⁰ Fysiska institutionen, Lunds universitet, Lund, Sweden
- ¹⁰¹ Departamento de Física Teórica C-15 and CIAFF, Universidad Autónoma de Madrid, Madrid, Spain
- ¹⁰² Institut für Physik, Universität Mainz, Mainz, Germany
- ¹⁰³ School of Physics and Astronomy, University of Manchester, Manchester, United Kingdom
- ¹⁰⁴ CPPM, Aix-Marseille Université, CNRS/IN2P3, Marseille, France
- ¹⁰⁵ Department of Physics, University of Massachusetts, Amherst, MA, United States of America
- ¹⁰⁶ Department of Physics, McGill University, Montreal, QC, Canada
- ¹⁰⁷ School of Physics, University of Melbourne, Victoria, Australia
- ¹⁰⁸ Department of Physics, University of Michigan, Ann Arbor, MI, United States of America
- ¹⁰⁹ Department of Physics and Astronomy, Michigan State University, East Lansing, MI, United States of America
- ¹¹⁰ Group of Particle Physics, University of Montreal, Montreal, QC, Canada
- ¹¹¹ Fakultät für Physik, Ludwig-Maximilians-Universität München, München, Germany
- ¹¹² Max-Planck-Institut für Physik (Werner-Heisenberg-Institut), München, Germany
- ¹¹³ Graduate School of Science and Kobayashi-Maskawa Institute, Nagoya University, Nagoya, Japan
- ^{114a} Department of Physics, Nanjing University, Nanjing
- ^{114b} School of Science, Shenzhen Campus of Sun Yat-sen University
- ^{114c} University of Chinese Academy of Science (UCAS), Beijing, China
- ¹¹⁵ Department of Physics and Astronomy, University of New Mexico, Albuquerque, NM, United States of America
- ¹¹⁶ Institute for Mathematics, Astrophysics and Particle Physics, Radboud University/Nikhef, Nijmegen, Netherlands
- ¹¹⁷ Nikhef National Institute for Subatomic Physics and University of Amsterdam, Amsterdam, Netherlands
- ¹¹⁸ Department of Physics, Northern Illinois University, DeKalb, IL, United States of America
- ^{119a} New York University Abu Dhabi, Abu Dhabi
- ^{119b} United Arab Emirates University, Al Ain, United Arab Emirates
- ¹²⁰ Department of Physics, New York University, New York, NY, United States of America
- ¹²¹ Ochanomizu University, Otsuka, Bunkyo-ku, Tokyo, Japan
- ¹²² Ohio State University, Columbus, OH, United States of America
- ¹²³ Homer L. Dodge Department of Physics and Astronomy, University of Oklahoma, Norman, OK, United States of America
- ¹²⁴ Department of Physics, Oklahoma State University, Stillwater, OK, United States of America
- ¹²⁵ Joint Laboratory of Optics, Palacký University, Olomouc, Czech Republic
- ¹²⁶ Institute for Fundamental Science, University of Oregon, Eugene, OR, United States of America
- ¹²⁷ Graduate School of Science, University of Osaka, Osaka, Japan
- ¹²⁸ Department of Physics, University of Oslo, Oslo, Norway
- ¹²⁹ Department of Physics, Oxford University, Oxford, United Kingdom
- ¹³⁰ LPNHE, Sorbonne Université, Université Paris Cité, CNRS/IN2P3, Paris, France
- ¹³¹ Department of Physics, University of Pennsylvania, Philadelphia, PA, United States of America
- ¹³² Department of Physics and Astronomy, University of Pittsburgh, Pittsburgh, PA, United States of America
- ^{133a} Laboratório de Instrumentação e Física Experimental de Partículas - LIP, Lisboa
- ^{133b} Departamento de Física, Faculdade de Ciências, Universidade de Lisboa, Lisboa
- ^{133c} Departamento de Física, Universidade de Coimbra, Coimbra
- ^{133d} Centro de Física Nuclear da Universidade de Lisboa, Lisboa
- ^{133e} Departamento de Física, Escola de Ciências, Universidade do Minho, Braga
- ^{133f} Departamento de Física Teórica y del Cosmos, Universidad de Granada, Granada, Spain
- ^{133g} Departamento de Física, Instituto Superior Técnico, Universidade de Lisboa, Lisboa, Portugal
- ¹³⁴ Institute of Physics, Czech Academy of Sciences, Prague, Czech Republic
- ¹³⁵ Czech Technical University in Prague, Prague, Czech Republic
- ¹³⁶ Faculty of Mathematics and Physics, Charles University, Prague, Czech Republic
- ¹³⁷ Particle Physics Department, Rutherford Appleton Laboratory, Didcot, United Kingdom
- ¹³⁸ IRFU, CEA, Université Paris-Saclay, Gif-sur-Yvette, France
- ¹³⁹ Santa Cruz Institute for Particle Physics, University of California Santa Cruz, Santa Cruz, CA, United States of America
- ^{140a} Departamento de Física, Pontificia Universidad Católica de Chile, Santiago
- ^{140b} Millennium Institute for Subatomic physics at high energy frontier (SAPHIR), Santiago
- ^{140c} Instituto de Investigación Multidisciplinario en Ciencia y Tecnología, y Departamento de Física, Universidad de La Serena

- ^{140d} Department of Physics, Universidad Andres Bello, Santiago
- ^{140e} Universidad San Sebastian, Recoleta
- ^{140f} Instituto de Alta Investigación, Universidad de Tarapacá, Arica
- ^{140g} Departamento de Física, Universidad Técnica Federico Santa María, Valparaíso, Chile
- ¹⁴¹ Department of Physics, Institute of Science, Tokyo, Japan
- ¹⁴² Department of Physics, University of Washington, Seattle, WA, United States of America
- ^{143a} Institute of Frontier and Interdisciplinary Science and Key Laboratory of Particle Physics and Particle Irradiation (MOE), Shandong University, Qingdao
- ^{143b} School of Physics, Zhengzhou University, China
- ^{144a} School of Physics and Astronomy, State Key Laboratory of Dark Matter Physics, Shanghai Jiao Tong University, Key Laboratory for Particle Astrophysics and Cosmology (MOE), SKLPPC, Shanghai, China
- ^{144b} State Key Laboratory of Dark Matter Physics, Tsung-Dao Lee Institute, Shanghai Jiao Tong University, Shanghai, China
- ¹⁴⁵ Department of Physics and Astronomy, University of Sheffield, Sheffield, United Kingdom
- ¹⁴⁶ Department of Physics, Shinshu University, Nagano, Japan
- ¹⁴⁷ Department Physik, Universität Siegen, Siegen, Germany
- ¹⁴⁸ Department of Physics, Simon Fraser University, Burnaby, BC, Canada
- ¹⁴⁹ SLAC National Accelerator Laboratory, Stanford, CA, United States of America
- ¹⁵⁰ Department of Physics, Royal Institute of Technology, Stockholm, Sweden
- ¹⁵¹ Departments of Physics and Astronomy, Stony Brook University, Stony Brook, NY, United States of America
- ¹⁵² Department of Physics and Astronomy, University of Sussex, Brighton, United Kingdom
- ¹⁵³ School of Physics, University of Sydney, Sydney, Australia
- ¹⁵⁴ Institute of Physics, Academia Sinica, Taipei, Taiwan
- ^{155a} E. Andronikashvili Institute of Physics, Iv. Javakhishvili Tbilisi State University, Tbilisi
- ^{155b} High Energy Physics Institute, Tbilisi State University, Tbilisi
- ^{155c} University of Georgia, Tbilisi, Georgia
- ¹⁵⁶ Department of Physics, Technion, Israel Institute of Technology, Haifa, Israel
- ¹⁵⁷ Raymond and Beverly Sackler School of Physics and Astronomy, Tel Aviv University, Tel Aviv; Israel
- ¹⁵⁸ Department of Physics, Aristotle University of Thessaloniki, Thessaloniki, Greece
- ¹⁵⁹ International Center for Elementary Particle Physics and Department of Physics, University of Tokyo, Tokyo, Japan
- ¹⁶⁰ Graduate School of Science and Technology, Tokyo Metropolitan University, Tokyo, Japan
- ¹⁶¹ Department of Physics, University of Toronto, Toronto, ON, Canada
- ^{162a} TRIUMF, Vancouver, BC
- ^{162b} Department of Physics and Astronomy, York University, Toronto, ON, Canada
- ¹⁶³ Division of Physics and Tomonaga Center for the History of the Universe, Faculty of Pure and Applied Sciences, University of Tsukuba, Tsukuba, Japan
- ¹⁶⁴ Department of Physics and Astronomy, Tufts University, Medford, MA, United States of America
- ¹⁶⁵ Department of Physics and Astronomy, University of California Irvine, Irvine, CA, United States of America
- ¹⁶⁶ University of West Attica, Athens, Greece
- ¹⁶⁷ Department of Physics and Astronomy, University of Uppsala, Uppsala, Sweden
- ¹⁶⁸ Department of Physics, University of Illinois, Urbana, IL, United States of America
- ¹⁶⁹ Instituto de Física Corpuscular (IFIC), Centro Mixto Universidad de Valencia - CSIC, Valencia, Spain
- ¹⁷⁰ Department of Physics, University of British Columbia, Vancouver, BC, Canada
- ¹⁷¹ Department of Physics and Astronomy, University of Victoria, Victoria, BC, Canada
- ¹⁷² Fakultät für Physik und Astronomie, Julius-Maximilians-Universität Würzburg, Würzburg, Germany
- ¹⁷³ Department of Physics, University of Warwick, Coventry, United Kingdom
- ¹⁷⁴ Waseda University, Tokyo, Japan
- ¹⁷⁵ Department of Particle Physics and Astrophysics, Weizmann Institute of Science, Rehovot, Israel
- ¹⁷⁶ Department of Physics, University of Wisconsin, Madison, WI, United States of America
- ¹⁷⁷ Fakultät für Mathematik und Naturwissenschaften, Fachgruppe Physik, Bergische Universität Wuppertal, Wuppertal, Germany
- ¹⁷⁸ Department of Physics, Yale University, New Haven, CT, United States of America
- ¹⁷⁹ Yerevan Physics Institute, Yerevan, Armenia
- ^a Also at Affiliated with an institute formerly covered by a cooperation agreement with CERN
- ^b Also at An-Najah National University, Nablus, Palestine
- ^c Also at Borough of Manhattan Community College, City University of New York, New York, NY, United States of America
- ^d Also at Center for Interdisciplinary Research and Innovation (CIRI-AUTH), Thessaloniki, Greece
- ^e Also at Centre of Physics of the Universities of Minho and Porto (CF-UM-UP), Portugal
- ^f Also at CERN, Geneva, Switzerland
- ^g Also at Département de Physique Nucléaire et Corpusculaire, Université de Genève, Genève, Switzerland
- ^h Also at Departament de Física, Universitat Autònoma de Barcelona, Barcelona, Spain
- ⁱ Also at Department of Financial and Management Engineering, University of the Aegean, Chios, Greece
- ^j Also at Department of Mathematical Sciences, University of South Africa, Johannesburg, South Africa
- ^k Also at Department of Modern Physics and State Key Laboratory of Particle Detection and Electronics, University of Science and Technology of China, Hefei, China
- ^l Also at Department of Physics, Bolu Abant İzzet Baysal University, Bolu, Türkiye
- ^m Also at Department of Physics, King's College London, London, United Kingdom
- ⁿ Also at Department of Physics, Stanford University, Stanford, CA, United States of America
- ^o Also at Department of Physics, Stellenbosch University, South Africa
- ^p Also at Department of Physics, University of Fribourg, Fribourg, Switzerland
- ^q Also at Department of Physics, University of Thessaly, Greece
- ^r Also at Department of Physics, Westmont College, Santa Barbara, United States of America
- ^s Also at Faculty of Physics, Sofia University, 'St. Kliment Ohridski', Sofia, Bulgaria
- ^t Also at Faculty of Physics, University of Bucharest, Romania
- ^u Also at Hellenic Open University, Patras, Greece
- ^v Also at Henan University, China
- ^w Also at Imam Mohammad Ibn Saud Islamic University, Saudi Arabia
- ^x Also at Institutio Catalana de Recerca i Estudis Avancats, ICREA, Barcelona, Spain
- ^y Also at Institut für Experimentalphysik, Universität Hamburg, Hamburg, Germany
- ^z Also at Institute for Nuclear Research and Nuclear Energy (INRNE), Bulgarian Academy of Sciences, Sofia, Bulgaria
- ^{aa} Also at Institute of Applied Physics, Mohammed VI Polytechnic University, Ben Guerir, Morocco

^{ab} Also at Institute of Particle Physics (IPP), Canada
^{ac} Also at Institute of Physics and Technology, Mongolian Academy of Sciences, Ulaanbaatar, Mongolia
^{ad} Also at Institute of Physics, Azerbaijan Academy of Sciences, Baku, Azerbaijan
^{ae} Also at Institute of Theoretical Physics, Ilia State University, Tbilisi, Georgia
^{af} Also at National Institute of Physics, University of the Philippines Diliman (Philippines), Philippines
^{ag} Also at The Collaborative Innovation Center of Quantum Matter (CICQM), Beijing, China
^{ah} Also at TRIUMF, Vancouver, BC, Canada
^{ai} Also at Università di Napoli Parthenope, Napoli, Italy
^{aj} Also at Department of Physics, University of Colorado Boulder, Colorado, United States of America
^{ak} Also at University of Sienna, Italy
^{al} Also at Washington College, Chestertown, MD, United States of America
^{am} Also at Physics Department, Yeditepe University, Istanbul, Türkiye

†Deceased

References

- [1] P.V. Landshoff, J.C. Polkinghorne, Calorimeter triggers for hard collisions, *Phys. Rev. D* 18 (1978) 3344. <https://doi.org/10.1103/PhysRevD.18.3344>
- [2] F. Takagi, Multiple Production of Quark Jets off Nuclei, *Phys. Rev. Lett.* 43 (1979) 1296. <https://doi.org/10.1103/PhysRevLett.43.1296>
- [3] C. Goebel, D.M. Scott, F. Halzen, Double Drell-Yan annihilations in hadron collisions: Novel tests of the constituent picture, *Phys. Rev. D* 22 (1980) 2789. <https://doi.org/10.1103/PhysRevD.22.2789>
- [4] R. Kirschner, Generalized Lipatov-Altarelli-Parisi Equations and Jet Calculus Rules, *Phys. Lett. B* 84 (1979) 266. [https://doi.org/10.1016/0370-2693\(79\)90300-9](https://doi.org/10.1016/0370-2693(79)90300-9)
- [5] V.P. Shelest, A.M. Snigirev, G.M. Zinovjev, Gazing into the multiparton distribution equations in QCD, *Phys. Lett. B* 113 (1982) 325. [https://doi.org/10.1016/0370-2693\(82\)90049-1](https://doi.org/10.1016/0370-2693(82)90049-1)
- [6] M. Mekhfi, Correlations in Color and Spin in Multiparton Processes, *Phys. Rev. D* 32 (1985) 2380. <https://doi.org/10.1103/PhysRevD.32.2380>
- [7] N. Paver, D. Treleani, Multiquark scattering and large- p_T jet production in hadronic collisions, *Nuovo Cim. A* 70 (1982) 215. <https://doi.org/10.1007/BF02814035>
- [8] N. Paver, D. Treleani, Multiple parton interactions and multijet events at collider and tevatron energies, *Phys. Lett. B* 146 (3) (1984) 252–256. [https://doi.org/https://doi.org/10.1016/0370-2693\(84\)91029-3](https://doi.org/https://doi.org/10.1016/0370-2693(84)91029-3)
- [9] M. Mekhfi, Multiparton processes: an application to the double Drell-Yan mechanism, *Phys. Rev. D* 32 (1985) 2371. <https://doi.org/10.1103/PhysRevD.32.2371>
- [10] B. Humpert, Are there multiquark interactions? *Phys. Lett. B* 131 (1983) 461. [https://doi.org/10.1016/0370-2693\(83\)90540-3](https://doi.org/10.1016/0370-2693(83)90540-3)
- [11] B. Humpert, The production of gauge boson pairs by pp colliders, *Phys. Lett. B* 135 (1) (1984) 179. [https://doi.org/10.1016/0370-2693\(84\)90479-9](https://doi.org/10.1016/0370-2693(84)90479-9)
- [12] B. Humpert, R. Odorico, Multi-parton scattering and QCD radiation as sources of four-jet events, *Phys. Lett. B* 154 (1985) 211. [https://doi.org/10.1016/0370-2693\(85\)90587-8](https://doi.org/10.1016/0370-2693(85)90587-8)
- [13] D. Ametller, L.L. and Paver, N. and Treleani, Possible signature of multiple parton interactions in collider four-jet events, *Phys. Lett. B* 169 (1986) 289. [https://doi.org/10.1016/0370-2693\(86\)90668-4](https://doi.org/10.1016/0370-2693(86)90668-4)
- [14] F. Halzen, P. Hoyer, W.Y. Stirling, Evidence for multiple parton interactions from the observation of multi-muon events in Drell-Yan experiments, *Phys. Lett. B* 188 (1987) 375. [https://doi.org/10.1016/0370-2693\(87\)91400-6](https://doi.org/10.1016/0370-2693(87)91400-6)
- [15] R.M. Godbole, S. Gupta, J. Lindfors, Double parton scattering contribution to $W +$ jets, *Z. Phys. C* 47 (1990) 69. <https://doi.org/10.1007/BF01551914>
- [16] ATLAS Collaboration, Measurement of hard double-parton interactions in $W(\rightarrow \nu) + 2$ jet events at $\sqrt{s} = 7$ TeV with the ATLAS detector, *New J. Phys.* 15 (2013) 033038. arXiv:1301.6872. <https://doi.org/10.1088/1367-2630/15/3/033038>
- [17] CMS Collaboration, Study of double parton scattering using $W + 2$ -jet events in proton–proton collisions at $\sqrt{s} = 7$ TeV, *JHEP* 03 (2014) 032. arXiv:1007.1727. [https://doi.org/10.1007/JHEP03\(2014\)032](https://doi.org/10.1007/JHEP03(2014)032)
- [18] CDF Collaboration, Measurement of double parton scattering in $\bar{p}p$ collisions at $\sqrt{s} = 1.8$ TeV, *Phys. Rev. Lett.* 79 (1997) 584. <https://doi.org/10.1103/PhysRevLett.79.584>
- [19] CMS Collaboration, Event generator tunes obtained from underlying event and multiparton scattering measurements, *Eur. Phys. J. C* 76 (2016) 155. arXiv:1512.00815. <https://doi.org/10.1140/epjc/s10052-016-3988-x>
- [20] D0 Collaboration, Double parton interactions in $\gamma + 3$ jet events in $\bar{p}p$ collisions at $\sqrt{s} = 1.96$ TeV, *Phys. Rev. D* 81 (2010) 052012. arXiv:0912.5104. <https://doi.org/10.1103/PhysRevD.81.052012>
- [21] ATLAS Collaboration, Observation and measurements of the production of prompt and non-prompt J/ψ mesons in association with a Z boson in pp collisions at $\sqrt{s} = 8$ TeV with the ATLAS detector, *Eur. Phys. J. C* 75 (2015) 229. arXiv:1412.6428. <https://doi.org/10.1140/epjc/s10052-015-3406-9>
- [22] LHCb Collaboration, Production of associated Υ and open charm hadrons in pp collisions at $\sqrt{s} = 7$ and 8 TeV via double parton scattering, *JHEP* 07 (2016) 052. arXiv:1510.05949. [https://doi.org/10.1007/JHEP07\(2016\)052](https://doi.org/10.1007/JHEP07(2016)052)
- [23] D0 Collaboration, Evidence for simultaneous production of J/ψ and Υ mesons, *Phys. Rev. Lett.* 116 (2016) 082002. arXiv:1511.02428. <https://doi.org/10.1103/PhysRevLett.116.082002>
- [24] CMS Collaboration, Observation of triple J/ψ meson production in proton–proton collisions, *Nat. Phys.* 19 (2023) 338–350. arXiv:2111.05370. <https://doi.org/10.1038/s41567-022-01838-y>
- [25] The Axial Field Spectrometer Collaboration, Double parton scattering in pp collisions at $\sqrt{s} = 63$ GeV, *Z. Phys. C* 34 (1987) 163. <https://doi.org/10.1007/BF01566757>
- [26] UA2 Collaboration, A study of multi-jet events at the CERN $\bar{p}p$ collider and a search for double parton scattering, *Phys. Lett. B* 268 (1991) 145. [https://doi.org/10.1016/0370-2693\(91\)90937-L](https://doi.org/10.1016/0370-2693(91)90937-L)
- [27] CDF Collaboration, Study of four-jet events and evidence for double parton interactions in $\bar{p}p$ collisions at $\sqrt{s} = 1.8$ TeV, *Phys. Rev. D* 47 (1993) 4857. <https://doi.org/10.1103/PhysRevD.47.4857>
- [28] CDF Collaboration, Double parton scattering in $\bar{p}p$ collisions at $\sqrt{s} = 1.8$ TeV, *Phys. Rev. D* 56 (1997) 3811. <https://doi.org/10.1103/PhysRevD.56.3811>
- [29] LHCb Collaboration, Observation of double charm production involving open charm in pp collisions at $\sqrt{s} = 7$ TeV, *JHEP* 06 (2012) 141. arXiv:1205.0975. [https://doi.org/10.1007/JHEP06\(2012\)141](https://doi.org/10.1007/JHEP06(2012)141)
- [30] CMS Collaboration, Constraints on the double-parton scattering cross section from same-sign W boson pair production in proton–proton collisions at $\sqrt{s} = 8$ TeV, *JHEP* 02 (2018) 032. arXiv:1712.02280. [https://doi.org/10.1007/JHEP02\(2018\)032](https://doi.org/10.1007/JHEP02(2018)032)
- [31] ATLAS Collaboration, Study of the hard double-parton scattering contribution to inclusive four-lepton production in pp collisions at $\sqrt{s} = 8$ TeV with the ATLAS detector, *Phys. Lett. B* 790 (2019) 595. arXiv:1811.11094. <https://doi.org/10.1016/j.physletb.2019.01.062>
- [32] CMS Collaboration, Measurement of double-parton scattering in inclusive production of four jets with low transverse momentum in proton–proton collisions at $\sqrt{s} = 13$ TeV, *JHEP* 01 (2022) 177. arXiv:2109.13822. [https://doi.org/10.1007/JHEP01\(2022\)177](https://doi.org/10.1007/JHEP01(2022)177)
- [33] CMS Collaboration, Study of Z boson plus jets events using variables sensitive to double-parton scattering in pp collisions at 13 TeV, *JHEP* 10 (2021) 176. arXiv:2105.14511. [https://doi.org/10.1007/JHEP10\(2021\)176](https://doi.org/10.1007/JHEP10(2021)176)
- [34] D0 Collaboration, Observation and studies of double J/ψ production at the Tevatron, *Phys. Rev. D* 90 (2014) 111101. arXiv:1406.2380. <https://doi.org/10.1103/PhysRevD.90.111101>
- [35] D0 Collaboration, Double Parton Interactions in $\gamma + 3$ Jet and $\gamma + b/c$ jet + 2 Jet Events in $\bar{p}p$ Collisions at $\sqrt{s} = 1.96$ TeV, *Phys. Rev. D* 89 (7) (2014) 072006. arXiv:1402.1550. <https://doi.org/10.1103/PhysRevD.89.072006>
- [36] D0 Collaboration, Study of double parton interactions in diphoton + dijet events in $\bar{p}p$ collisions at $\sqrt{s} = 1.96$ TeV, *Phys. Rev. D* 93 (5) (2016) 052008. arXiv:1512.05291. <https://doi.org/10.1103/PhysRevD.93.052008>
- [37] ATLAS Collaboration, Study of hard double-parton scattering in four-jet events in pp collisions at $\sqrt{s} = 7$ TeV with the ATLAS experiment, *JHEP* 11 (2016) 110. arXiv:1608.01857. [https://doi.org/10.1007/JHEP11\(2016\)110](https://doi.org/10.1007/JHEP11(2016)110)
- [38] ATLAS Collaboration, Measurement of the prompt J/ψ pair production cross-section in pp collisions at $\sqrt{s} = 8$ TeV with the ATLAS detector, *Eur. Phys. J. C* 77 (2017) 76. arXiv:1612.02950. <https://doi.org/10.1140/epjc/s10052-017-4644-9>
- [39] CMS Collaboration, Observation of $\Upsilon(1S)$ pair production in proton–proton collisions at $\sqrt{s} = 8$ TeV, *JHEP* 05 (2017) 013. arXiv:1610.07095. [https://doi.org/10.1007/JHEP05\(2017\)013](https://doi.org/10.1007/JHEP05(2017)013)
- [40] LHCb Collaboration, Measurement of the J/ψ pair production cross-section in pp collisions at $\sqrt{s} = 13$ TeV, *JHEP* 06 (2017) 047. arXiv:1612.07451. [https://doi.org/10.1007/JHEP06\(2017\)047](https://doi.org/10.1007/JHEP06(2017)047)
- [41] W.James. Gaunt, Jonathan R. and Stirling, Double parton distributions incorporating perturbative QCD evolution and momentum and quark number sum rules, *JHEP* 03 (2010) 005. arXiv:0910.4347. [https://doi.org/10.1007/JHEP03\(2010\)005](https://doi.org/10.1007/JHEP03(2010)005)
- [42] M. Diehl, J.R. Gaunt, K. Schönwald, Double hard scattering without double counting, *JHEP* 06 (2017) 083. arXiv:1702.06486. [https://doi.org/10.1007/JHEP06\(2017\)083](https://doi.org/10.1007/JHEP06(2017)083)
- [43] M. Diehl, P. Plöchl, A. Schäfer, Proof of sum rules for double parton distributions in QCD, *Eur. Phys. J. C* 79 (3) (2019) 253. arXiv:1811.00289. <https://doi.org/10.1140/epjc/s10052-019-6777-5>
- [44] J.R. Gaunt, T. Kasemets, Transverse momentum dependence in double parton scattering, *Adv. High Energy Phys.* 2019 (2019) 3797394. arXiv:1812.09099. <https://doi.org/10.1155/2019/3797394>
- [45] B. Cabouat, J.R. Gaunt, K. Ostrolenk, A Monte-Carlo simulation of double parton scattering, *JHEP* 11 (2019) 061. arXiv:1906.04669. [https://doi.org/10.1007/JHEP11\(2019\)061](https://doi.org/10.1007/JHEP11(2019)061)
- [46] L. Evans, P. Bryant, LHC Machine, *JINST* 3 (2008) S08001. <https://doi.org/10.1088/1748-0221/3/08/S08001>
- [47] CMS Collaboration, Observation of Same-Sign W/W Production from Double Parton Scattering in Proton–Proton Collisions at $\sqrt{s} = 13$ TeV, *Phys. Rev. Lett.* 131 (2023) 091803. arXiv:2206.02681. <https://doi.org/10.1103/PhysRevLett.131.091803>
- [48] J.R. Gaunt, C.-H. Kom, A. Kulesza, W.J. Stirling, Same-sign W pair production as a probe of double-parton scattering at the LHC, *Eur. Phys. J. C* 69 (2010) 53–65. arXiv:1003.3953. <https://doi.org/10.1140/epjc/s10052-010-1362-y>

- [49] F.A. Ceccopieri, M. Rinaldi, S. Scopetta, Parton correlations in same-sign W pair production via double parton scattering at the LHC, *Phys. Rev. D* 95 (11) (2017) 114030. arXiv:1702.05363. <https://doi.org/10.1103/PhysRevD.95.114030>
- [50] ATLAS Collaboration, Luminosity determination in pp collisions at $\sqrt{s} = 13$ TeV using the ATLAS detector at the LHC, *Eur. Phys. J. C* 83 (2023) 982. arXiv:2212.09379. <https://doi.org/10.1140/epjc/s10052-023-11747-w>
- [51] G. Avoni, et al., The new LUCID-2 detector for luminosity measurement and monitoring in ATLAS, *JINST* 13 (2018) P07017. <https://doi.org/10.1088/1748-0221/13/07/P07017>
- [52] ATLAS Collaboration, The ATLAS Experiment at the CERN Large Hadron Collider, *JINST* 3 (2008) S08003. <https://doi.org/10.1088/1748-0221/3/08/S08003>
- [53] ATLAS Collaboration, Performance of the ATLAS trigger system in 2015, *Eur. Phys. J. C* 77 (2017) 317. arXiv:1611.09661. <https://doi.org/10.1140/epjc/s10052-017-4852-3>
- [54] ATLAS Collaboration, Software and computing for Run 3 of the ATLAS experiment at the LHC, *Eur. Phys. J. C* 85 (2025) 234. arXiv:2404.06335. <https://doi.org/10.1140/epjc/s10052-024-13701-w>
- [55] ATLAS Collaboration, The ATLAS simulation infrastructure, *Eur. Phys. J. C* 70 (2010) 823. arXiv:1005.4568. <https://doi.org/10.1140/epjc/s10052-010-1429-9>
- [56] S. Agostinelli, et al., GEANT4 – a simulation toolkit, *Nucl. Instrum. Meth. A* 506 (2003) 250. [https://doi.org/10.1016/S0168-9002\(03\)01368-8](https://doi.org/10.1016/S0168-9002(03)01368-8)
- [57] T. Sjöstrand, S. Mrenna, P. Skands, A brief introduction to PYTHIA 8.1, *Comput. Phys. Commun.* 178 (2008) 852–867. arXiv:0710.3820. <https://doi.org/10.1016/j.cpc.2008.01.036>
- [58] NNPDF Collaboration, R.D. Ball, et al., Parton distributions with LHC data, *Nucl. Phys. B* 867 (2013) 244. arXiv:1207.1303. <https://doi.org/10.1016/j.nuclphysb.2012.10.003>
- [59] ATLAS Collaboration, The Pythia 8 A3 tune description of ATLAS minimum bias and inelastic measurements incorporating the Donnachie–Landshoff diffractive model, *ATL-PHYS-PUB-2016-017*, 2016. <https://cds.cern.ch/record/2206965>.
- [60] D.J. Lange, The EvtGen particle decay simulation package, *Nucl. Instrum. Meth. A* 462 (2001) 152. [https://doi.org/10.1016/S0168-9002\(01\)00089-4](https://doi.org/10.1016/S0168-9002(01)00089-4)
- [61] C. Bierlich, S. Chakraborty, N. Desai, L. Gellersen, I. Helenius, P. Ilten, L. Lönnblad, S. Mrenna, S. Prestel, C.T. Preuss, T. Sjöstrand, P. Skands, M. Uthheim, R. Verheyen, A comprehensive guide to the physics and usage of PYTHIA 8.3, *SciPost Phys. Codeb.* (2022) 8. arXiv:2203.11601. <https://doi.org/10.21468/SciPostPhysCodeb.8>
- [62] ATLAS Collaboration, ATLAS Pythia 8 tunes to 7 TeV data, *ATL-PHYS-PUB-2014-021*, 2014. <https://cds.cern.ch/record/1966419>.
- [63] M. Bähr, et al., Herwig++ physics and manual, *Eur. Phys. J. C* 58 (2008) 639. arXiv:0803.0883. <https://doi.org/10.1140/epjc/s10052-008-0798-9>
- [64] J. Bellm, et al., Herwig 7.0/Herwig++ 3.0 release note, *Eur. Phys. J. C* 76 (4) (2016) 196. arXiv:1512.01178. <https://doi.org/10.1140/epjc/s10052-016-4018-8>
- [65] NNPDF Collaboration, R.D. Ball, et al., Parton distributions for the LHC Run II, *JHEP* 04 (2015) 040. arXiv:1410.8849. [https://doi.org/10.1007/JHEP04\(2015\)040](https://doi.org/10.1007/JHEP04(2015)040)
- [66] ATLAS Collaboration, Measurement and interpretation of same-sign W boson pair production in association with two jets in pp collisions at $\sqrt{s} = 13$ TeV with the ATLAS detector, *JHEP* 04 (2024) 026. arXiv:2312.00420. [https://doi.org/10.1007/JHEP04\(2024\)026](https://doi.org/10.1007/JHEP04(2024)026)
- [67] E. Bothmann, et al., Event generation with Sherpa 2.2, *SciPost Phys.* 7 (3) (2019) 034. arXiv:1905.09127. <https://doi.org/10.21468/SciPostPhys.7.3.034>
- [68] T. Gleisberg, S. Höche, Comix, a new matrix element generator, *JHEP* 12 (2008) 039. arXiv:0808.3674. <https://doi.org/10.1088/1126-6708/2008/12/039>
- [69] F. Cascioli, P. Maierhöfer, S. Pozzorini, Scattering Amplitudes with Open Loops, *Phys. Rev. Lett.* 108 (2012) 111601. arXiv:1111.5206. <https://doi.org/10.1103/PhysRevLett.108.111601>
- [70] S. Schumann, F. Krauss, A parton shower algorithm based on Catani–Seymour dipole factorisation, *JHEP* 03 (2008) 038. arXiv:0709.1027. <https://doi.org/10.1088/1126-6708/2008/03/038>
- [71] J. Alwall, R. Frederix, S. Frixione, V. Hirschi, F. Maltoni, O. Mattelaer, H.-S. Shao, T. Stelzer, P. Torrielli, M. Zaro, The automated computation of tree-level and next-to-leading order differential cross sections, and their matching to parton shower simulations, *JHEP* 07 (2014) 079. arXiv:1405.0301. [https://doi.org/10.1007/JHEP07\(2014\)079](https://doi.org/10.1007/JHEP07(2014)079)
- [72] T. Sjöstrand, S. Ask, J.R. Christiansen, R. Corke, N. Desai, P. Ilten, S. Mrenna, S. Prestel, C.O. Rasmussen, P.Z. Skands, An introduction to PYTHIA 8.2, *Comput. Phys. Commun.* 191 (2015) 159. arXiv:1410.3012. <https://doi.org/10.1016/j.cpc.2015.01.024>
- [73] B. Cabouat, T. Sjöstrand, Some dipole shower studies, *Eur. Phys. J. C* 78 (3) (2018) 226. arXiv:1710.00391. <https://doi.org/10.1140/epjc/s10052-018-5645-z>
- [74] S. Höche, F. Krauss, M. Schönherr, F. Siegert, A critical appraisal of NLO+PS matching methods, *JHEP* 09 (2012) 049. arXiv:1111.1220. [https://doi.org/10.1007/JHEP09\(2012\)049](https://doi.org/10.1007/JHEP09(2012)049)
- [75] S. Höche, F. Krauss, M. Schönherr, F. Siegert, QCD matrix elements + parton showers. The NLO case, *JHEP* 04 (2013) 027. arXiv:1207.5030. [https://doi.org/10.1007/JHEP04\(2013\)027](https://doi.org/10.1007/JHEP04(2013)027)
- [76] S. Catani, F. Krauss, B.R. Webber, R. Kuhn, QCD matrix elements + parton showers, *JHEP* 11 (2001) 063. arXiv:hep-ph/0109231. <https://doi.org/10.1088/1126-6708/2001/11/063>
- [77] S. Höche, F. Krauss, S. Schumann, F. Siegert, QCD matrix elements and truncated showers, *JHEP* 05 (2009) 053. arXiv:0903.1219. <https://doi.org/10.1088/1126-6708/2009/05/053>
- [78] R. Frederix, E. Re, P. Torrielli, Single-top t -channel hadroproduction in the four-flavour scheme with POWHEG and aMC@NLO, *JHEP* 09 (2012) 130. arXiv:1207.5391. [https://doi.org/10.1007/JHEP09\(2012\)130](https://doi.org/10.1007/JHEP09(2012)130)
- [79] P. Nason, A new method for combining NLO QCD with shower Monte Carlo algorithms, *JHEP* 11 (2004) 040. arXiv:hep-ph/0409146. <https://doi.org/10.1088/1126-6708/2004/11/040>
- [80] S. Frixione, P. Nason, C. Oleari, Matching NLO QCD computations with parton shower simulations: the POWHEG method, *JHEP* 11 (2007) 070. arXiv:0709.2092. <https://doi.org/10.1088/1126-6708/2007/11/070>
- [81] S. Alioli, P. Nason, C. Oleari, E. Re, A general framework for implementing NLO calculations in shower Monte Carlo programs: the POWHEG BOX, *JHEP* 06 (2010) 043. arXiv:1002.2581. [https://doi.org/10.1007/JHEP06\(2010\)043](https://doi.org/10.1007/JHEP06(2010)043)
- [82] ATLAS Collaboration, Modelling and computational improvements to the simulation of single vector-boson plus jet processes for the ATLAS experiment, *JHEP* 08 (2022) 089. arXiv:2112.09588. [https://doi.org/10.1007/JHEP08\(2022\)089](https://doi.org/10.1007/JHEP08(2022)089)
- [83] ATLAS Collaboration, Performance of electron and photon triggers in ATLAS during LHC Run 2, *Eur. Phys. J. C* 80 (2020) 47. arXiv:1909.00761. <https://doi.org/10.1140/epjc/s10052-019-7500-2>
- [84] ATLAS Collaboration, Performance of the ATLAS muon triggers in Run 2, *JINST* 15 (2020) P09015. arXiv:2004.13447. <https://doi.org/10.1088/1748-0221/15/09/p09015>
- [85] ATLAS Collaboration, ATLAS data quality operations and performance for 2015–2018 data-taking, *JINST* 15 (2020) P04003. arXiv:1911.04632. <https://doi.org/10.1088/1748-0221/15/04/P04003>
- [86] ATLAS Collaboration, Vertex Reconstruction Performance of the ATLAS Detector at $\sqrt{s} = 13$ TeV, *ATL-PHYS-PUB-2015-026*, 2015. <https://cds.cern.ch/record/2037717>.
- [87] ATLAS Collaboration, Electron and photon performance measurements with the ATLAS detector using the 2015–2017 LHC proton–proton collision data, *JINST* 14 (2019) P12006. arXiv:1908.00005. <https://doi.org/10.1088/1748-0221/14/12/P12006>
- [88] ATLAS Collaboration, Muon reconstruction and identification efficiency in ATLAS using the full Run 2 pp collision data set at $\sqrt{s} = 13$ TeV, *Eur. Phys. J. C* 81 (2021) 578. arXiv:2012.00578. <https://doi.org/10.1140/epjc/s10052-021-09233-2>
- [89] ATLAS Collaboration, Measurement of the W charge asymmetry in the $W \rightarrow \mu\nu$ decay mode in pp collisions at $\sqrt{s} = 7$ TeV with the ATLAS detector, *Phys. Lett. B* 701 (2011) 31. arXiv:1103.2929. <https://doi.org/10.1016/j.physletb.2011.05.024>
- [90] M. Cacciari, G.P. Salam, G. Soyez, The anti- k_t jet clustering algorithm, *JHEP* 04 (2008) 063. arXiv:0802.1189. <https://doi.org/10.1088/1126-6708/2008/04/063>
- [91] M. Cacciari, G.P. Salam, G. Soyez, FastJet user manual, *Eur. Phys. J. C* 72 (2012) 1896. arXiv:1111.6097. <https://doi.org/10.1140/epjc/s10052-012-1896-2>
- [92] ATLAS Collaboration, Jet reconstruction and performance using particle flow with the ATLAS Detector, *Eur. Phys. J. C* 77 (2017) 466. arXiv:1703.10485. <https://doi.org/10.1140/epjc/s10052-017-5031-2>
- [93] ATLAS Collaboration, Performance of pile-up mitigation techniques for jets in pp collisions at $\sqrt{s} = 8$ TeV using the ATLAS detector, *Eur. Phys. J. C* 76 (2016) 581. arXiv:1510.03823. <https://doi.org/10.1140/epjc/s10052-016-4395-z>
- [94] ATLAS Collaboration, Jet energy scale and resolution measured in proton–proton collisions at $\sqrt{s} = 13$ TeV with the ATLAS detector, *Eur. Phys. J. C* 81 (2021) 689. arXiv:2007.02645. <https://doi.org/10.1140/epjc/s10052-021-09402-3>
- [95] ATLAS Collaboration, ATLAS flavour-tagging algorithms for the LHC Run 2 pp collision dataset, *Eur. Phys. J. C* 83 (2023) 681. arXiv:2211.16345. <https://doi.org/10.1140/epjc/s10052-023-11699-1>
- [96] ATLAS Collaboration, ATLAS b -jet identification performance and efficiency measurement with $\bar{t}t$ events in pp collisions at $\sqrt{s} = 13$ TeV, *Eur. Phys. J. C* 79 (2019) 970. arXiv:1907.05120. <https://doi.org/10.1140/epjc/s10052-019-7450-8>
- [97] ATLAS Collaboration, Calibration of the light-flavour jet mistagging efficiency of the b -tagging algorithms with Z +jets events using 139fb^{-1} of ATLAS proton–proton collision data at $\sqrt{s} = 13$ TeV, *Eur. Phys. J. C* 83 (2023) 728. arXiv:2301.06319. <https://doi.org/10.1140/epjc/s10052-023-11736-z>
- [98] ATLAS Collaboration, Measurement of the c -jet mistagging efficiency in $\bar{t}t$ events using pp collision data at $\sqrt{s} = 13$ TeV collected with the ATLAS detector, *Eur. Phys. J. C* 82 (2022) 95. arXiv:2109.10627. <https://doi.org/10.1140/epjc/s10052-021-09843-w>
- [99] ATLAS Collaboration, The performance of missing transverse momentum reconstruction and its significance with the ATLAS detector using 140fb^{-1} of $\sqrt{s} = 13$ TeV pp collisions, *Eur. Phys. J. C* 85 (2025) 606. arXiv:2402.05858. <https://doi.org/10.1140/epjc/s10052-025-14062-8>
- [100] S.M. Lundberg, S. Lee, A unified approach to interpreting model predictions, in: Proceedings of the 31st International Conference on Neural Information Processing Systems, 2017, arXiv:1705.07874.
- [101] ATLAS Collaboration, Tools for estimating fake/non-prompt lepton backgrounds with the ATLAS detector at the LHC, *JINST* 18 (2023) T11004. arXiv:2211.16178. <https://doi.org/10.1088/1748-0221/18/11/T11004>
- [102] ATLAS Collaboration, Measurement of $W^\pm Z$ production cross sections and gauge boson polarisation in pp collisions at $\sqrt{s} = 13$ TeV with the ATLAS detector, *Eur. Phys. J. C* 79 (2019) 535. arXiv:1902.05759. <https://doi.org/10.1140/epjc/s10052-019-7027-6>
- [103] ATLAS Collaboration, Study of multiple hard-scatter processes from different pp interactions in the same ATLAS event, *ATL-PHYS-PUB-2018-007*, 2018. <https://cds.cern.ch/record/2320419>.
- [104] ATLAS Collaboration, Measurement of the Inelastic Proton–Proton Cross Section at $\sqrt{s} = 13$ TeV with the ATLAS Detector at the LHC, *Phys. Rev. Lett.* 117 (2016) 182002. arXiv:1606.02625. <https://doi.org/10.1103/PhysRevLett.117.182002>
- [105] J. Butterworth, et al., PDF4LHC recommendations for LHC Run II, *J. Phys. G* 43 (2016) 023001. arXiv:1510.03865. <https://doi.org/10.1088/0954-3889/43/2/023001>

- [106] W.A. Rolke, A.M. Lopez, J. Conrad, Limits and confidence intervals in the presence of nuisance parameters, *Nucl. Instrum. Meth. A* 551 (2005) 493–503. [arXiv:physics/0403059](https://arxiv.org/abs/physics/0403059). <https://doi.org/10.1016/j.nima.2005.05.068>
- [107] G. Cowan, K. Cranmer, E. Gross, O. Vitells, Asymptotic formulae for likelihood-based tests of new physics, *Eur. Phys. J. C* 71 (2011) 1554. [arXiv:1007.1727](https://arxiv.org/abs/1007.1727). <https://doi.org/10.1140/epjc/s10052-011-1554-0>
- [108] ATLAS Collaboration, ATLAS Computing Acknowledgements, ATL-SOFT-PUB-2025-001, 2025. <https://cds.cern.ch/record/2922210>.
- [109] CERN, CERN Open Data Policy for the LHC Experiments, CERN-OPEN-2020-013, 2020. <https://cds.cern.ch/record/2745133>.